Controlling cell adhesion at the nanoscale

Duncan S. Sutherland[1]

[1]*Nanobiointerfaces group, Interdisciplinary Nanoscience Center (iNANO), Aarhus University, Denmark*

The microenvironment around a cell critically determines its function and behavior. Nanometer scale topographic and chemical structures can provide cues and organization signals imposing a pattern on the extracellular matrix molecules adsorbing to nanostructured materials. Here a route to define cell instructive nanostructured interfaces based on colloidal monolayer masks and traditional lithographic steps will be described. Dispersed monolayers resulting from sequential electrostatic binding to oppositely charged surfaces results in short range ordered arrays of particles and can be utilized to generate one nanostructure per particle. The generated patterns have no long range order and are homogeneous over large areas (10's of cm^2) and can be chemically functionalized to enable protein patterning. These materials are used to pattern specific ECM and cell-cell adhesion molecules for use in understanding and steering development and signaling at adhesive complexes such as integrin based focal adhesions and cadherin based adherence junctions. Examples of studies with different ECM protein patterns (e.g. Fibronectin [1], Vitronectin [2], Laminin, Collagen,) and cell-cell adhesion proteins (e.g. E-Cadherin [3] and I-CAM) and their influence on cell adhesion and differentiation will be given. Both the size scale of the protein patches and the specific proteins immobilized are critical to determining and steering the cellular response. The size scale of the patterns in the range 60-3000 nm systematically controls the cellular attachment but with different critical sizes in specific systems. A clear role and importance for the specific ligand pattern was observed with nanopatterns of fibronectin and vitronectin showing clear differences in the mechanism of adhesion [2]. Colloidal lithographic techniques represent a useful tool for use in the study of the mechanics of cellular adhesion and control of differentiation.

REFERENCES: [1] J. Malmström, B. Christensen, H.P. Jakobsen, J. Lovmand, E.S. Sørensen, D.S. Sutherland (2010) *Nano Letters* **10**:2 686-94. [2]J. Malmström, J. Lovmand, S. Kristensen, M. Sundh, M. Duch, D.S. Sutherland (2011) *Nano Letters* **11**:6 2264-71 (2011) [3] S. Kristensen, G. Pedersen, L. N. Nejsum, D.S. Sutherland (2012) *Nano Letters* **12**(4):2129-33.

Making tissue by injection

JG Hilborn[1], K Bergman[2], D Ossipov[1], O Varghese[1], T Bowden[1], C Aulin[3], S Piskounova[1], T Engstrand[4]

[1] Department of Chemistry,Uppsala University, Sweden. [2] Termira AB Stockholm, Sweden, [3] Department of Medicine, Karolinska Institutet, [4] Department of Molecular Medicine and Surgery, Solna, Sweden

INTRODUCTION: Synthetic scaffolds composed of various biomolecules that are an integral part of extracellular matrix (ECM) components, such as hyaluronic acid or hyaluronan (HA), chondroitin sulphate, heparin sulphate etc., play an essential role in various drug delivery applications. Specifically, the hydrogel forms of these synthetic ECM mimetic materials serve as a suitable matrices for tissue engineering and regenerative medicine. We have recently developed HA based injectable hydrogels that have been used as a depot for HA linked prodrugs such as bisphosphonate, as well as for the delivery of growth factor, namely BMP-2 (bone morphogenetic protein-2) to form ectopic bone at the site of injection, regenerate cartilage and unexpectedly to form tendon-like structures in vivo.

METHODS: Aldehyde functionalized hyaluonan (HA-A) and hydrazide functional crosslinker(PVA-H) were prepared as discribed in (1). Gel preparation.: Equimolar amounts of HA-A and PVA-H at 1.5% solid in water was rapidly mixed using a dual barel syringe or two interconnected syringes by pushing back and forth followed by injection to induce the reaction between HYA-A and PVA-H. Bone morphogentic protein (BMP-2) and hydroxyapatite powder was added to selected formulations prior mixing.

RESULTS & DISCUSSION: The selection of suitable ECM component as building block is critical. We have focussed on HA which is a non immunogenic linear polysaccharide, and serves important functions within the ECM. As a result of these specific biological properties along with in vivo enzymatic degradability, HA derivatives have been extensively evaluated for various biomedical applications.

Scheme 1. Network forming reaction

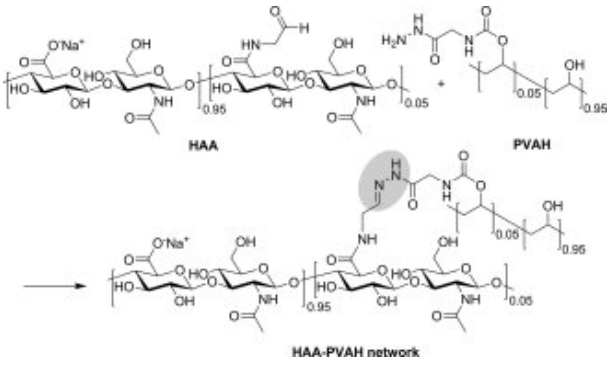

Our synthetic strategy involves pre-derivatisation and purification of two multifunctional polymers that may react spontaneously and selectively with each other in aqueous solutions to form a cross-linked network held together by hydrazone linkages (Scheme 1). We have demonstrated bone formation in small and large animals and also capability of cartilage regeneration without added cells [1-3]. Surprisingly, immunohistochemistry of representative samples from a 5-week post injection time-point into the rat model was performed to demonstrate the presence of not only bone but also tendon and cartilage, Figure 1.

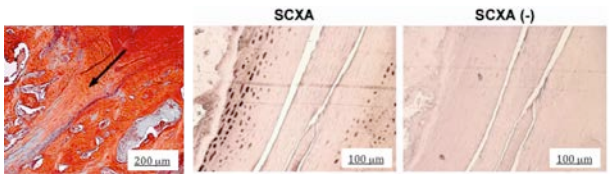

Figure 1. Left: Histological examination of samples in the HAP group also revealed the presence of cartilage and tendon like structures (arrow) indicative of enthesis. Middle/Right: Immunohistochemistry on histological sections confirmed the presence of tendon by staining with scleraxis (SCXA).

CONCLUSIONS: The studies presented demonstrate the possibility to induce bone and interconnecting musculoskeletal tissue by single injections of HA-based hydrogels. The advantage of not having to rely on transplantation of cells, in combination with the non-invasive procedure, makes this approach particularly attractive for clinical use.

REFERENCES: [1]Bergman K, Engstrand T, Hilborn J, et al., (2009) *J. Biomed. Mater. Res. Part A*, 91A **4:**1111-1118 [2]Docherty-Skogh AC, Bergman K, Waern MJ, et al., (2010) *Plastic and Reconstructive Surgery*, **5**:1383-1392 [3]Aulin C, Bergman K, Jensen-Waern M, Hedenqvist P, et al., (2011) *Journal of Tissue Engineering and Regenerative Medicine* **8**:188-96.

Development of nanoprobes for imaging foreign body reactions

J Zhou, YT Tsai, H Weng, EN Tang, D Baker, L Tang

Department of Bioengineering, University of Texas at Arlington, Arlington, Texas, USA.

INTRODUCTION: Material implants often trigger foreign body reactions, which are accompanied with the accumulation of macrophages (MΦ) and polymorphonuclear leukocytes (PMN). Although histological staining is widely used to determine the extent of foreign body reactions, a large number of animals are needed to monitor the kinetics of inflammatory reactions. Taking advantage of recent development of *in vivo* imaging, MΦ-targeting and PMN-targeting imaging probes were developed and then tested for their ability to monitor the process of immune cell responses to biomaterial implants.

METHODS: Recent studies show that activated MΦs express high levels of folic acid receptors, which has a high affinity to folate. On the other hand, it is well established that activated PMNs have up-regulated formyl peptide receptors, which can bind to the Phe-Leu-Phe-Leu-Phe (cFLFLF) peptide without triggering cell degranulation [1,2] To image activated MΦs and PMNs, folate- and cFLFLF-conjugated near-infrared (NIR) probes were fabricated by covalently linking peptide ligands with NIR dye-labeling 8-armed PEG core as described in previous publication. [1] The ability of these probes to image immune cells and to quantify the extent of foreign body reactions was investigated both *in vitro* and *in vivo.*

RESULTS: We found that the folate-conjugated (MΦ-targeting) probes had significantly higher affinity (9X) to activated MΦs than control probes *in vitro* (Fig. 1A). When incubated with peritoneal lavage cells, cFLFLF-conjugated probes were found to have high affinity to some cells, which were also stained positive with an anti-PMN antibody (Fig. 1B). Only activated PMNs (stained with antibody, green color) were associated with the PMN-targeting probe (red color). The ability of these two probes to quantify the degree of implant-associated inflammatory responses was tested *in vivo*. Briefly, Balb/C mice (20 gram body weight) were subcutaneously implanted with particles made of poly-lactic acid (PLA) (known to prompt strong inflammation), polyethylene glycol (PEG) particles (a biocompatible material), and saline (as a negative control) for 24 hours prior to probe injection. After probe administration for 18 hours, the animal imaging analyses were carried out using the KODAK In vivo FX Pro (Kodak, USA). As expected, we find that the accumulation of MΦ-targeting and PMN-targeting probes at the implant sites in the following: PLA > PEG > saline (Fig 1C-D).

Fig. 1: In vitro tests to assess the probe (A) to have high affinity to activated MΦ and (B) to be able to

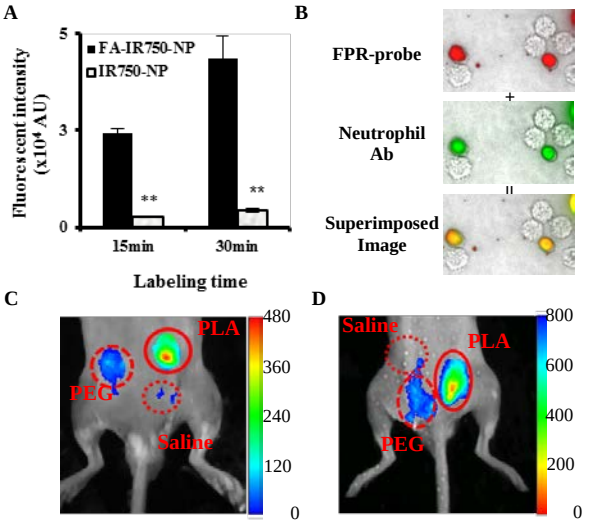

identify activated PMN. The ability of these probes to monitor foreign body reactions was assessed using subcutaneous biomaterial implant model. Whole body fluorescent images show that a stronger accumulation of (C) MΦ-targeting probes and (D) PMN-targeting probes at the PLA implant sites than PEG implant sites and saline controls.

DISCUSSION & CONCLUSIONS: These results demonstrate that the MΦ-targeting and PMN-targeting imaging probes can be fabricated to monitor MΦ's and PMN's responses to biomaterial implants. These probes may be used to assess the dynamic of foreign body reactions real-time without the need for large number of animals.

REFERENCES: [1] J. Zhou, Y.T. Tsai, H. Weng, D. W. Baker, L. Tang (2011) *Biomaterials* **32**: 9383-90. [2] Y. Zhang, B. Kundu, K.D. Fairchild, L. Locke, S.S. Berr, J. Linden and D. Pan (2007) *Bioorg. Med. Chem. Lett.* **17**: 6876-78.

ACKNOWLEDGEMENTS: This work was supported by NIH RO1 EB007271.

Towards load-bearing bone graft substitutes: synthesis of hexagonal β-tricalcium phosphate platelets with controlled size

M Bohner[1], L Galea[1], N Doebelin[2]

[1] *RMS Foundation, Bischmattstrasse 12, 2544 Bettlach, CH.*

INTRODUCTION: In the field of bone graft substitution, there are a few challenges remaining. One of them is the absence of materials associating resorbability, biocompatibility and load-bearing properties [1]. Several classes of materials partially fulfil these conditions. For example, polylactides and Mg alloys can be used to mechanically stabilize bone defects, but their poor biocompatibility limits their use to small implants, e.g. for maxillofacial applications. Processed cortical bone allografts, stainless steel and Ti alloys can also be used in such applications, but their very slow resorption rate may lead to mechanical instabilities or even fatigue fractures. Many ceramic based bone graft substitutes combine resorption and biocompatibility, but their inherent brittleness limits their use to mechanically stable bone defects.

One potential solution to this dilemma is to copy the strategy used in natural materials such as bone and nacre: ceramic single crystals with controlled size and shape are used to reinforce a soft but resilient organic matrix. The use of single crystals with a size below a critical value warrants mechanical properties close to the theoretical mechanical properties, whereas their high aspect ratio (10 for nacre) provides an ideal toughening effect.

Two approaches are generally used for the synthesis of nacre-like structure: (i) a bottom-up "layer-by-layer approach", and (ii) a two step approach during which a perfectly structured material (e.g. the ceramic) is reinforced by infiltration of a second material (e.g. the polymer / organic phase). Unfortunately, the synthesis of artificial nacre using these two approaches remains a challenge. Part of these difficulties stems from the absence of suitable building blocks: to the best of our knowledge, there is no study describing the synthesis of a resorbable ceramic (e.g. calcium carbonate, calcium phosphate) with controlled composition, size, shape and degree of agglomeration. Therefore, our interest was raised by a study of Tao et al [2], describing the synthesis of non-agglomerated hexagonal β-tricalcium phosphate single crystals. These crystals had a diameter inferior to 1 μm and a thickness close to 300 nm.

This presentation aims at discussing the various aspects described in this abstract. A focus is set on the synthesis of β-TCP platelets (Fig 1), the theoretical predictions of an ideal aspect ratio, and first approaches to produce ordered composites.

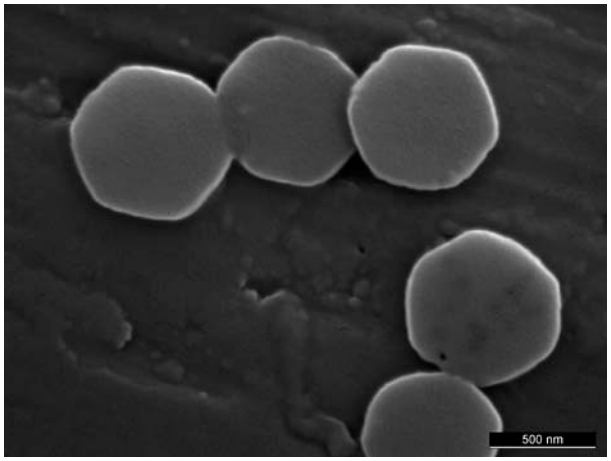

Fig. 1: β-TCP platelets obtained with the method of Tao et al [2].

REFERENCES: [1] M. Bohner, L. Galea, N. Doebelin (2012) *J Eur Ceram Soc* In Press. [2] J. Tao et al *Cryst Growth Des* (2009), 9(7): 3154-60.

ACKNOWLEDGEMENTS: The authors kindly acknowledge the financial support of Mathys Ltd.

Biomimetic processing of calcium phosphates: tailoring porosity from the nano- to the macroscale for bone regeneration and drug delivery applications

MP Ginebra[1,2], C Canal[1,2], E Montufar[1,2,3], M Espanol[1,2]

[1] Biomaterials, Biomechanics and Tissue Engineering Group. Dept. of Materials Science and Metallurgy, Technical University of Catalonia, Barcelona, Spain. [2] Biomedical Research Networking Center in Bioengineering, Biomaterials, and Nanomedicine (CIBER-BBN), Spain. [3]Institute for Bioengineering of Catalonia, Barcelona, Spain.

Calcium phosphate (CaP) materials have long been used as bone substitutes, owing to their excellent biological behaviour and their biocompatibility, bioactivity and osteoconductivity. Putting aside all these advantages, one property that is arising great interest among these materials is their porosity. Porosity at any level ranging from the nano- to the macro-scale has been shown to control various biological mechanisms which greatly determine the bone healing response and the regeneration capability of the material. While interconnected macropores are needed for bone ingrowth, nano and micropores affect the protein pattern at the surface of the material and, in turn, cell interaction. Moreover, in the design of biomaterials for controlled drug delivery in the musculoskeletal system, where CaP have much to contribute, control of the porosity is also crucial.

One type of CaP of particular interest are calcium phosphate cements (CPCs). Cements are self-setting materials which are formed by mixing a solid phase with a liquid phase. The setting reaction allows obtaining hydrated compounds with morphologies and compositions very similar to the calcium phosphates found in the mineralized tissues. Moreover, the entangled network of crystals that are formed via cementitious reactions do not simply mimic the composition of the mineral phase in bone but they also generate porous structures with specific nano/micro porosities [1]. The intrinsic porosity of CPCs allows the incorporation of drugs, biologically active molecules or even cells, without thermal denaturalization or loss of activity during preparation or implantation. Thus, CPCs emerge as potential controlled drug delivery systems for local treatment [2]. The incorporation of active molecules can be used to increase the bone regeneration capacity of the material or to target specific skeletal disorders or pathologies. Moreover, these materials are injectable, making them very attractive for minimally invasive surgery. Although these features have often been the rationale for using them as biomaterials, one additional advantage of CPCs is their simplicity in processing, which makes them extremely versatile and compatible with many techniques [3].

The combination of CPCs with surface active molecules, such as low molecular weight surfactants or some proteins, has allowed obtaining CPC foams, with interconnected macroporosity and controlled textural properties, with porosities ranging from the nano- to the macroscale (Fig. 1). The increased permeability of these structures allows designing drug delivery systems with enhanced release kinetics and higher degradability. Macroporosity provides also an optimum support for cell and tissue penetration, thus improving bone regeneration.

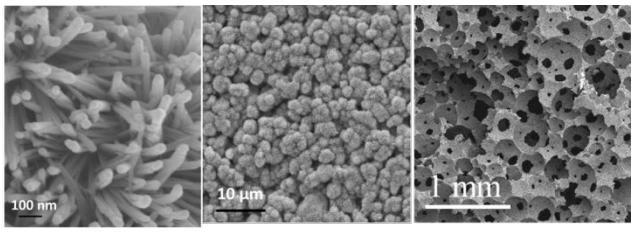

Fig.1: CPCs offer the possibility to modulate the porosity at different scales

In a different approach, porous microspheres with controlled micro and nanostructures can be obtained by emulsion of CPCs in hydrophobic liquids, which can be used as cell microcarriers or as drug release systems [4].

In summary, CPCs provide an excellent platform for the combination of the whole range of porosities, from the nano to the macro level, which can allow orchestrating specific biological events.

REFERENCES: [1]M. Espanol, RA Perez, EB Montufar, et al (2009) *Acta Biomater* **5**:2752–62. [2]MP Ginebra, C Canal, M Espanol (2012) *Adv. Drug Deliv. Rev*. doi:10.1016/j.addr.2012.01.008 [3]MP Ginebra, M Espanol, EB Montufar et al (2010) *Acta Biomater* **6:**2863–73. [4]RA Perez, S Del Valle, G Altankov et al (2011) *J Biomed Mater Res B: Appl Biomater* **97**:156–66.

Bone tissue response to topographically nanopatterned model implants

S Petronis[1,2], H Agheli[2,3], A Ballo[2,4], O Omar[2,4], L Emanuelsson[2,4], J Lausmaa[1,2], P Thomsen[2,4]

[1]*Department of Chemistry and Materials, SP Technical Research Institute of Sweden, Borås, SE.* [2]*BIOMATCELL, VINN Excellence Center of Biomaterials and Cell Therapy, Gothenburg, SE.* [3]*Applied Physics, Chalmers University of Technology, Gothenburg, SE.* [4]*Department of Biomaterials, University of Gothenburg, Gothenburg, SE.*

INTRODUCTION: Previously, we have developed a model system which enables systematic studies of nanotopography effects on implant osseointegration in rat tibia [1]. It was demonstrated, that superposition of 60-nm semispherical nanostructures on the microscale topography of machined Ti implant increased the extent of bone development when compared to just machined surface or 110 and 220 nm nanopatterns of identical chemical composition. The distribution density and surface curvature of the nanostructures were identified as important topographic parameters causing the observed tissue response. In this study, we further investigate the mechanistic details of the tissue response to nanotopography which led to the improved osseointegration.

METHODS: Colloidal lithography [1,2] was used to nanopattern machined cylindrical titanium implants by semispherical nanobumps of 60 nm diameter (*Fig.1*). The machined titanium implants without nanobumps were used as a control. Both types of implants were sputter-coated with 20 nm titanium layer to assure identical chemical composition of the surfaces. The implants were placed randomly into both tibias of 24 male Sprague-Dawley rats. After 3, 6 and 28 days, the implants were retrieved for analysis of the implant surface and the surrounding tissues. SEM and EDX were used to analyze the organic and inorganic matrix formed in direct contact to the implant surfaces. Immunohistochemistry and qPCR were used to investigate the type and activity of cells and tissues in vicinity to the implants.

RESULTS: SEM revealed increasing matrix formation on both type of implants over time. Ca/P ratio reached 0.9-1.5 after 28 days, which is in agreement to values determined in natural bone [3]. Furthermore, measured CaP content was higher on the nanopatterned implant compared to control (*Fig. 2*). Gene expression analysis showed no differences between machined and nanopatterned surfaces regarding the osteogenic differentiation and bone formation genes (ALP, OC and Runx2). Nevertheless, the nanopatterned surface was associated with lower expression of TNF-α (marker of inflammation) after 3 days and cathepsin K (marker for bone resorption activation) after 6 days.

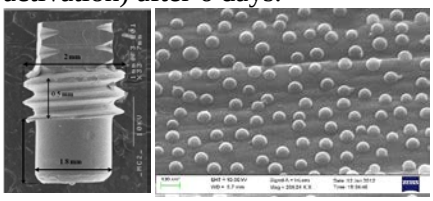

Fig. 1: SEM image of implant design and nanopatterned surface

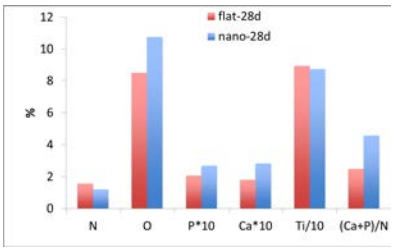

Fig 2. EDX analysis of N, O, P, Ca and Ti content on the retrieved implants after 28 days

DISCUSSION & CONCLUSIONS: Nanostructured implants induced higher amounts of mineralised matrix on the implant surface after 28 days, which supports our earlier observations of higher bone-implant contact established on the implants nanopatterned by 60 nm semispheres. As indicated by the gene expression profile, this effect might be related to the suppressed immune response towards nanostructured surface at early stages of implant healing. Such hypothesis is in agreement with immune complement activation attenuation observed on Au topographic nanopatterns *in vitro* [4].

REFERENCES: [1] A. Ballo et al (2011) *Int J Nanomedicine* **6**:3415-28. [2] P. Hanarp et al (1999) *Nanostructured Materials* **12**:429-32. [3] V. Kyriazis and M. Tzaphlidou (2004) *Sci World J* 4:1027–34. [4] M Hulander et al (2011) *Int J Nanomedicine* **6**:2653-66.

ACKNOWLEDGEMENTS: The work was supported by Biomatcell Vinn Excellence Centre.

Nano concentration of nano particles induce activation of blood cascade systems

J Hong[1], B Ekstrand-Hammarström[2], Kristina N. Ekdahl [1,3] A Bucht[2], B Nilsson[1]

[1] Department of Immunology, Genetics and Pathology, Uppsala University, Rudbeck Laboratory, Uppsala Sweden. [2] Division of CBRN Defence and Security, Swedish Defence Research Agency. [3] School of Natural Sciences, Linnæus University, SE-391 82 Kalmar, Sweden.

INTRODUCTION: Inhaled nanosized particles (NPs) are concerned as a contributing factor to the unfavourable health effects of air pollution, particularly in individuals with asthma or cardiovascular disease [1]. Reactions towards NPs are described in terms of oxidative stress, inflammation, and procoagulant effects [1]. Nanosized titanium dioxide (TiO_2) is produced in increasing amounts for energy and environmental applications, as well as use in pigments and medical implants. Recently it was shown that TiO_2 NPs when inhaled by rats causes activation of both innate and adaptive immune systems [2]. There is concern that NPs can be transported from the lungs into the blood stream due to increased endothelial permeability by the lung inflammation [3]. In addition it is previously shown that titanium is a highly thrombogenic material [4].

The aim of this study was to evaluate the effect of TiO_2 nano particles on blood cascade systems.

METHODS: Tubes with a internal diameter of 4 mm and a length of 20 cm with a total volume of 2,5ml coated with Corline immobilized heparin were used. Tubes were then filled with 2.0ml of freshly drawn blood with no anti-coagulant, from healthy donors with heparinized equipment. Increasing amounts of TiO_2 NPs (P25) suspended in PBS and sonicated were added to the loops. Final concentration of NPs ranged between 10ng/ml to 5µg/ml blood. The loops were then closed into circuits with connectors of stainless steel coated with immobilized heparin (Chandler loop). As a negative control we used heparinisized PVC tubes with addition of only PBS. The loops were rotated for 60 min vertically at 20 rpm in a 37°C water bath. The blood was then collected in EDTA and citrate analyzed for consumption of platelets, platelet granule release (thrombospondin), thrombin-antithrombin (TAT) generation, contact activation of coagulation (FXIIa-C1INH, FXIIa-AT, FXIa-C1INH and FXIa-AT) and complement activation (C3a and sC5b-9).

RESULTS: Preliminary results show that the introduction of nano particles at an amount of 100ng/ml to the system causes a significant ($p<0.05$) depletion of platelets compared to PBS control. In addition there is an enhanced activation of contact activation with increasing amounts of particles. In contrast the complement activation did not show clear difference when nanoparticles were added to the loops. One observation is that there is a great variation of thrombogenic response between individual blood donors.

DISCUSSION & CONCLUSIONS: We show that the Chandler loop blood model is a versatile tool for detecting the impact of small amounts of NPs on blood cascade systems. Even small amounts of nanoparticles cause activation of the contact activation pathway of coagulation followed by thrombin generation and subsequent platelet depletion. The observed inter individual variation may have implication for identification of individuals susceptible for high risk when exposed to airborne particles.

REFERENCES: [1] N.L. Mills, H. Törnqvist, M.C. Gonzalez et al (2007) *New Engl J Med* **357**:1075–82. [2] Å. Gustafsson, E. Lindstedt, L.S. Elfsmark et al (2011) *J Immunotoxicol* **8**(2):111-21. [3] A. Furuyama, S. Kanno, T. Kobayashi, S. Hirano et al (2009) *Arch Toxicol* **83**(5):429-37. [4] J. Hong, J. Andersson, K. Nilsson-Ekdahl et al (1999) *Thromb Haemost.* **82**(1):58-64.

ACKNOWLEDGEMENTS: This work was supported by grants from the Swedish Research Council (VR) 2009-4675, 2009-4462, the Swedish Research Council, and the Swedish Research Council/SSF/Vinnova contract grant number 60761701, and by faculty grants from the Linnæus University.

ECM-inspired Nanopatterns for Biomaterial Research

A.Lundgren, M.Hulander, H.Elwing, M.Berglin

Gothenburg University, Gothenburg, Sweden.

INTRODUCTION: Cellular organization *in vivo* is critically dependent on biochemical nanopatterns, the extracellular matrix (ECM) being an excellent example. For example, it is known that growth factors form gradients by binding to heparin present in ECM, thereby inducing a directed angiogenesis. [1] For biomaterial research, understanding the mechanisms that govern cell function and location is very important. Patterned substrates with composition and organization at the single protein level, similar to the ECM are therefore attractive for *in vitro* cell studies.

METHODS: A simplistic method for preparation of (bio)chemical nano pattern in the sub-100 nanometer regime is the electro-statically restricted self-arrangement of charged gold nanoparticles adsorbing onto gold-binding substrates, e.g. dithiol modified gold surfaces. The negatively charged gold nanoparticles form short-range ordered arrays with nanoparticle separation between 5 and 75 nm depending on the ion content of the gold sol. [1,2] Also gradients with high concentration of particles at one end and low at the other end of a surface may be prepared (fig1). After assembly, particle surfaces and surrounding surfaces were modified to have different functionality (fig2). *For example*, heparin was bound to the particles, whereas surrounding surfaces was modified with RGD-peptide (fig3a). In other experiments, proteins were presented vs. non-fouling PEG (fig3b), this way creating gradients in chemical composition. Gradients with several different protein and peptide patterns were prepared and used to study adhesion, proliferation and polarization of primary human epithelial cells after 24h incubation.

RESULTS & DISCUSSION: Correlation with iSPR-data as presented in fig.3 allowed quantitative evaluation of the number of proteins or peptides needed to induce cell binding and cell-spreading respectively. In the steep gradient region cells were polarized along the gradient, indicating cell migration. Similarly, imaging SPR-data could be used to determine the critical gradient in number of proteins needed to induce cell polarization. Interestingly, co-grafting RGD-peptides with biologically active heparin, instead of non-fouling PEG, did not increase the cell-adhesion. However, a general positive effect on cell spreading, with an optimum mixing concentration was seen. This underlines the potential impact of multifunctional patterning for cell models.

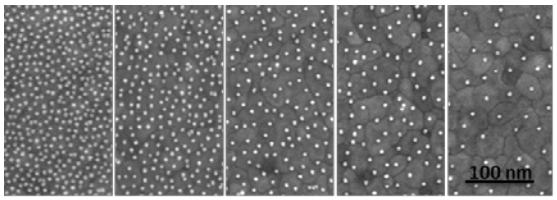

Fig. 1: SEM micrograph from a gold surface (10x10 mm) used for cell studies. 10 nm gold nanoparticles were bound in a density gradient along the surface, as shown by the micrographs taken at different positions.

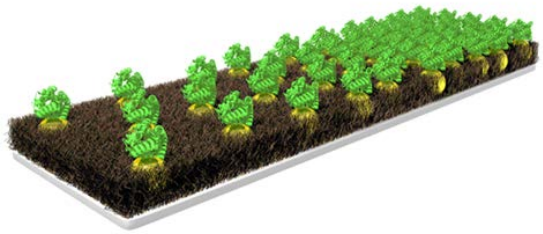

Fig. 2: Cartoon schematically describing how particles and surrounding areas can be chemically modified.

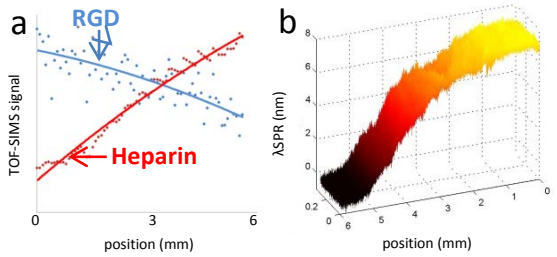

Fig. 3: (a) A gradient of Heparin presented vs. a back-ground modified with RGD-peptides measured with TOF-SIMS. (b) A gradient of protein presented vs. PEG measured with imaging SPR.

REFERENCES: [1] C. Ruhrberg et al (2002) Genes Dev. **16**:2684-98. [2] A. Lundgren et al (2008) *Nano Lett.* **8**:3989-92. [3] A. Lundgren et al (2011) *Angew. Chem. Int. Ed.* **50**:3450-53

ACKNOWLEDGEMENT: Olle Andersson is acknowledged for iSPR measurements. This research was funded by Vetenskapsrådet.

Magnetic core-shell particles for biomedical applications

T Gulin[1], A Duchanoy[1], M Lee[2], L Qian[2], H Jiang[3], Y Ma[2], H Xu[2], C Zhang[2], C Sahlgren[4], M Lindén[5], H-C Gu[2], JM Rosenholm[1]

[1] Center for Functional Materials, Laboratory of Physical Chemistry, Åbo Akademi, Turku, Finland. [2] Nano Biomedical Research Center, Med-X Institute, Shanghai Jiao Tong University, China [3] Department of Applied Physics, Aalto University, Espoo, Finland. [4] Turku Centre for Biotechnology, University of Turku and Åbo Akademi University. [5] Inorganic Chemistry II, University of Ulm, Germany.

INTRODUCTION: Magnetic nanoparticles are a major class of nanoscaled materials with the potential to revolutionize current clinical diagnostic and therapeutic techniques. The abilities of these nanodevices show much promise as contrast agents for magnetic resonance imaging (MRI), as carriers for targeted drug delivery and magnetic bioseparation. The magnetic nanoparticles can be manipulated by an external magnetic field gradient and this 'action at a distance', combined with the intrinsic penetrability of magnetic fields in to human tissue, opens up for many new bioapplications.

METHODS: Large-pore silica shells [1] were synthesized on magnetic cores [2]. The core-shell particles were further amino-functionalized [3] and different fluorophores were incorporated to render the nanoparticles suitable for fluorescence-based characterization techniques. Magnetically enhanced cellular uptake, as well as magnetic resonance imaging (MRI) *in vitro*, was demonstrated. Coupled to the study of the cellular uptake, also a sulfur-sulfur reduction-based release of a model compound has been demonstrated *in situ* and will be further demonstrated *in vitro*. Magnetically-aided cell separation was demonstrated with different setups for the magnetic field.

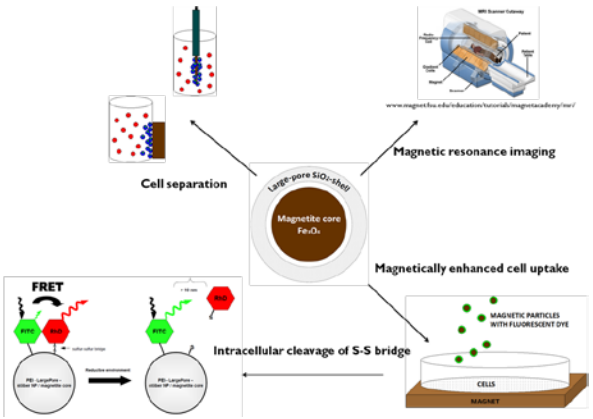

Fig. 1: The studied bioapplications of the magnetic nanoparticles.

RESULTS: A large difference in cellular uptake efficiency of the magnetic nanoparticles of varying size and surface functionality could be observed when comparing cells which had been in contact with a magnetic field and non-magnetized cells (see figure 2). These results could be confirmed by magnetic resonance imaging, where the MRI signal intensity was much more pronounced for the magnetized cells.

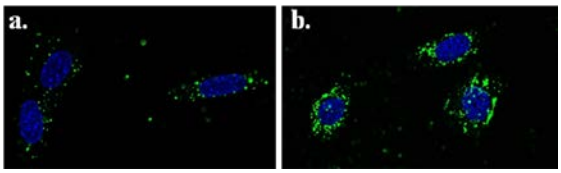

Fig. 2: NIH-3T3 cells labelled with 200 nm fluorescent (green) magnetite particles, (a) without and (b) in presence of an external magnetic field.

Larger magnetic beads (600 nm) were also readily taken up by HeLa cells. Due to the large magnetic moment of these particles, they were very effective in cell separation. Cells containing these particles could easily be separated from a mixture of different cells.

DISCUSSION & CONCLUSIONS: Silica-magnetite composite particles were proven to be useful for a range of different bio-related applications. An external magnetic field could be used to enhance the uptake of magnetic particles of variable size into different cell lines. Once inside the cell, redox-sensitive coupling of bioactive "satellite" entities could provide for selective and/or efficient transport of cell-impermeable biomolecules into specific cell lines (by magnetic targeting).

REFERENCES: [1] J. Rosenholm, J. Zhang, S. Wei, H. Gu (2011) *Microp Mesop Mat* **145**:14-20. [2] H. Xu, L. Cui, N. Tong, H. Gu (2006) *J Am Chem Soc* **128**: 15582-83. [3] J. Rosenholm, M. Lindén (2007) *M Chem Mater* **19**: 5023-34.

Recombinant spider silk with IgG-binding capacity used for cell capture

R Jansson[1], U Johansson[1], M Widhe[1], A Rising[1,2], P-Å Nygren[3], J Johansson[1,2], M Hedhammar[1]

[1] Department of Anatomy, Physiology and Biochemistry, Swedish University of Agricultural Sciences, Uppsala, Sweden. [2] Department of Neurobiology, Care Science and Society, Karolinska Institutet, Stockholm, Sweden. [3] Department of Molecular Biotechnology, Royal Institute of Technology, Stockholm, Sweden.

INTRODUCTION: Spider silk has for a long time been considered as an interesting candidate for novel biomaterials, with proposed applications in medicine and biotechnology. The great potential of spider silk mainly originates from its high mechanical strength, light weight and observed biocompatibility. However, recombinant production of spider silk has proven difficult, mainly due to the long, repetitive and aggregation-prone sequence of spider silk proteins [1].

Our group has managed to clone and express a recombinant spider silk protein, 4RepCT, which self-assembles into macroscopic fibres under physiological-like conditions [2]. Recently, we also functionalised self-assembled 4RepCT fibres in order to conduct electricity [3]. In the present study, 4RepCT was fused to the Z domain, an engineered version of the immunoglobulin G (IgG) binding domain B of staphylococcal protein A [4]. This fusion resulted in a recombinant spider silk protein, Z-4RepCT, able to bind IgG in both fibre and film format. Moreover, IgG-coated films and fibres of Z-4RepCT were assessed for the ability to capture lymphocytic cells.

METHODS: A Z-4RepCT construct was created by fusion of the Z domain to 4RepCT on the DNA level. The fusion protein was then expressed in *Escherichia coli*, purified and allowed to form fibres and films. Next, fibres and films were allowed to bind the Fc (fragment, crystallisable) region of fluorescently labelled IgG, via the Z domain. Bound IgGs, directed towards the CD3 molecule of human T lymphocytes, were then exposed to isolated lymphocytes. Captured cells were stained with DAPI nucleic acid stain. Fibres and films were assessed for IgG and cell binding using fluorescence microscopy. 4RepCT without Z was used as control.

RESULTS: Fluorescence microscopy revealed that both fibres and films of Z-4RepCT bound IgG, while fibres and films of 4RepCT without Z did not bind IgG (*Fig. 1A-B*). Furthermore, IgG-coated fibres and films of Z-4RepCT were able to bind lymphocytic cells, whereas no cell binding was observed for 4RepCT (*Fig. 1C-D*).

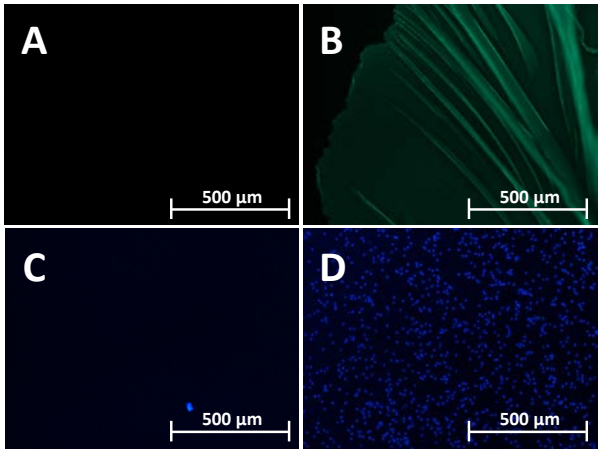

Fig. 1: Fluorescence micrographs showing binding of fluorescently labelled IgG to 4RepCT and Z-4RepCT films (A and B, respectively), and captured lymphocytes onto IgG-coated 4RepCT and Z-4RepCT films (C and D, respectively).

DISCUSSION & CONCLUSIONS: Here we report on the expression and purification of the recombinant spider silk-Z fusion protein Z-4RepCT. Both the silk-like properties of 4RepCT and the IgG-binding ability of the Z domain are retained in fibres and films of Z-4RepCT. Moreover, initial data showed that IgG-coated Z-4RepCT films and fibres have the ability to capture lymphocytic cells, although the binding specificity has to be further investigated. In general, Z-4RepCT fibres and films could be decorated with IgG directed towards any suitable target.

REFERENCES: [1] A. Rising, M. Widhe, J. Johansson, et al (2011) *Cell Mol Life Sci* **68**:169-84. [2] M. Stark, S. Grip, A. Rising, et al (2007) *Biomacromolecules* **8**:1695-1701. [3] C. Müller, R. Jansson, A. Elfwing, et al (2011) *J Mater Chem* **21**:2909-15. [4] B. Nilsson, T. Moks, B. Jansson, et al (1987) *Protein Eng* **1**:107-13.

ACKNOWLEDGEMENTS: The authors would like to acknowledge Vinnova, Formas and The Swedish Research Council for funding.

Fibria-Mediated Adhesion of E.Coli to Material Surfaces

A.Lundgren, M.Hulander, H.Elwing, M.Berglin

Gothenburg University, Gothenburg, Sweden.

INTRODUCTION: Invasion of *E. coli* (G- rods) is a common reason to catheter associated infections. It is generally believed that type 1 fimbria of *E. coli* is an important virulence factor due to the presence of FimH, a mannose binding protein at the tip of the fimbria; it seems that *E. coli* uses the Type 1 fimbria to attach to host cells, e.g. epithelial cells in the urinary tract. However, a topic of discussion has also been the involvement of fimbriae for surface adhesion in general.

METHODS: To examine this, gold surfaces coated with dithiol were modified with 10 nm gold nanoparticles; forming a gradient in nanoparticle density along the 1 cm long surface, see fig. 1. The distance between the particles was controlled by the ionic strength of the gold sol during particle adsorption as reported previously. [1] After binding, the particles were modified with different thiols to become either hydrophobic (general adhesive), to display mannose (pos. control for FimH binding) or to display a hydrophilic mannose analogue (neg. control). Areas surrounding the particles were blocked with non-fouling PEG, thereby creating a ***gradient in number*** of 10 nm adhesive patches. [2] Additionally, gradient surfaces were also prepared where PEG was bound as a corona on the particles, and surrounding areas were made hydrophobic. These surfaces constitute a ***gradient in size*** of the adhesive patch, ranging from approx. 50 to 0 nm. Contact angle at all positions of the gradients were measured using the Wilhelmy plate technique. Bacterial adhesion and desorption experiment were performed using a simple laminar flow system where bacteria were allowed to adsorb under static conditions and then rinsed off under moderate flow.

RESULTS & DISCUSSION: On ***gradients in number*** of hydrophobic or mannose-modified 10 nm particles, bacteria bound in stoichiometric relation to particle number. The formed bonds seemed fairly stable towards flow pressure. Thus, we suggest that bacteria mainly bind to these surfaces via fimbriae. [3] In contrast, on ***gradients in size*** of hydrophobic patches, bacteria bound in three distinct levels: For particle separation >40nm, very high binding was observed, however this binding was sensitive to flow, indicating physisorption. For smaller particle separation, lower but stronger binding was observed, as explained in fig3. Together our results indicate a role for fimbriae in establishing strong bonds to surfaces, also when only small patches are available. We also note that *E. coli* binding was more dependent on molecular nano-arrangement than water contact angle.

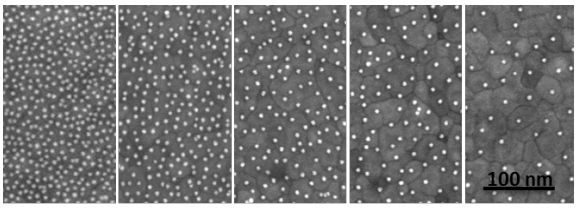

Fig. 1: SEM micrograph from a gold surface (10x10 mm) used for adhesion experiments. 10 nm gold nanoparticles were bound in a density gradient along the surface, as shown by the micrographs taken at different positions.

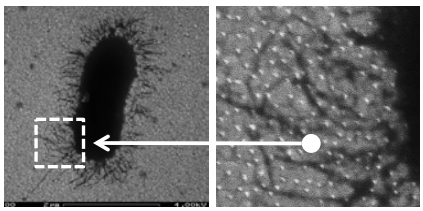

Fig. 2: "Footprint" of E. Coli on nano-patterned surface.

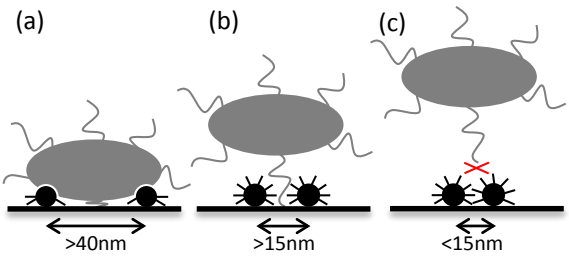

Fig. 3: Cartoon (not to scale) illustrating the different binding observed on a gradient in size of hydrophobic patches between PEG-modified nanoparticles; (a) mainly physisorption, (b)mainly fimbria mediated, (c) no binding.

REFERENCES: [1] A. Lundgren et al (2008) *Nano Lett.* **8**:3989-92. [2] A. Lundgren et al (2011) *Angew. Chem. Int. Ed.* **50**:3450-53 [3] E. Sokurenko (2008) *Cell Host Microbe*. **4**: 314–323

Vascular repair by anchoring of a macromolecular heparin conjugate

S Nordling[1], J Hong[1], B Nilsson[1], R Larsson[1], P.U Magnusson[1]

[1] *Department of Immunology, Genetics and Pathology, Uppsala University, The Rudbeck Laboratory, Dag Hammarskjolds vag 20, SE-751 85 Uppsala, Sweden*

INTRODUCTION: A macromolecular conjugate of heparin (Corline Heparin Conjugate, CHC) has successfully been utilized for preparing artificial and biological surfaces with immobilized heparin by implementing multi-step procedures [1, 2]. CHC is composed of approximately seventy heparin molecules covalently linked by a hetero-bifunctional coupling reagent to a linear aliphatic backbone. Consequently, due to its multiple binding sites, CHC exerts enhanced binding to substrates displaying heparin affinity concomitant with the presentation of free heparin chains available for interaction with cofactors such as antithrombin.

METHODS & RESULTS: We have earlier published results of CHC utilized in combination with endothelial cells, which show the capacity of CHC to bind vascular endothelial growth factor (VEGF) and how this affects endothelial cell function [3]. The present study is aimed at investigating the capacity of CHC to interact and bind directly towards basement membrane proteins such as fibrin and collagen. Here we show that there is, indeed, a direct interaction between the CHC and the basement membrane proteins and that such binding significantly abrogates the inherent thrombo-genicity of collagen.

In a Chandler loop model, in which PVC tubings were pre-coated with collagen, we show that the thrombogenicity of collagen is unaffected by exposure to heparin but is significantly abrogated by allowing CHC to bind to collagen prior to blood contact. Using human blood, collagen-coated tubings (with or without heparin treatment) induced severe clotting, whereas collagen-coated tubings treated with CHC did not induce any clotting during one hour rotation with a platelet count of more than 90% of the baseline level. Parameters for activation of coagulation and complement (thrombin antithrombin (TAT), C3a and C5b-9) were significantly reduced.

In a wound assay where primary human umbilical vein endothelial cells (HUVEC) are cultured on collagen coated glass slides, a scratch (i.e. wound) is created in the confluent endothelial cell layer exposing the collagen surface. We show that CHC can bind towards the exposed collagen surface of the wound in a direct manner. By combining the wound assay with our newly developed blood endothelial cell chamber model we present distinct binding of platelets, as detected by immunofluorescent staining of P-selectin, towards the exposed collagen surface. However, when the HUVEC and uncovered collagen alike are coated with CHC the adherence of platelets is barely noticeable after 30 and 60 minutes of incubation with blood. Furthermore, plasma samples prepared from the blood exhibit decreased thrombospondin-1 and TAT following CHC treatment, suggesting reduced activation of the platelets and less pro-thrombotic activity, respectively.

CONCLUSIONS: This study demonstrates the feasibility of the heparin conjugate to repair a damaged vasculature such as in the scenario of a donated organ exposed to ischemia, creating a less reactive vasculature upon reperfusion during transplantation.

REFERENCES: [1] M. Johnell et. al. (2002) *J Thoracic Cardiovasc Surg* **124**: 321-32. [2] S. Cabric etal (2007) *Diabetes* **56**: 2008-15 [3] S. Cabric et al (2010) *Tissue Eng Part A*, **16**: 961-70.

ACKNOWLEDGEMENTS: This study was supported by grants from the Swedish Research Council (90293501, A0290401, A0290402, 2009-4675, 2009-4462), the Swedish Foundation for Strategic Research and VINNOVA (6076170, 60761701), the NovoNordisk Foundation and Barndiabetesfonden (Children's Diabetes Association).

Tissue engineering of bladder wall patch at the surgical table

F Ajalloueian[1,2], S Zeiai[3,4], R Rojas[1], M Fossum[3,4], J Hilborn[1],

[1] *Department of Materials Chemistry, Uppsala University, Uppsala, Sweden ,[2] Textile Department Isfahan University of Technology, Isfahan, Iran. [3] Department of Women's and Children's Health, Karolinska Institutet, Stockholm, Sweden [4] Department of Paediatric Surgery, Astrid Lindgren Children's Hospital, Karolinska University Hospital, Stockholm, Sweden*

INTRODUCTION: Bladder tissue regeneration has attracted a lot of attention during recent years. Culturing autologous urothelial cells and transplanting them can be considered as an appropriate method to restore bladder tissue [1]. However, draw-backs include the demand of in-house cell culture facilities, laborious and time consuming procedures which limits the use in ordinary surgical units. Bladder mucosa tissue can be considered as an alternative to in vitro culturing of urothelial cells [2]. Despite some success with this technique, the lack of mechanical support has prevented this technique to move forward. In this study, we have integrated a polycaprolactone (PCL)-knitted mesh within two plastic compressed collagen gels mixed with bladder mucosa tissue as a hybrid scaffold. The aim of this study was to construct transplants with autologous proliferating cells that could be used in bladder tissue regeneration treatments.

METHODS: Type I Collagen gel formation and plastic compression of the construct including a PCL knitted fabric between two cubes of collagen gel was carried out by a technique described previously [3]. Bladder mucosa was mechanically separated from an excised pig bladder and minced to obtain tissue particles with dimensions around 0.04 mm^2. Minced tissue seeding was done in two different ways: either inside and on top of the hybrid structure "Mixed method" or only on top "Top method". The scaffolds containing the minced tissue were cut and cultured in 12 well plates. Plates were incubated at specific culture conditions with cell culture medium to stimulate proliferation and analyzed at 2, 4, and 6 weeks in respect to morphology, histology and scanning electron microscopy (SEM) imaging.

RESULTS: Our preliminary studies showed successful proliferation of urothelial cells when minced tissue was placed only on top (Fig.1), while no viability or growth was seen in the "Mixed method".

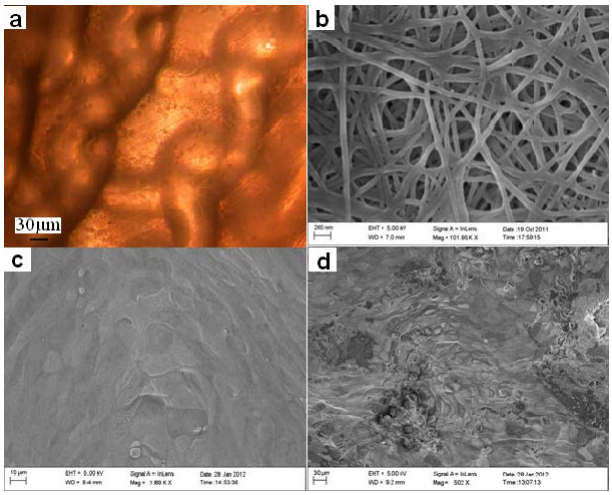

Fig. 1: Phase contrast microscopy and SEM images of minced tissue particles seeded in hybrid scaffolds: (a) microscopy at 4 weeks, (b) SEM of the scaffold with no transplanted tissue, (c) SEM with confluent cells at 4 weeks, (d) SEM with multi-layered cells at 6 weeks in cell culture

DISCUSSION & CONCLUSIONS: As demonstrated in Fig.1, cells can migrate and proliferate from the minced tissue particles that were incorporated in the hybrid structure to the surface of the scaffold. The cells are viable and proliferative with morphological features characteristic of urothelial cells. After four weeks, the hybrid scaffold is confluent, while at 6 weeks a multi-layered confluent urothelium has been formed. We conclude that such a hybrid construct can be a future approach for bladder augmentation purposes. By doing this, an in vivo cell expansion could be established without the need for conventional in vitro cell culturing. The method is simple, can be used in a one-staged procedure and in ordinary sterile surgical unit conditions.

REFERENCES: [1] A. Atala, S.B. Bauer, S. Soker et al (2006) *Lancet* **367**:1241-1246. [2] M. Fossum, B. Zuhaili, J. Malte Spielmann et al. (2010) *J Urol*, **184**: 757-761, [3] R. Brown, M. Wiseman, C. Chuo, et al (2005), *Adv Funct Mater* **15**: 1762-1770.

A novel design of an artificial islet-carrier; the evaluation of islet support, adherence and function

U Johansson[1], K Åvall[2], A Rising[1,3], I Schenning[3], J Johansson[1], SV Zaitsev[2], PO Berggren[2], M Hedhammar[1]

[1]Department of Anatomy, Physiology and Biochemistry, Swedish University of Agricultural Sciences, The Biomedical Centre, Uppsala, Sweden. [2]The Rolf Luft Research Center for Diabetes and Endocrinology, Karolinska Institute, Stockholm, Sweden. [3]Spiber Technologies AB, Uppsala

INTRODUCTION: Transplantation of the islets of Langerhans is one of the most promising approaches as a widely applicable treatment for diabetes. Unfortunately currently available procedures suffer from low efficacy due to loss of function and survival of the pancreatic cells. The low success rates are incompletely understood but prior to transplantation, during islet isolation, the environment surrounding the cells is disrupted. This has been implicated as a major cause of the limited survival and function. The endocrine parts of the pancreas, unlike the exocrine part, do not produce a basement membrane of their own, indicating again that the right niche might be of importance. Therefore establishment of an environment optimized for islets is necessary both for the study and propagation of pancreatic islets, and for the design of a possible artificial, islet-carrier for transplantation. In order to do so, a highly versatile biomaterial is needed as a scaffold.

METHODS: Recently our group at the Swedish University of Agricultural Sciences has succeeded in producing recombinant spider silk, 4RepCT, under physiological conditions [1]. The 4RepCT is a strong and highly versatile material that can acquire various forms e.g. three-dimensional fiber meshes, foams or films [1-2]. This newly generated synthetic variant of spider proteins; both the wild type and variants modified by incorporation of different intergrin and laminin related cell-binding motifs (e.g RGD, IKVAV and YIGSR) were used as scaffolds to define an optimal environment for maintaining pancreatic islet function and survival after isolation. Isolated human and mouse pancreatic islets were plated onto wells coated with the 4RepCT protein in the various forms and with incorporation of the different cell-binding motifs. Islets cultured on uncoated wells served as control. The adherence to the protein was analyzed as well as insulin release and the cytoplasmic free Ca^{2+} concentration and compared to control islets.

RESULTS: The islet adherence to the 4RepCT various forms e.g. three-dimensional fiber meshes, foams or films showed that islets do adhere with an increased number to the foam structure. There is also a preferable for adherence onto the foam with RGD cell-binding motif.

The function of the adhered islets was investigated and the results show that the islets on the RGD-4RepCT release insulin equally well as control islets and show a better free cytoplasmic Ca^{2+} oscillating response after high glucose stimuli.

After long termed culture more islets on RGD-4RepCT were functional compared to control. Among and between these existing islets on the RGD-4RepCT we found outgrowth of cells and sprouts from endothelial cells following the foam structure (Figure 1).

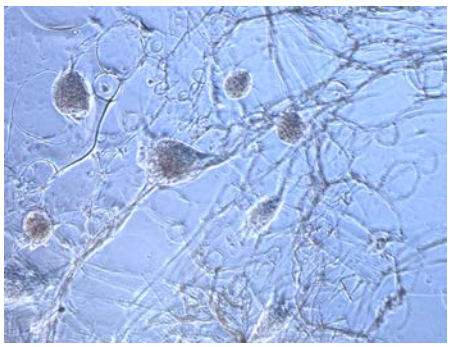

Fig. 1 Islets after long termed culture on RGD-4RepCT

DISCUSSION & CONCLUSIONS: The properties of recombinant spider silk, 4RepCT can be used as an excellent candidate in the production of scaffolds mimicking the natural cell environment thus providing support for the islets of Langerhans after isolation.

REFERENCES: [1] M. Hedhammar et al (2008) *Biochemistry* **47**(11):3407-17. [2] M. Stark et al (2007) *Biomacromolecules* **8**(5):1695-701.

ACKNOWLEDGEMENTS: The authors would like to thank Vinnova and Barndiabetesfonden for providing financial support to this project.

Combination of bioactivity, antibacterial properties and controlled drug delivery in one chemically bonded bioceramic material

L. Hermansson[1] and J. Lööf[1]

[1]*Doxa AB, Axel Johanssons gata 4-6, SE-75451 Uppsala*

INTRODUCTION: The paper describes characteristics of a Ca-aluminate (CA) based biomaterial with focus on the nanostructure. This opens up for some specific applications related to dental applications where anti-bacterial and bacteriostatic aspects are of importance. Nano-size porosity is essential also for carriers for controlled drug delivery.

METHODS: Phases and microstructures were evaluated using SEM, TEM, HRTEM, XRD, XPS and STEM with EDX. Compressive and flexure strength, Young´s modulus, fracture toughness as well as chemical and wear resistance were studied using methods presented in details in [1-2]. *In vitro* bioactivity was evaluated using ISO standard 23317, and bacterial leakage and antibacterial properties using the direct contact test [3].

RESULTS: Precipitation of nanocrystals in the CA-system results in complete cavity/void filling with low porosity. The nano-crystals (10-40 nm crystals with nanopores 1-3 nm) bond to surrounding implant materials and to tissues. The nanostructure influences the properties positively, and yield biomaterials for load-bearing applications [1-2]. Table 1 below summarizes physical properties of the CA-based biomaterial.

Table 1. Mean values of fundamental properties of Ca-aluminate based biomaterial.

Property	Typical value
Compression strength	200 MPa
Young's modulus	10 GPa
Flexural strength	45 MPa
Fracture toughness	0.7 $MPam^{1/2}$
Total porosity	< 10 %
Dimensional stability	< 0.2 % expansion
Corrosion resistance	< 0.01 mm reduction

The CA-based biomaterial exhibits antibacterial properties, and the nanostructure including nanoporosity makes the CA- material suitable as carrier for drug delivery.

DISCUSSION & CONCLUSIONS: The oral environment with high bacterial activity causes the most common dental problem - caries formation. The hydration reactions, the stability of the hydrates formed, and the nano-structure developed make the CA-material suitable as an injectable material into tissue, within odontology as cements and restoratives, and within orthopaedics as augmentation materials [4].

The bacteriostatic and antibacterial profile of the Ca-aluminate based biomaterial is ascribed the following features;
1) pH during hardening – antibacterial effect at low and high pH,
2) F-ions presence – similarity in size to hydroxyl ions,
3) The nanostructure developed – entrapping of bacteria and growth inhibition,
4) The surface – fastening of bacteria to the nano-porosity structured surface and growth inhibition, and
5) No shrinkage during hardening, just a limited expansion - contributes to nano-structural integration towards tissue and other biomaterial contacts with no bacterial leakage.

The antibacterial features of the CA based materials do not affect the established bioactivity of these biomaterials [1,4].

REFERENCES: [1]J. Loof, H. Engqvist, L. Hermansson and N.O. Ahnfelt (2004) *Key Eng Mater* **254-256**:51-54, [2]EN **29917**: 1994/ISO 9917:1991, [3]E Weiss, M. Shalhav and Z. Fuss, (1996) *Endod Dent Traumatol* **12**:179-84. [4]L. Hermansson, J. Loof, T. Jarmar (2009) *Key Eng Mater* **396-398**:183-186.

ACKNOWLEDGEMENTS: The authors express their gratitude to all the Doxa personnel for valuable input under a ten year period.

Porosity engineering in bioactive glasses: a sol-gel approach.

J Soulié[1,2], J Lao[1], E Jallot[1], JM Nedelec[2]

[1]Clermont Université, Université Blaise Pascal, CNRS/IN2P3, Laboratoire de Physique Corpusculaire, Clermont-Ferrand, France. [2]Clermont Université, ENSCCF, ICCF, Clermont-Ferrand, France

INTRODUCTION: Among the various biomaterials used as bone substitutes or as prosthesis coatings in orthopedic surgery, bioactive glasses have attracted considerable interest [1,2]. When in contact with living tissues, dissolution and precipitation take place at the material / biological medium interface, and this leads to the formation of a phosphocalcic layer. This apatite-like layer is used as a mineralization site for bone cells and finally allows an intimate chemical bond between the glass and the bone.

A fine control of bioactivity can be achieved by using soft chemistry routes to tailor the morphology and the texture of such porous bioactive glasses. Pore size can span several orders of magnitude (from nm to mm). Each level of porosity (meso, macro,…) could then have biological usefulness, like for drug delivery, vascularization of the implant, or cell adhesion for tissue engineering. With this respect, mesoporous, macroporous and glass foams have been prepared.

METHODS: Mesostructured glasses (Fig1a) have been prepared by using surfactant as directing agent whereas polystyrene opals were used as template for the production of macroporous glasses with different pore size (Figure 1b). Finally using a surfactant and adapted dispersive equipment, a air/liquid foam has been used as template to obtain monolithical glass foams (Fig 1c).

RESULTS: All samples have been characterized using a various set of techniques including gas sorption, SAXS, thermoporosimetry, helium pycnometry and SEM/TEM microscopies. The control of the pore size and pores organization is demonstrated for meso and macro porous glasses. Glass foams exhibit a multiscale porosity with a high fraction of void making these materials attractive for tissue engineering applications. Finally interactions between acellular biological medium and the different glasses have been studied for different delays. At each time period, quantitative chemical maps of samples were recorded with a micrometer resolution using Particle Induced X-ray Emission coupled to Rutherford Backscattering spectroscopy (PIXE-RBS)[3].

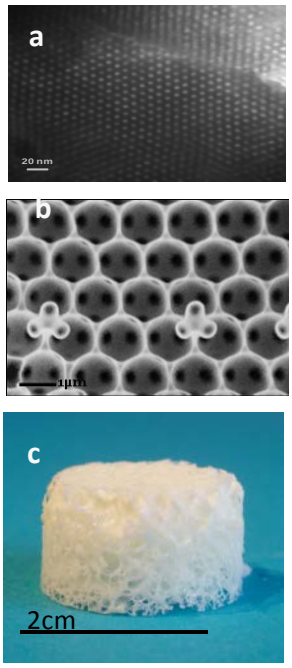

Figure 1: a) TEM image of a mesotructured bioactive glass (scale bar 20 nm), b) SEM image of a macroporous sample (scale bar 1 µm) and c) picture of a monolithic glass foam (scale bar 2cm).

This technique allows monitoring spatial and chronological evolutions of elemental concentrations, thanks to measurements with an excellent sensitivity (10^{-6} g/g). The influence of porosity on the bioactivity has been determined.

DISCUSSION & CONCLUSIONS: Comparison of mesoporous glasses exhibiting or not spatial ordering is provided. Determining parameter for the biomineralization onto macroporous glasses is found to be the size of the interconnection window and a criterion is proposed for the homogeneous nucleation for HAp in glass foams.

REFERENCES: [1]Hench, L. (1998) *J Biomed Mater Res* **41**:511-18.[2] J. Lao, E. Jallot, J.-M. Nedelec, (2008) *Chem Mat* **20**(15): 4969-73; [3] E. Jallot, O. Raissle, J. Soulie, J. Lao, G. Guibert, J.M. Nedelec (2010) *Adv Biomater* **12**(7): B245-B255. [4] E. Jallot, J. Lao, Ł. John, J. Soulié, P. Moretto, J.M. Nedelec (2010) *Appl Mater Interfaces* **2**(6): 1737-42.

Investigation of cerium substituted hydroxyapatites

L Bauermeistere[1], A Viksna[1], A Kareiva[2], KA Gross[3]

[1] Faculty of Chemistry, University of Latvia, Riga, Latvia. [2] Faculty of Chemistry, Vilnius University, Vilnius, Lithuania. [3]Institute of Biomaterials and Biomechanics, Riga Tecnical University, Riga, Latvia.

INTRODUCTION: Hydroxyapatites (HAp) are widely used in implants, but show insufficient antibacterial properties. The antibacterial properties can be improved by substituting calcium with cerium in the HAp structure [1]. Cerium is an element with low toxicity. Electronegativity and ionic radii of Ce^{3+} ion is 1.1 and 0.100 nm respectively, which are very close to the values of Ca^{2+} (1.00 and 0.101 nm). For this reason the substitution of calcium with cerium in HAp is achievable. Cerium ions in nature usually have two oxidation states – +3 and +4. Both of these oxidation states can also occur in cerium substituted HAp (Ce-HAp). This work investigates the quantitative determination of cerium content in each oxidation state by using potentiometric titration with iron ions in an acidic medium.

METHODS: Cerium substituted HAp were synthesized in the Faculty of Chemistry, Vilnius University with the sol-gel method. Four different Ce-HAp samples with total theoretical amount of 1, 3, 5 and 10 Ce wt% were produced. The total amount of Ce^{4+} ions was obtained by titrating solutions of Ce-HAp with a solution that contained Fe^{2+} ions. Meanwhile, the Ce^{3+} ion content was obtained by titrating with a solution that contained Fe^{3+} ions. The samples were prepared for titration by dissolving Ce-HAp powders in 0.1M hydrochloric acid at atmospheric pressure and in 0.5 wt% nitric acid at increased pressure and temperature. Total amount of cerium was determined using the ICP-MS method.

RESULTS: The results of total amount of cerium in Ce-HAp determined by ICP-MS, show that all of the added cerium incorporates in the HAp structure with the sol-gel route. Potentiometric titration is applicable for determination of cerium oxidation states in Ce-HAp. However, the limiting factor is the low solubility of Ce-HAp, which decreases at increasing concentrations of cerium.

Table 1. Comparison between theoretical and ICP-MS determined Ce concentration

Sample	Theoretical, wt%	ICP-MS, wt%
Ce-1	1	1.2
Ce-3	3	2.9
Ce-5	5	5.4
Ce-10	10	10.1

DISCUSSION & CONCLUSIONS: The acquired titration curves for Ce-HAp samples dissolved in 0.1M hydrochloric acid show a rapid drop of potential from 0.93 to 0.78 V at the beginning followed by a slow decrease caused by further dissolution of Ce-HAp, Fig. 1.

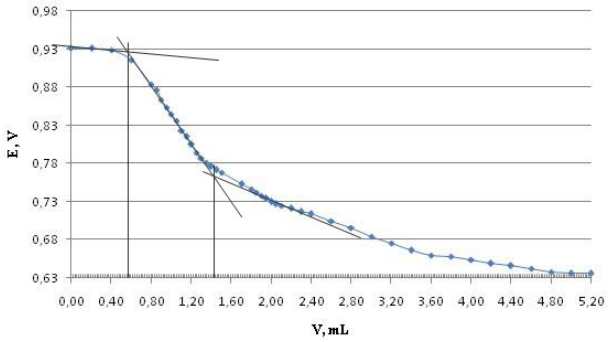

Fig.1. Titration curve for sample Ce-10 with 0.001M Fe^{2+} solution. Black lines mark a titration jump, equivalence point is at 1.11 mL.

Sintered cerium substituted apatites contain a small amount of tricalcium phosphate that increases with cerium addition. The solubility could be encouraged by heat treatment at a lower temperature, thus facilitating dissolution for the analysis of the cerium content.

The oxidation state of cerium in Ce-HAp is possible with potentiometric titration by optimizing the titration conditions (temperature, solution media) and inorganic solvents, used for dissolving the Ce-HAp.

REFERENCES: [1]Y.G. Lin et al (2007) *J Rare Earths* **25:** 452-56

ACKNOWLEDGEMENTS: Support has been provided by the Cooperation project “Nanoscaled functional materials for biotechnological and optical applications”

Preformulation of orthopaedic cements used as drug delivery systems: use of percolation theory

S Cazalbou, S Cavalie, F Brouillet, A Tourrette, P Kirilov, F Rodriguez

Université de Toulouse, CIRIMAT, UPS-INPT-CNRS, Faculté de Pharmacie, Toulouse, France

INTRODUCTION: Calcium phosphate cements (CPC) are widely used as biomaterial in clinical applications. Moreover, they can be used also as drug delivery systems to which several drug such as antibiotic, antitumor, anti-inflammatory drugs [1,2], and so on can easily be added. Nevertheless, the formulation of these new composites needs to answer the following question: "which amount of porogenic agent and which size will permit to obtain a material with interconnected pore network apt to release the totality of drug introduced?"

We propose to use the percolation theory in order to solve this problem and permit the use of new parameter (the percolation threshold) as element of preformulation of CPC.

METHODS: The calcium phosphate cements used in this study were Cementek, commercialised by Teknimed™ (France). A spherical porogenic agent containing 50 wt% of Ibuprofen were used with various amount (5, 10, 20, 30 and 40 wt%) and various granulometry (<315 µm, 400 µm<Ø<500 µm, 500<Ø<630 µm). Cement containing Ibuprofen were moulded into cylinder with 1cm diameter. *In-vitro* drug release has been performed in paddle dissolutest in tris(hydroxymethyl) amino methane buffer solution with pH=7.4 at 37°C. Ibuprofen release was quantified by UV spectroscopy.

RESULTS: The data obtained from the dissolution studies were analysed using Higuchi representation. The property, β, of each composite was calculated according to the Leuenberger and Bonny method [2]. This property derived from de diffusion coefficient of the drug. Plotting β *versus* ε, the drug percolation threshold (ε_c) can be readily calculated as the point of intersection with the abscissa (fig 1). This percolation threshold corresponds to a critical porosity, ε_c, where the pore network just begins to span the whole matrix and depends of the granulometry of the porogenic agent introduced. The percolation threshold of composites containing various diameter of porogen has been determined using the same method as describe above.

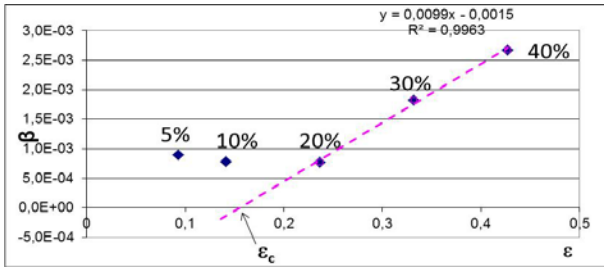

Fig 1: β parameter plotted versus total porosity ε of cements containing various amount of porogen containing Ibuprofen.

The weight percentage of porogenic agent which permit the total percolation of the composite are represented in table 1.

Table 1: percentage of porogen corresponding to the percolation threshold of composites.

Porogen diameter	ε_c [% (w/w)]
Ø<315 µm	11.2%
400 µm<Ø<500 µm	15%
500 µm <Ø<630 µm	20.1%

DISCUSSION & CONCLUSIONS: The formulation of porous cements with interconnected macropore is an important challenge for this material which contains only micropores. The determination of percolation threshold of various systems allows us to determine the amount of porogen we have to introduce in order to induce the formation of an infinite cluster which percolates the whole cement. The knowledge of this parameter can thus be used by the formulator as element for preformulation of interconnected pore cements.

REFERENCES:

[1] MP. Ginebra et al (2006) *Biomaterials* **27**:2171-77. [2] D. Yu, J. Wong, Y Matsuda, JL. Fox, WI. Higuchi, M. Otsuka (1992), *J Pharm Sci* **81**(6): 529-31. [3] J.D. Bonny, H. Leuenberger (1991) *Pharm Acta Helv* **66**:160-64.

From wet precipitation synthesis of calcium phosphates to porous ceramics

J Locs[1], V Zalite[1], A Skageris[2], L Berzina-Cimdina[1]

[1]*Riga Biomaterials Innovation and Development Centre, Riga Technical University, Riga, Latvia*
[2] *Institute of Stomatology, Riga Stradins University, Riga, Latvia*

INTRODUCTION: Calcium phosphates are very promising materials for regeneration applications in locations of damaged or resorbed areas of bone tissue due to chemical similarity to inorganic bone component, osteoconductivity and biocompatibility. One of the easiest approaches to produce calcium phosphates (hydroxyapatite (HAp and β-tricalcium phosphate (β-TCP)) is wet precipitation method that gives opportunity to modify ratio between calcium and phosphorus. Various phase compositions have influence on the solubility and bioactivity of implant materials under physiological conditions [1]. To diversify application and to improve properties of calcium phosphate ceramics, it is important to modify existing and develop new technological methods.

METHODS: Calcium phosphates were obtained by wet precipitation synthesis using calcium hydroxide ($Ca(OH)_2$) suspension and orthophosphoric acid (H_3PO_4) solution. H_3PO_4 was dropwise added to $Ca(OH)_2$ suspension while it was heated and continuously stirred. The pH value of the mixture was adjusted from 6 to 9, followed by stirring for 1 hour. Obtained precipitates were vacuum filtrated and left wet or dried overnight at 105 ^oC and then grinded into powder form. Those two kinds of precipitates were used to obtain porous ceramics by viscous ceramic mass foaming process *in situ*. Ammonium bicarbonate (NH_4HCO_3) was as pore forming agent. Glycerol was added to attain a viscous/plastic mixture. The green-bodies were sintered at 1150 ^oC for 2 hours. The morphology of the obtained ceramics was examined by field emission scanning electron microscopy (SEM) and phase and chemical composition was determined by X-ray diffractometry (XRD) and Fourier transform infrared spectrometry (FTIR). The porosity was determined with Archimedes method.

RESULTS: Phase composition and chemical structure analysis revealed that pure stoichiometric HAp, mixture of HAp and β-TCP and pure β-TCP can be obtained by wet precipitation method choosing the ending pH in range from 9 to 6. Porosity of bioceramics produced by foaming process *in situ* is 50 to 72 %. Calcium phosphate bioceramics obtained from wet precipitates or dried and grinded powder as raw material shows significantly different microstructure after sintering (see *Fig.1*).

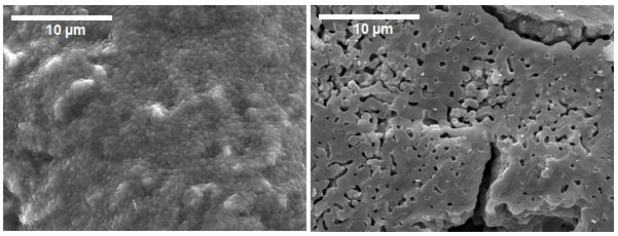

Fig. 1: SEM images of calcium phosphate fracture surface of ceramic pore wall microstructure a) ceramics obtained from wet precipitates, b) ceramics obtained from powder.

DISCUSSION & CONCLUSIONS: The pore wall microstructure of ceramics obtained using the wet precipitates as raw materials is more dense and homogenous compare to the ceramics obtained from dried powders. The difference in microstructure can be explained by avoid of agglomerate formation in case of wet precipitates, that occurs during the preparation of dried powder raw material. The preparation technology of viscous ceramic mass troubles the disintegration of dried agglomerates, what restricts the possibility to avoid the microporosity in pore walls. The use of wet precipitates for preparation of porous calcium phosphate ceramics by viscous ceramic mass foaming process *in situ* permits the formation of more dense pore walls after sintering in relatively low temperature. Such microstructures have advantages from improved mechanical point of view unless certain wall microporosity is requested for special applications like drug immobilisation or polymer impregnation.

In both cases the FTIR and XRD analysis of ceramics obtained did not showed any changes of phase or chemical composition caused by applied *in situ* foaming technology.

REFERENCES: [1]S.V.Dorozhkin (2011) *@CCAAS BIO* **1**:1-51.

ACKNOWLEDGEMENTS: This work have been done within the support of National Research programm of Latvia in materials science N^{o}4 “Novel materials and technologies for implantation and evaluation of biological tissues” V7709.

Feeding tubes for neonates – leaching of plasticizers in food simulating solutions and resulting changes in mechanical properties

HM Kopperud[1], NR Gjerdet[2]

[1] *Nordic Institute of Dental Materials (NIOM), Oslo, Norway.* [2] *Biomaterial Research Cluster, University of Bergen, Norway*

INTRODUCTION: Leaching of plasticizers, especially the phthalate DEHP (diethylhexyl phthalate), from PVC materials is well-known, and health-concerns are raised with regards to human exposure to DEHP leached from the materials [1]. Still, PVC tubes are used as feeding tubes, also for neonates and prematures. At Haukeland University Hospital (Bergen, Norway), the use of PVC-feeding tubes was questioned after observing property changes (stiffening) of the tubes upon use for some days. Recently, the DEHP plasticizer was exchanged with TOTM (trioctyl trimellitate) in some tubing materials. The aim of this study was to analyse the leaching of plasticizers from feeding tubes in combination with the evaluation of changes in mechanical properties as measured by tensile testing.

METHODS: Feeding tubes made from silicone, polyurethane or PVC were tested. The leaching of plasticizers from different tubes was measured (chromatographic analysis, GC/MS and LC/MS) in hydrophilic and lipophilic solutions to simulate gastric fluid and feeding solutions, respectively.

The property changes of the feeding tubes were investigated using a tensile test (Fig. 1) measuring the relative elongation and the elastic modulus of the feeding tubes as delivered, and after soaking in simulated feeding solution for 48 h.

RESULTS: Only minor amounts of plasticizer were found to leach into the hydrophilic solutions after 48 h. The amounts were estimated to be in the range 50-100 ng DEHP per ml solution for the PVC materials, corresponding to app. 15-30 ng/cm of tubing material. However, larger amounts of phthalates were found when soaking the tubes for 48 h in the lipophilic solutions: 833-2344 µg/ml DEHP was detected, corresponding to 1.7-4.7 mg/cm of tubing material. Feeding tubes of alternative materials (silicone and polyurethane) did not contain DEHP or TOTM.

The elastic moduli of the PVC-tubes increased with up to 80% after the tubes were soaked in lipophilic solution for 48 h. The elastic property of the other tested tubes of alternative materials (silicone and polyurethane) did not show such pronounced changes.

Fig. 1: Set-up for tensile testing of feeding tubes. Photo: NR Gjerdet.

DISCUSSION & CONCLUSIONS: The low water solubility of DEHP (reported between 1 and 1200 ng/ml) limits its migration into aqueous solutions. However, the solubility and migration into lipophilic solutions is much higher. Similar behaviour may be suggested for the alternative plasticizer TOTM. PVC tubes may thus still have unwanted property changes upon use with lipophilic solutions. Tubing materials of polyurethane or silicone seem to keep their properties after soaking in simulated feeding solutions.

REFERENCES: [1] SCENIHR (Scientific Committee on Emerging and Newly-Identified Health Risks), Scientific opinion on the safety of medical devices containing DEHP-plasticized PVC or other plasticizers on neonates and other groups possibly at risk, 6 February 2008.

ACKNOWLEDGEMENTS: The support from Haukeland University Hospital and Norwegian suppliers of feeding tubes is appreciated.

Biological performance of TiO_2 thin films loaded with alendronate and raloxifene

N Harmankaya[1*], J Karlsson[2], A Palmquist[1], M Halvarsson[3], M Andersson[2], P Tengvall[1]

[1]*Dept of Biomaterials, Sahlgrenska Academy at University of Gothenburg, Göteborg, Sweden.* [2]*Dept of Chemical and Biological Engineering.* [3]*Applied Physics, Chalmers University of Technology, Göteborg, Sweden*

INTRODUCTION: There is a great need for improved technologies for treating osteoporotic patients without systemic effect of pharmacotics and other patient groups with deficient bone growth [1]. The use of local administration of drugs is one route, where the implant surface could serve as a drug delivery vehicle [2]. In this study, mesoporous TiO_2 surfaces immobilized with the osteoporosis drugs [3], alendronate (AL), a bisphosphonate, and the estrogen receptor modulator, raloxifene (RA), have been evaluated for biological performance *in vivo* in a rat model.

METHODS:

Synthesis and drug immobilization Cubic mesoporous TiO_2 thin films were synthesized on implants of Ti using the evaporation induced self assembly (EISA) method. Implants were spin coated, which resulted in mesoporous thin films. The mesoporous TiO_2 coatings were characterized using SEM and TEM. The films were subsequently loaded with approximately 500 ng/cm^2 AL and RA (0.8 mg/ml).

Animal Experiment A total of 42 male Sprague–Dawley male rats were used for the *in vivo* evaluation. Four different groups of Ti-impants were then inserted into the einto the proximal position of the tibia in a randomized manner: mesoporous Ti control (MPAC), mesoporous Ti with AL (MPA), mesoporous Ti with RA (MPR) and hydrophobic mesoporous Ti control (MPRC). Implants were harvested after 24 hours or 28 days for analysis by qPCR, Removal Torque (RTQ) and histomorphometry.

RESULTS: Mesoporous TiO_2 films were characteerised by TEM (Fig. 1R). The oxide showed cubic arrangement with a pore size of 6 nm and layer thickness of 200 nm. The RTQ-measurements after 4 weeks showed strongest bone apposition to RA-releasing implants (41% higher than control). The RA-containing implants showed 19% higher values compared to those AL-releasing (Fig. 1L). A significantly enhanced expression of bone remodeling markers supported the above observation. Histology and histomorphometry are pending.

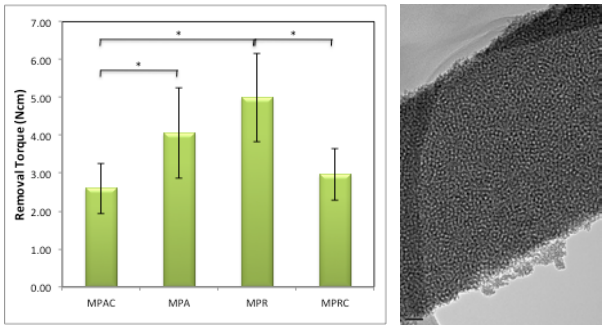

Fig. 1: Removal Torque results 28 days post-surgery showing the highest bone attachment to Raloxifene-releasing implant (left), TEM image of mesoporous Ti film (right).

DISCUSSION & CONCLUSIONS: A succesful immobilization of osseoinductive drugs into mesoporous Ti implants was achieved. Interestingly, Raloxifene promoted at 4 weeks of implantation in rat tibia a superior bone attachment in comparison to control as well as alendronate containing surfaces. A strong correlation between gene expression and measured bone strength constitutes this observation which implies a high potential applicability of mesoporous Ti-implants for local drug release.

REFERENCES: [1]O. Omar (2010) *J. Biomed Mater Res A* **92**(4): 1552-1566. [2]L. Wermelin (2008) *J. Biomed Mater Res A* **86** (1): 220-227. [3]M. Andersson (2005) *Chem. Mater.* **17**: 1409-1415.

ACKNOWLEDGEMENTS: The authors would like to thank the Materials Area of Advance at Chalmers University of Technology for providing financial support.

A new screening in-vitro method to study drug release in early development of transdermal drug delivery systems

B Cai[1], K Söderkvist[2], H Engqvist[1], S Bredenberg [1,2*]

[1] *Division for Applied Materials Science, Department of Engineering Sciences, Uppsala University, Sweden.*
[2] *Orexo AB, Uppsala, Sweden*

INTRODUCTION: Dissolution is the required characterization test to evaluate new materials for transdermal drug delivery [1]. However the conventional dissolution tests, recommended by United State Pharmacopeia (USP), cannot provide results with good correlation with *in vivo* drug release, especially for patches that mainly depends on skin resistance to drug diffusion [2]. Other dissolution methods, such as Franz diffusion cell, horizontal permeation system and flow-through diffusion cell, can provide skin resistance and penetration effects and are commonly used to study skin permeation assay [3]. However, these tests are costly and the swelling of stratum corneum increases penetration and uptake of drug [4]. The purpose of this study was to develop a novel, selective and easy-to handle *in vitro* method, which could better than the USP method imitate the diffusion and moisture level of skin. Further, this method can be especially helpful to study the drug release profiles of different transdermal formulations in early development.

METHODS: Durogesic patches of two strengths (12 and 75 µg/hr) were used as model transdermal devices in all experiments. One patch was placed on a piece of synthetic skin simulator (SSS) (2×2.5cm^2 or 5.5×6 cm^2) that was wetted with pH 6.8 buffer (300µl or 1800µl). The patch and simulator were wrapped and fixed on flat surfaces to minimize the evaporation and displacement. The patch was moved to a new wetted SSS, while the former piece was collected and soaked in pH1.0 buffer for 3 hours for complete extraction. The concentrations of fentanyl were analyzed by HPLC with UV detector in triplicates. Data was plotted as the cumulative amount of drug released as a function of time. For comparison, the patches were also tested with the standard USP dissolution bath (Sotax AT7 Smart, Sotax AG, Switzerland) equipped with mini vessels and paddles. The dissolution tests were taken place in phosphate buffer with pH 6.8 and the concentrations were measured in duplicates.

RESULTS: Durogesic patch is a controlled release transdermal device, which could release fentanyl drug at constant rate for three days. As shown in figure 1, Durogesic patches of both dosing strengths released over 90% of drug within 6 hours by the USP method. The drug release profile obtained by the SSS method was more comparable with the stated clinical release. The standard deviation (denoted as error bars in figure 1) indicated that the SSS method had small variations between the measurements of the drug release from the patches.

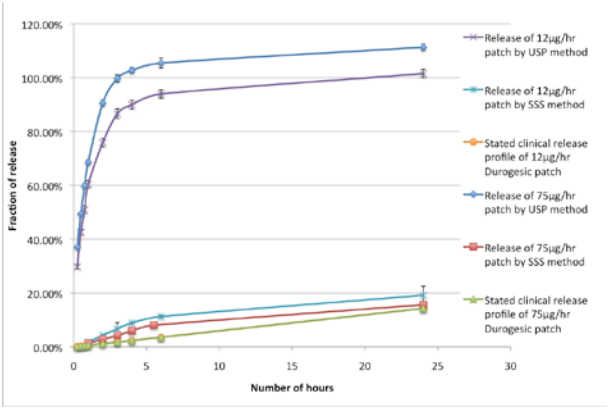

Figure 1. Drug release profiles of durogesic patches (12 and 75µ/hr) measured by USP and SSS methods were compared with the stated clinical release.

DISCUSSION & CONCLUSIONS: The experiment showed that the new *in vitro* testing method could provide significantly more comparable dissolution profile to the *in vivo* uptake than the USP method. This simple method could be particularly helpful to select appropriate formulations for transdermal patches in early development.

REFERENCES: [1] Purdon, Carryn H., et al. (2006) *Penetration enhancement by skin hydration.* In Eric W. Smith and Howard I. Maibach. *Percutaneous penetration enhancers.* s.l. : CRC Press, pp. 67-71. [2] Anand, O, et al (2011) *AAPS J.* **13**:328-35. [3] Azarmi, S., Roa, W. and Löbenberg, R. (2007) *Int J Pharm* **328(1)**:12-21.[4] Hadgraft, J., et al. (1991) *Int J Pharm* **73(2)**:125-130.

ACKNOWLEDGEMENTS: Orexo AB is acknowledged for supplying the materials and analytical support and Vinnova is acknowledged for financial contribution.

Interactions between tissue growth, pore geometry and cell mechanics

J Knychala[1], N Bouropoulos[2], M Taylor[1], BG Sengers [1]

[1] Bioengineering Science Research Group, *Faculty of Engineering and the Environment, University of Southampton, Highfield, Southampton, UK.* [2] Department of Materials Science, University of Patras, Patras, Greece

INTRODUCTION: Pore architecture has a dramatic effect on tissue formation in porous biomaterials used in tissue engineering. However, the wide variety of 3D structures used indicates there is a clear need for the optimal design of pore architecture to maximize tissue formation and ingrowth. Moreover, the shape in which tissue is organized can influence multi-cellular growth patterns. Indeed, different pore architecture leads to tissue shape variations such as the level of curvature resulting in different growth patterns[1]. Furthermore, shape dependent tissue formation in 2D can be the result of local variations of internal mechanical forces that are distributed throughout the cytoskeleton [2]. Nevertheless, understanding how cell generated forces affect tissue organisation and formation in a 3D environment in different pore geometry *in vitro* remains to be understood. Thus, the first aim of this study was to characterize tissue growth solely as a function of pore geometry. Secondly, to observe the involvement of cell mechanics potentially governed by actin organization. Tissue formation was monitored and recorded in an *in vitro* system with well defined open pore slots of varying width, providing a 3D environment for tissue formation while minimizing nutrient limitations.

METHODS: Cell culture and seeding: HBMSCs were cultured on TCP structures in α-MEM medium with 10% FBS under standard conditions (37ºC and 5% CO_2). Imaging: Samples were imaged every 24h using an inverted optical bright-field microscope (IX71, *Olympus Corporation*, Tokyo, Japan). Time-Lapse was recorded by keeping the sample at 37˚C and 5% CO_2 for 48h. Samples were labelled for F-actin with Alexa-Fluor 568-Phalloidin (Molecular probes, Invitrogen). Samples were imaged using a laser confocal microscope (Leica TCS SP2, Germany).

RESULTS: Results demonstrated that tissue formation was strongly influenced by pore geometry. Tissue formation was greater as pores became narrower (fig.1). The level of curvature of the tissue front was seen to change depending on the pore geometry (fig.1 & 2). This can be associated with distinct patterns of actin organisation depending on pore width, indicative of the role of active cell generated forces (fig.2). Time-lapse revealed the highly dynamic nature of tissue formation involving a pulling stress generated by the leading cell that could potentially be provided by acto-myosin contraction and drive tissue growth.

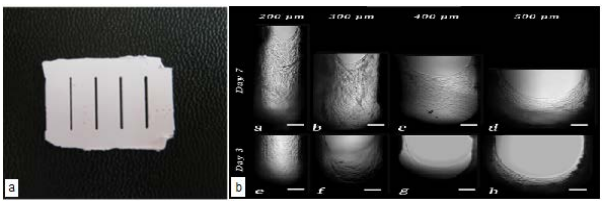

Fig. 1:a) TCP structures, pore width: 200, 300, 400, 500 µm from left to right. b) Tissue front at day 3 (bottom), day 7 (top). Pore size 200, 300, 400, 500 µm from left to right. Scale bar: 100 µm

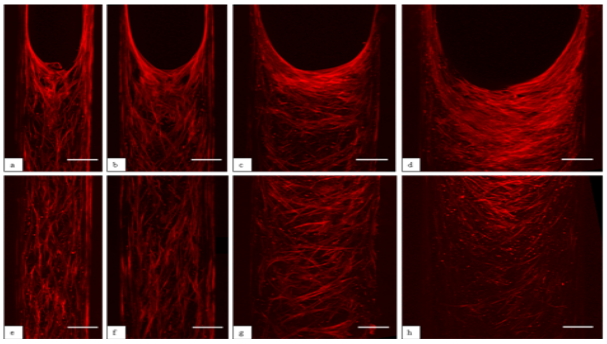

Fig. 2 Actin network in TCP constructs (scale bar = 100 µm). Front of migration (a, b, c, d), tissue bulk (e, f, g, h)

DISCUSSION & CONCLUSIONS: In this study we have clearly demonstrated the relationships between pore geometry, tissue growth and curvature, and implicated the role of actin organisation in this process. The type of experimental system developed could serve as a platform to accurately quantify growth in different culture conditions, as well as to assess the impact of biomaterial, surface modification and biochemical factors**.**

REFERENCES:[1]M. Rumpler, A. Woesz, J. W. Dunlop et al., (2008). *J R Soc Interface* **27**, 1173 1180. [2]C.M. Nelson, R.P. Jean, J.L. Tan et al., *P.N.A.S* **33**, 11594 (2005).

A novel alginate TiO_2 composite scaffold for cell based bone tissue engineering

E Østrup[1,2], H Tiainen [1], JE Reseland[1], JE Melvik[3], SP Lyngstadaas[1], JE Brinchmann[2]

[1]Department of Biomaterials, Institute for Clinical Dentistry, University of Oslo, Norway. [2]Norwegian Center for Stem Cell Research and Institute of Immunology, Oslo University Hospital Rikshospitalet, University of Oslo, Norway. [3]NovaMatrix/FMC Biopolymer, Sandvika, Norway

INTRODUCTION: Mesenchymal stem cells (MSCs) represent, in combination with scaffolds, an outstanding tool for bone tissue engineering. However, the ballance between cell growth conditions and loadbearing properties remains a challenge. Ultra porous TiO_2 scaffolds have high strength, excellent biocompatibility and allow for attachment and growth of MSCs [1, 2]. The aim of the present study is on improving conditions for cell growth on porous ceramic scaffolds focusing on viability, bone differentiation and extra-cellular matrix (ECM) deposition.

METHODS: Cylindrical ultra-porous titanium dioxide scaffolds (4mmx9mm) with a pore-size of 400µm were produces as previously described [1]. Scaffolds were incubated in 2% Ca-alginate suspension (NovaMatrix) for 30 minutes followed by centrifugation at 500 rpm for 2 minutes. Subsequently, 150µl 1% LVG alginate (NovaMatrix) solution was added to the Ca-alginate coated scaffolds. The alginate was allowed to gel for 30 minutes before centrifugation at 500rpm to remove un-gelled alginate from the scaffold. The alginate coated scaffolds were stabilized in 50 mM SrCl for 5 minutes. The resulting composite scaffold was stained by Periodic acid Shiffs (PAS) staining to visualize the alginate. Confocal laser scanning microscopy (CLSM) was used to estimate the thickness of the alginate coat by PAS fluorescence emission (543nm excitation /555-625nm emission). Human adipose tissue derived MSCs were either seeded on uncoated TiO2 scaffolds (500.000 cells/100 ul) or mixed in the 1% Na-alginate solution and seeded on Ca-alginate coated scaffolds as described. Cell seeded scaffolds were cultured in a standard culture medium for 14 days. Lactate dehydrogenase (LDH) activity in medium was measured every 2nd day to asses cell death. At day 14, the relative expression of the skeletal precursor markers *RUNX2* and *SOX9*, as well as the osteogenic markers *COL1A1*, and *ALPL* was determined by RT-qPCR. Type 1 collagen (COL1) protein expression was evaluated by CLSM. Cell viability and proliferation rate was evaluated based on CLSM of ethidium bromide /acridine orange stainings (day 7 and 14).

RESULTS: The alginate layer coating the struts had evaluated thickness of 15µm. Seeding of MSCs in the alginate coating significantly improved conditions for growth and viability as indicated by low cell death, reduced LDH activity, and increased proliferation. Moreover, differentiation towards skeletal progenitor cells was induced as shown by significantly increased expression of *RUNX2* and *SOX9*. Expression of the osteogenic markers *COL1A1*, and *ALPL* however showed no significant differences between the two types of scaffolds. The COL1 staining showed increased deposition in ECM.

DISCUSSION & CONCLUSIONS: The significant increase in *RUNX2* and *SOX9* mRNA in cells cultured in alginate coated scaffolds indicates differentiation of MSC into skeletal progenitor cells. Interestingly immunocytochemical staining showed increased COL1 in the alginate coated scaffolds. It has been speculated previously that culturing cells in porous scaffolds may be accompanyed by the risk of washing out ECM molecules by the culture media [3]. In conclusion, seeding MSCs in an alginate coating improves growth conditions, primes the cells towards osteogenic differentiation, and retains secreted ECM proteins.

REFERENCES: [1] H. Tiainen, SP. Lyngstadaas, JE. Ellingsen, HJ. Haugen (2010) *J Mater Sci Mater Med.* **21**(10):2783-92. [2] R. Sabetrasekh, H. Tiainen, SP. Lyngstadaas, J. Reseland, H. Haugen (2011) *J Biomater Appl.* **25**(6):559-80. [3]RB. Jakobsen, A. Shahdadfar, FP. Reinholt, JE. Brinchmann (2010) *Knee Surg Sports Traumatol Arthrosc.* **18**(10):1407-16.

Biosensing platforms to study ECM carbohydrate-protein interactions

N Altgärde[1], E Nilebäck[1,2], J Becher[3], FE Weber[4], M Schnabelrauch[3], S Svedhem*[1]

[1] Dept. of Applied Physics, Chalmers University of Technology, Göteborg, Sweden, [2] Q-Sense, Västra Frölunda, Sweden, [3] Dept. of Biomaterials, INNOVENT e.V., Jena, Germany, [4] Division of Cranio-Maxillofacial and Oral Surgery, Oral Biotechnology & Bioengineering, University Hospital, 8091 Zurich, Switzerland

INTRODUCTION: Glycosaminoglycans (GAGs) in the extra cellular matrix (ECM) take part in important interactions with proteins, e.g. growth factors. Understanding these interactions is important when engineering supports for cell and tissue cultures. Here, platforms for studying GAG related interactions based on self-assembled monolayers (SAMs) and supported lipid bilayers (SLBs) are described. The platforms enable detailed studies of GAG related interactions, e.g recombinant bone morphogenetic protein (BMP-2).

METHODS: Chondroitin sulfate (CS) and hyaluronoic acid (HyA) were functionalized with biotin or adipic dihydrazide. SAMs were prepared by adsorbing disulfide OEG chains, SS-OEG and SS-OEG-biotin (Polypure) on gold surfaces [1]. SLBs were formed on SiO_2 using POPC, DOPE-COOH, and DOPE-NH_2 lipids (Avanti Lipids). GAGs were immobilized to SLBs using conventional carbodiimide-based coupling reactions [2] or pre-treatment of biotin-SAMs with streptavidin, and the process was followed in real time monitored using quartz crystal microbalance with dissipation monitoring, QCM-D (Q-sense). Subsequent interactions with proteins, e.g. BMP-2 and aggrecan were studied.

RESULTS: CS and HyA were successfully immobilized to both SLBs (Fig. 1) and to SAMs, although immobilized amount varied between strategies. GAGs were immobilized in a side-on configuration to SLB and both side-on as well as end-on to SAMs. The specificity of the BMP-2/CS interaction was studied using low and high ionic strength buffer. At high ionic strength, (150mM) CS immobilized to SLB could load large amounts of BMP-2 and QCM-D dissipation data indicates a densification of the layer (Fig. 1). The interaction between HyA and aggrecan was pH dependent, an effect that can be traced to events in inflamed tissue. Unspecific binding of protein was negligible, a positive aspect when using SLBs.

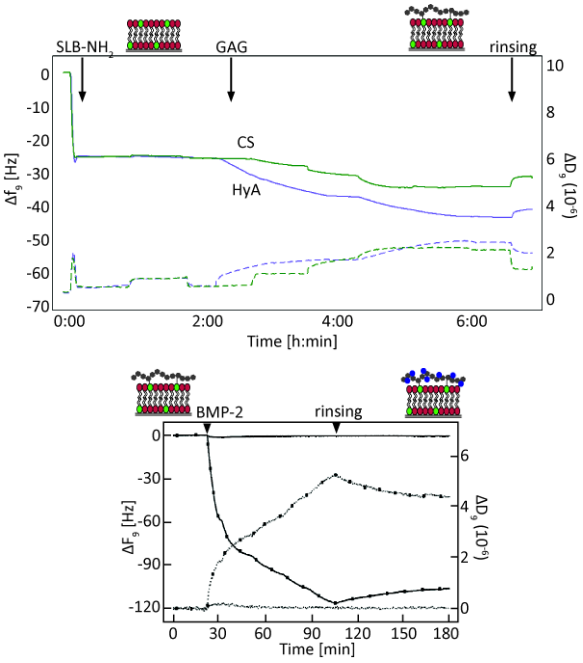

Fig. 1: QCM-D data of GAG immobilization to a SLB (top) and BMP-2 binding to immobilized CS (bottom). Decrease in frequency (solid) corresponds to uptake of mass at the sensor surface. This is paralleled by an increase in dissipation (dashed), showing how soft the layer is.

DISCUSSION & CONCLUSIONS: Platforms for biomolecular interaction studies based on immobilization of GAGs to SLB or SAMs have been investigated. Interaction between CS and growth factor BMP-2 shows the ability of CS to load large amounts of BMP-2. These results contribute to the use of SLBs in interaction studies and also to engineering of supports mimicking the ECM for improving cell and tissue cultures.

REFERENCES: [1] E. Nilebäck, L. Feuz, H. Uddenberg, R. Valiokas, S. Svedhem, *Biosens. Bioelectron.* (2011) **28**:407. [2] N. Altgärde, J. Becher, S. Möller, FE. Weber, M. Schnabelrauch, S. Svedhem (2012) submitted.

ACKNOWLEDGEMENTS: These results were obtained with funding from the EU 7th Framework Programme (FP7/2007-2013) under grant agreement no NMP4-SL-2009-229292 (Find&Bind).

Inositol Hexakisphosphate Inhibits Osteoclastogenesis and Stimulates Activity of Mature Osteoclasts

M. M. Arriero[1], J. M. Ramis[1], J. Perelló[2], M. Monjo[1]
[1]*Research Institute on Health Sciences (IUNICS). University of Balearic Islands, Palma de Mallorca, Spain.* [2] *Sanifit Laboratoris S.L., Palma de Mallorca, Spain.*

INTRODUCTION: Inoxitol hexakisphosphate (IP6) has been found to have an important role in biomineralization and a direct effect inhibiting mineralization of osteoblasts in vitro without impairing extracellular matrix production and expression of alkaline phosphatase [1]. IP6 has been proposed to exhibit similar effects to those of bisphosphonates on bone resorption, however, its direct effect on osteoclasts (OCL) is presently unknown. The aim of the present study was to investigate the effect of IP6 on cell viability, proliferation, differentiation and activity of the RAW 264.7 monocyte/macrophage mouse cell line to OCL.

METHODS: Undifferentiated and mature OCL treated with IP6 were tested for specific differentiation and functional markers using real-time RT-PCR and TRAP-staining. Activity of OCL was also determined by resorption of dentin discs and actin ring formation.

RESULTS: We show that IP6 decreases the osteoclastogenesis in RAW 264.7 cells induced by RANKL, without affecting cell proliferation or cell viability. The number of TRAP positive cells and mRNA levels of osteoclast markers such as TRAP, calcitonin receptor, cathepsin K and MMP-9 was decreased by IP6 on RANKL-treated cells. Also bone resorption activity on dentin discs and actin ring formation was reduced with IP6 (Fig. 1). On the contrary, when giving IP6 to mature osteoclasts after RANKL treatment, a significant increase of bone resorption activity, actin ring formation and TRAP mRNA levels was found.

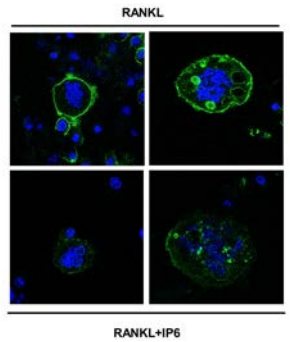

Fig 1. Actin ring formation of mature osteoclasts treated with 1µM of IP6 for 24 h was evaluated using confocal microscopy. Actin was stained with FITC-Phalloidin (green) and nucleus were stained with DAPI (blue). Representative images are shown.

DISCUSSION & CONCLUSIONS: Our results demonstrate that IP6 differentially modulates RANKL-induced osteoclastogenesis by inhibiting OCL differentiation and function of non-committed RAW 264.7 precursor cells and by potentiating OCL function of RANKL-committed cells. Due to the short life span of mature osteoclast and as a consequence that IP6 directly inhibits osteoclast formation (40% at 1 µM IP6 dose), it is therefore expected that the net effect of IP6 on OCL is the inhibition of bone resorption, in agreement to in vivo [2] and clinical findings [3,4]. Moreover, it was found that treatment with IP6 during osteoclastogenesis impaired actin ring formation, contributing to the inhibition of bone resorption.

REFERENCES: [1]W.N. Addison, M.D. McKee MD (2010) *Bone* **46**: 1100-1107. [2] F.Grases, P. Sanchis, R.M. Prieto, J. Perello, A.A. Lopez-Gonzalez (2010) *J Med Food* **13**: 1301-1306. [3]A.A. Lopez-Gonzalez, F. Grases, P. Roca, et al. (2008) *J Med Food* **11**: 747-752. [4] A.A. Lopez-Gonzalez, F. Grases, J. Perello J, et al. (2010) *Front Biosci (Elite Ed)* **2**: 1093-1098.

ACKNOWLEDGEMENTS: The authors are especially thankful for the support from Dr. Fernando Tur and Prof. Felix Grases. This work was supported by INVEST IN SPAIN, European Regional Development Fund (ERDF) from the European Union, Eureka-Eurostars Project Application E!5069 NewBone, Interempresas Internacional Program from the CDTI and the MICINN (Torres Quevedo contract to J.M. Ramis, and Ramón y Cajal contract to M. Monjo).

Weak effect of strontium on early implant fixation in rat tibia

P Linderbäck[1, 2], F Agholme[3], K Wermelin[3], T Närhi[2], P Tengvall[4] P Aspenberg[3]

[1] Laboratory of applied physics, Linköping University, Sweden [2] Turku Clinical Biomaterial Centre, The University of Turku, Finland [3] Section for orthopaedics, faculty of Health Sciences, Linköping University, Sweden [4] Department of Biomaterials, Sahlgrenska Academy, University of Gothenburg, Sweden

INTRODUCTION: Improved early implant fixation in bone can be achieved by increasing the bone formation rate or by improvement of bone quality adjacent to the implants. The recently developed anti-osteoporotic drug strontium ranelate shows good potential for the treatment of osteoporosis [1-2]. Also other drugs, such as bisphosphonates (BP) and parathyroid hormone (PTH), are in clinical use to treat osteoporosis, and have demonstrated a positive effect on fixation of intraosseous implants [3, 4]. The purpose of the present study was to investigate whether systemic strontium treatment could improve the short term implant fixation in an animal model where such effects were demonstrated with other drugs.

METHODS: Two osteoporosis drugs, alendronate and strontium ranelate (SR), were systemically delivered, and their effect compared in a rat implant model after 4 and 8 weeks of implantation. Implanted stainless steel (316L) screws with thread length 2.5 mm and outer diameter of 1.6 mm were used for the mechanical testing. Bone microarchitecture was studied by micro-computed tomography (μCT). To avoid metal artefacts on μCT imaging, polymethyl methacrylate (PMMA) screws of the same size were used. Histomorphometric analyses were performed after the μCT examination.

RESULTS: No significant effect on pullout force was observed upon systemic SR administration during 4 weeks (95% CI for treatment effect: − 41% to 35%), or during 8 weeks (95% CI: − 37% to 90%). In contrast, the systemic administration of alendronate enhanced the pullout force after 4 weeks by 91% and after 8 weeks by 98% (Fig. 1). The alendronate treatment increased the bone volume fraction (BV/TV %) in cancellous bone around PMMA screws by 126% after 4 weeks and by 195% after 8 weeks of implantation, as compared to untreated controls. Strontium ranelate (SR) treatment did not increase the bone volume fraction in the cancellous bone around the PMMA screws after either 4 weeks (95% CI for treatment effect − 31% to 80%) or 8 weeks (95% CI for treatment effect − 40% to 126%).

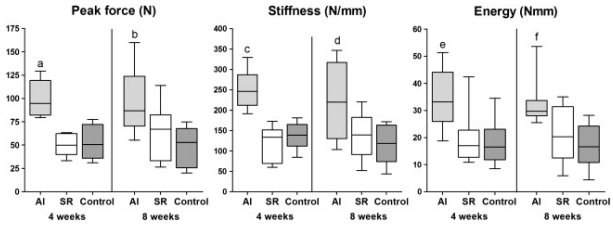

Fig. 1. Effects of alendronate (Al) and strontium ranelate (SR) treatment on screw fixation. Pull-out testing 4 and 8 weeks after screw insertion. SR had no significant effects on any parameter compared to controls. For Al treatment all parameters were significantly increased compared to controls.

DISCUSSION & CONCLUSIONS: Systemic delivery of strontium during 4 or 8 weeks showed no significant improvement of implant fixation in the rat tibia, despite a general increase in bone density. The results do, however, not exclude a small positive effect of SR during the remodeling phase.

REFERENCES: [1]P. Ammann. (2006) *Bone*, **38**: 15–18. [2] G.M. Blake, I. Fogelman (2006) *Clin Interv Aging*, **1**:367–375 [3] P. Aspenberg, K. Wermelin, P. Tengvall, A. Fahlgren. (2008) *Acta Orthop* **79**:111–115. [4] R. Skripitz, S. Bohling, W. Ruther, P. Aspenberg (2000) *Acta Orthop Scand*, **71**: 619–624.

ACKNOWLEDGEMENTS: This study was supported by the Swedish Research Council (VR-2009-6725), the local strategic research project Materials in Medicine funded by County Council of Östergötland and Linköpings Universitet, Sweden.

Effect of nanoporous TiO2 coating and anodized Ca2+ modification of titanium surfaces on early microbial biofilm formation

V Fröj[1,3], P Linderbäck[4,5] A Wennerberg[3,1], L Chávez de Paz[2], G Svensäter[2], JR Davies[2]

[1]Department of Prosthodontics, Malmo University, Sweden. [2]Department of Oral Biology, Malmo University, Sweden. [3]Department of Biomaterials, Institute of Clinical Sciences, Sahlgrenska Academy at the University of Gothenburg, Sweden. [4] Laboratory of applied physics, Linköping University, Sweden. [5] Turku Clinical Biomaterial Centre, The University of Turku, Finland

INTRODUCTION: The soft tissue around dental implants forms a barrier between the oral environment and the peri-implant bone and a crucial factor for long-term success of therapy is development of a good abutment/soft-tissue seal. Sol-gel derived nanoporous TiO_2 coatings have been shown to enhance soft-tissue attachment but their effect on adhesion and biofilm formation by oral bacteria is unknown.

METHODS: We have investigated how the properties of surfaces that may be used on abutments: turned titanium, sol-gel nanoporous TiO_2 coated surfaces and anodized Ca^{2+} modified surfaces, affect biofilm formation by two early colonizers of the oral cavity: Streptococcus sanguinis and Actinomyces naeslundii. The bacteria were detected using 16S rRNA fluorescence in situ hybridization together with confocal laser scanning microscopy.

RESULTS: Interferometry and atomic force microscopy revealed all the surfaces to be smooth (Sa≤0.22 μm). Incubation with a consortium of S. sanguinis and A. naeslundii showed no differences in adhesion between the surfaces over 2 hours. After 14 hours, the level of biofilm growth was low and again, no differences between the surfaces were seen. The presence of saliva increased the biofilm biovolume of S. sanguinis and A. naeslundii ten-fold compared to when saliva was absent and this was due to increased adhesion rather than biofilm growth.

DISCUSSION & CONCLUSIONS: Nano-topographical modification of smooth titanium surfaces had no effect on adhesion or early biofilm formation by S. sanguinis and A. naeslundii as compared to turned surfaces or those treated with anodic oxidation in the presence of Ca^{2+}. The presence of saliva led to a significantly greater biofilm biovolume but no significant differences were seen between the test surfaces. These data thus suggest that modification with sol-gel derived nanoporous TiO_2, which has been shown to improve osseointegration and soft-tissue healing in vivo, does not cause greater biofilm formation by the two oral commensal species tested than the other surfaces.

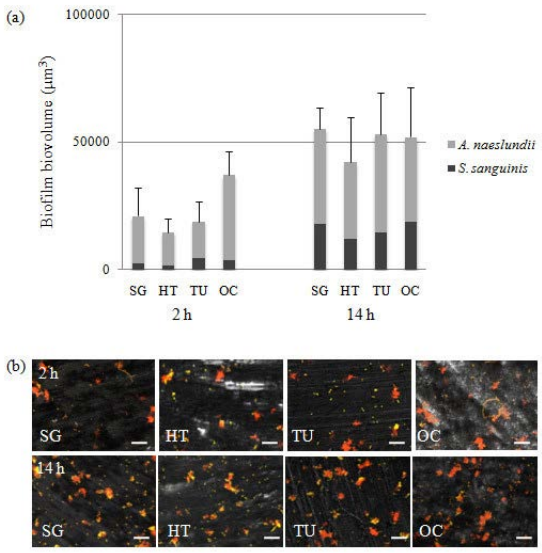

Fig. 1 Biofilm formation by S. sanguinis *and* A. naeslundii *over 2- and 14-hours on the smooth titanium surfaces. (a) Graphs showing the mean ± sd of biofilm volume generated from three independent sets of experiments. SG (sol-gel derived nanoporous TiO_2 coated), HT (heat-treated), TU (turned) and OC (anodically oxidized and Ca^{2+} incorporated). No significant differences were seen between the surfaces at each time point. (b) Representative images from CSLM of 2- and 14-hour biofilms visualized with 16S rRNA FISH.* S. sanguinis *cells appear yellow whereas* A. naeslundii *appears red.*

ACKNOWLEDGEMENTS: This study was supported by The Swedish Dental Society, the Hjalmar Svensson Research Foundation, the Swedish Research Council (AW), and the Knowledge Foundation, Sweden.

Mesoporous titania implant coatings with and without calcium and strontium ion incorporation

K Grandfield[1], S Pujari[1], M Ott[1], H Engqvist[1,2], W Xia[1,2]

[1] *Department of Engineering, Uppsala University, Uppsala, SE.* [2] *BIOMATCELL, VINN Excellence Center of Biomaterials and Cell Therapy, Gothenburg, SE*

INTRODUCTION: The chemistry, topography and morphology of implant surfaces are crucial determinants for implant success. For bone-interfacing applications, a highly tunable and functional biocompatible surface is desirable. Mesoporous titania coatings present several advantages due to the ability to tailor their pore size, chemical composition and topography in order to improve cell interaction, bone ingrowth and osseointegration. Mesoporous titanium dioxide coatings on titanium were produced by an evaporation-induced self-assembly method. The incorporation of calcium and strontium ions into the coatings altered the coating morphology and resulting pore size and surface area. Loading and release of antibiotics from the three-dimensional open-porous network was demonstrated. The surfaces of all compositions supported the proliferation of the SAOS-2 cell line on their surfaces.

METHODS: Four unique coating compositions with a low and high-concentration of calcium or strontium dopant, respectively, were produced according to an EISA method [1]. Plates were loaded with antibiotic by soaking in a 1 mg/ml Cephalothin aqueous solution under vacuum for 2 h. Drug-release was measured in a phosphate buffered saline solution (PBS) without Ca^{2+} or Mg^{2+} ions using a UV-Visible Spectrometer (Shimadzu, UV-1800). The morphology and porous structure were investigated using Scanning Electron Microscopy (FESEM, Leo 1550, Zeiss) with an acceleration voltage of 3 kV. The proliferation of the SAOS-2 cell line on the surface was studied over a two-week time period, similarly to a previous study [1].

RESULTS: The addition of ions resulted in the transformation from hexagonal to worm-like pore morphology shown in Figure 1 A and B. Pore volumes, suitable for drug loading, range from 3.8–5 nm. Sustained antibiotic release over 7 days with a slight burst was measured. SAOS-2 cells proliferated on the surfaces.

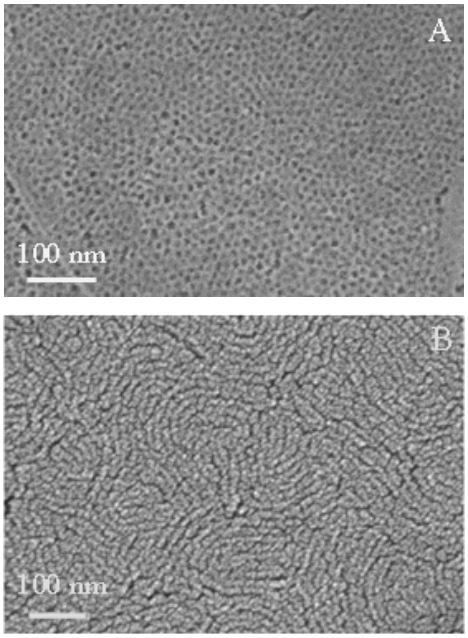

Fig. 1: High magnification SEM micrographs of A) mesoporous titania with hexagonal pore network, and B) Sr-doped mesoporous titania with worm-like pore network.

DISCUSSION & CONCLUSIONS: The coating morphology changed from hexagonally–packed to a worm-like porous system with the addition of calcium and strontium ions in the sol. All coating systems exhibited the potential to release drugs over a sustained time period. The addition of ions showed no adverse effect on the proliferation of the SAOS-2 cells on the surface. The results of this study suggest the potential for mesoporous coatings, with and without calcium or strontium incorporation, in direct bone-interfacing implant applications.

REFERENCES: [1] W. Xia, K. Grandfield, A. Hoess, A. Ballo, Y. Cai, H. Engqvist (2012) *J Biomed Mater Res Part B* **2012:100B:**82–93.

Surface modification using hyaluronic acid

I Berts[1,2], G Fragneto[2], J Hilborn[1], AR Rennie[3]

[1] *Department of Chemistry – Ångström Laboratory, Uppsala University, Sweden.* [2] *Institut Laue-Langevin, Grenoble, France.* [3] *Department of Physics and Astronomy, Uppsala University, Sweden*

INTRODUCTION: To improve an implantable material's performance and sustainability, one needs to understand the interfacial structure between the natural tissue and the biomaterial. Polysaccharide coatings are commonly used to increase the biocompatibility of an implant material and hyaluronic acid (HA), is presently the leading candidate for surface modifications [1]. We have investigated the structure and composition of grafted HA at a solid-liquid interface using neutron reflectivity.

METHODS: HA has been grafted on silica surfaces and titanium surfaces. In the first study, HA was immobilized on aminated silica surfaces by single- and two-stage deposition. In the second study, HA (functionalized with bisphosphonate groups) was immobilized on titanium surfaces. Due to the presence of additional cross-linkable groups, it was possible create a multilayer film of the titanium.

RESULTS: Single- and two-stage deposition of HA gave different polymer density profiles (Fig 1). A two-stage deposition process created a diffuse layer with an overall lower density but with HA further extended from the grafting site. The layer was affected by the exchange of counter-ions (from Na^+ to Ca^{2+}).

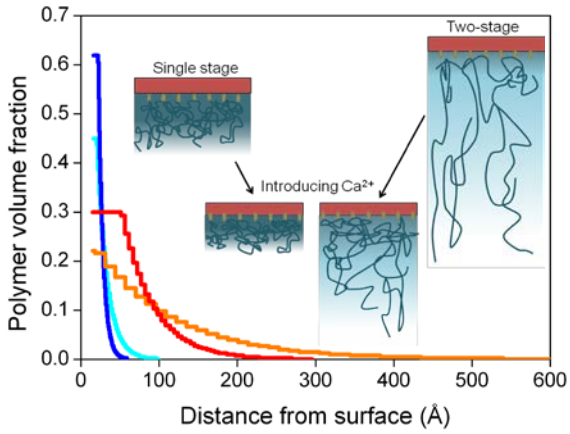

Fig. 1: Sample prepared by single deposition (--) with a small increase in surface polymer fraction after adding Ca^{2+}(--). Sample prepared by two-stage deposition (--) with a distinct increase in film thickness after adding Ca^{2+}(--).

A schematic diagram (Fig 1) illustrates the compression of the layers. In the second study, HA with bisphosphonate groups formed stable layers on titanium due to thermodynamically driven formation of Ti-O-P bonds. By further cross-linking, a multilayer film was created (Fig 2).

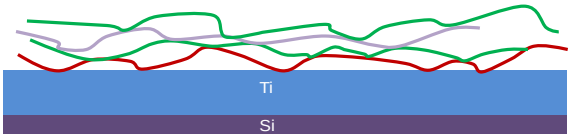

Fig. 2: Multilayer film on top of Ti surface.

Neutron reflectivity data (Fig 3) showed a distinct difference between the bare titanium surface and after the immobilization of HA.

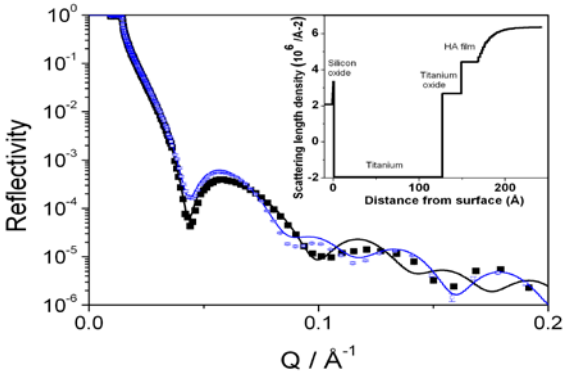

Fig. 3: Neutron reflectivity data of the bare titanium surface (□) and with the immobilized HA film (■). The scattering length density profile is shown in the inset. The modelled layers are silicon oxide, followed by atomic titanium (125 Å), titanium oxide (20 Å) and HA film (20 Å with additional density decay).

DISCUSSION & CONCLUSIONS: This study relates the method of surface functionalization to the HA structural outcome.

REFERENCES: [1] M. Morra (2003) *Biomacromolecules* **6(3)**:1205-23.

ACKNOWLEDGEMENTS: We are grateful to Dr. Kristoffer Bergman for providing the aldehyde derivative of HA, and Dr. Dmitri Ossipov for providing the bisphosphonate derivative of HA.

Analyzing the viability of bacteria after TiO_2 induced photocatalysis

Yanling Cai[1], Håkan Engqvist[2], Maria Strømme[*1] and Ken Welch[*1]

[1]*Division of Nanotechnology and Functional Materials, Ångström Laboratory, Uppsala University, Sweden.* [2]*Division of Applied Materials Science, Ångström Laboratory, Uppsala University, Sweden.*

INTRODUCTION: Bacterial infections are becoming a growing challenge and constitute a major cause of implant failure. In our former work [1], TiO_2 nanoparticle-containing dental adhesives (referred to as NP adhesives) have shown to be bioactive in terms of mineralization, and possess on-demand bactericidal properties via photocatalysis under UV-A irradiation. In order to assess the effectiveness of photocatalytic bactericidal treatments, it is essential to be able to determine the amount of viable bacteria using accurate and high-throughput methods.

The aim of the present work was to evaluate several methods for analyzing bacterial viability following antibacterial photocatalytic treatment.

METHODS: Bacterial strains, *Staphylococcus. epidermidis* and *Streptococcus. mutans* were employed in the antibacterial tests. A bacterial population of 10^7 cfu was spread on the surface the sample NP disks. Photocatalytic treatment was performed by irradiating the disks with UV-A light (0-14J/cm^2). After photocatalytic treatment, viability of the bacteria on each disk was examined using several methods, including Colony formation unit (CFU) counting, resazurin test (also known as Alamar blue test), a metabolic activity assay (MAA) based on phenol red, and Live/Dead (L/D) Baclight staining followed by fluorescent intensity measurements. Examination with L/D Baclight staining was also performed using laser scanning confocal microscopy and flow cytometery.

RESULTS: In antibacterial tests with *S. epidermidis*, the L/D staining method shows a much higher bacterial viability after medium to high UV-A doses (4-13.6J/cm^2) when compared to the cfu counting and resazurin method results. When the UV-A dose increased to 13.6J/cm^2, L/D staining showed 1 log reduction of viable bacteria while cfu counting and the resazurin test showed a 5 log or greater reduction in bacterial viability.

Similarly, in antibacterial tests with *S. mutans*, the MAA and resazruin tests showed that an increasing dose of UV-A irradiation leads to an increasing antibacterial effect. Generally, a population size of *S. mutans* of ~10^7 cfu on Φ8 mm disks can be disinfected (5 log reduction) by photocatalysis with a UV-A dose of 10J/cm^2. Again, compared to MAA and resazurin tests, L/D staining results showed a much higher bacterial viability after UV-irradiation tests for all doses. When the UV-A dose was increased to 13.6J/cm^2, L/D staining showed less than 2 log reduction of viable bacteria while MAA and resazurin tests showed more than 6 log viable bacteria reduction.

In the test with *S. epidermidis* (~2x10^8cfu on a Φ8mm disk), the results of flow cytometer based on L/D staining showed 39.2% viability after photocatalytic treatment with a UV-A dose of 40J/cm^2 while cfu counting showed a L/D ratio of 7.1x10^{-5}.

In an additional biofilm elimination test, a laser scanning confocal microscopy image of a biofilm stained with the L/D Baclight staining showed high viability after photocatalytic treatment with a UV-A dose of 40J/cm^2, while a MAA test showed that this dose lead to 5 log reduction of bacterial viability.

DISCUSSION & CONCLUSIONS: Multiple methods were compared for the assessment of bacterial viability after photocatalytic treatment. The results of cfu counting, resazurin test and MAA test based on phenol red showed correlation with each other, while tests based on the L/D Baclight staining differed significantly, showing much higher viability. Our results suggest that the use of L/D staining may not be applicable to the assessment of bacterial viability following antibacterial photocatalytic treatments.

REFERENCES: [1]K. Welch, Y. Cai, H. Engqvist, M. Strømme (2010) Dent Mater **26(5)**: 491-99.

Conducting nanocellulose polypyrrole membranes intended for hemodialysis

D O Carlsson[1], N Ferraz[1], J Hong[2], R Larsson[2], B Fellström[3], L Nyholm[4], M Strømme[1], A Mihranyan[1]

[1] Nanotechnology and Functional Materials, Uppsala University, Sweden. [2] Department of Immunology, Genetics and Pathology, Uppsala University, Sweden. [3] Renal Medicine, Uppsala University Hospital, Sweden. [4] Department of Chemistry, Uppsala University, Sweden

INTRODUCTION: Hemodialysis is based on ultrafiltration, a passive process, and is the only alternative to kidney transplantation for chronic renal failure patients. Dialysis is time-consuming and cannot mimic all kidney functions, e.g. secretion. Essential large proteins are inevitably removed during the treatment, while many small-size uremic toxins, e.g. phosphates and oxalates, accumulate to lethal levels. We have developed a porous (~70 %) and electroactive composite membrane, consisting of nanocellulose coated with the conducting polymer polypyrrole (PPy) [1]. Its ultrafiltration properties combined with potential controlled ion extraction could potentially improve solute removal efficiency. Present work is focused on improving the blood compatibility by heparinization and, specifically, on the stability and ion extraction properties of the heparinized composite.

METHODS: Composites were prepared as previously described [2] and coated with heparin through a modification of the Corline method (Corline Systems AB, Uppsala, Sweden). Coating stability was evaluated by avidin-Texas Red-X staining in combination with fluorescence microscopy and by an antithrombin (AT) binding assay before and after ten reduction-oxidation cycles using cyclic voltammetry (CV). Electrochemical extraction capacities for phosphate and oxalate were evaluated after ten CV-cycles in 0.1 M, pH 7.4 solutions. For further details, see [3]. Values are presented as mean value ± s.e. of the mean.

RESULTS: Composite heparinization lowers the thrombogenic properties to levels comparable to those of commercially available dialysis membranes, while both heparinized and non-heparinized composites generate similar or less complement activation (C3a and sC5b-9) as commercial membranes [3]. Fluorescence microscopy indicated that the heparin coating remained on the surface after CV-cycling (Fig. 1) and the AT-binding capacity remained unaffected by the cycling (Table 1). The ion extraction capacity of phosphate and oxalate was not affected by the heparin coating (Table 2).

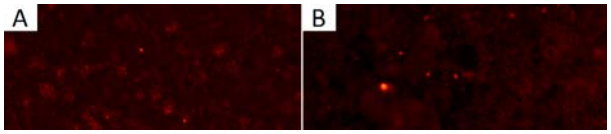

Fig. 1: Heparin coating of composites before (A) and after (B) CV-cycling.

Table 1. AT-binding capacity (n=6).

	Capacity (pmol/cm^2)
Non-heparinized	2 ± 1
Heparinized, before CV-cycling	9 ± 1
Heparinized, after CV-cycling	9 ± 1

Table 2. Ion extraction capacity (n=3).

	Phosphate (µmol/g)	Oxalate (µmol/g)
Non-heparinized	587 ± 23	579 ± 26
Heparinized	600 ± 26	523 ± 5

DISCUSSION & CONCLUSIONS: The heparinized composite exhibits good blood compatibility. The heparin coating stability was investigated in this work. The results indicate a stable heparin coating that, in addition, does not affect the ion extraction capacity of the membrane. Thus, it is a promising material for future dialysis systems. Ultrafiltration investigations are underway and ion extraction from more complex as well as flowing solutions will be studied.

REFERENCES: [1] A. Mihranyan, L. Nyholm, A. E. Garcia-Bennet, et al (2008) *J Phys Chem B* **112**: 12249-12255. [2] N. Ferraz, M. Strømme, B. Fellström, et al (2012) *J Biomed Mater Res A* **In press** (doi: 10.1002/jbm.a.34070). [3] N. Ferraz, D. O. Carlsson, J. Hong, et al (2012) *J R Soc Interface* **In press** (doi:10.1098/rsif.2012.0019).

ACKNOWLEDGEMENTS: Swedish Research Council, SSF, The Nordic Innovation Center, Bo Rydin Foundation and Stiftelsen Lars Hiertas Minne for financial support as well as S Pradhan, J Grawé and C Persson for their help.

Mathematical modelling of *in vivo* drug release from hydrogels for spinal cord injuries treatment

T. Casalini[1], F. Rossi[1,2], P. Torriani[1,2], M. Masi[1], P. Veglianese[2], G. Perale[1,2]

[1] *Department of Chemistry, Materials and Chemical Engineering, Politecnico di Milano, Milan, Italy* [2] *Neuroscience department, Mario Negri Institute for Pharmacological Research, Milan, Italy*

INTRODUCTION: Spinal cord injury (SCI) still represents one of the most debilitating condition among neurological diseases, because of acute and long-term health consequences. Hydrogels made of Carbomer (polyacrylic acid) and Agarose (polysaccharide) emerged as promising drug delivery systems for SCI repair application, thanks to their biocompatibility and the *in situ* gelation after injection that allows avoiding invasive surgical implantation procedures [1]. Here, first-principles mathematical modeling was applied in order to achieve a better understanding of the experimental behavior of *in vivo* drug release [1].

METHODS: Hydrogel was loaded with Hoechst 33258 (HC, 0.2 mg/mL) that can mimic neuroprotective agents commonly used in SCI repair [1]. The delivery kinetic of HC was studied *ex vivo* 7 days after gel positioning in injured mice. From a mathematical model point of view the system was then investigated through mass conservation equations and fluid dynamics equations [2]. Hydrogel and tissue behavior was described with Fick's law, while cerebrospinal fluid (CSF) was characterized through Navier Stokes equation (in order to determine the velocity field) and convection/diffusion equation. Both the three dimensional geometry construction and computations were performed by means of Comsol 3.5 software.

RESULTS: *Ex vivo* experimental data (Figure 1) showed a peculiar behavior, that is an oriented drug delivery to the caudal zone with respect to the gel-placing site. This can be related to the effect of cerebrospinal fluid (CSF) that, flowing in caudal direction, realizes a transport and tissue absorption of drug molecules far from placing site. Indeed CSF is formed in lateral, 3rd and 4th ventricles, it flows in the cisterna magna, and is then conveyed to the subarachnoid space surrounding the spinal cord, flowing in a rostral-to-caudal direction, till it is re-absorbed at the venus sinuses located in the caudal part of the spinal cord. In order to understand the hypothesized CSF effect on drug release, mathematical modeling was applied on the system.

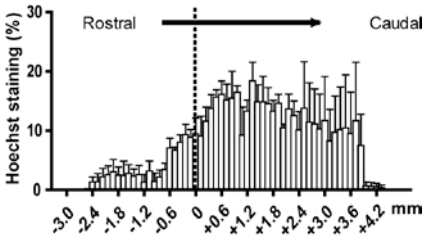

Fig. 1: Quantitative evaluation of the fraction of HC staining/section in a region encompassing the epicenter between -3.0 and +4.2 mm. Reproduced from Perale et al. (2012) ------

Computations confirmed the role of CSF in drug distribution, that is, the preferential delivery.

DISCUSSION & CONCLUSIONS: Mathematical modelling proved to be a powerful tool that, coupled with experimental activity, allowed obtaining a deeper understanding and an overall view of the involved phenomena. In particular, the system was not analyzed with regression formulas but through mass balances which represent fundamental conservation laws. Moreover, involved parameters (*e.g.* diffusion coefficients) have a physical meaning and can be properly and separately estimated. The model is able to qualitatively reproduce the experimental behavior of the system, since it captures the synergic effect of the main involved phenomena. Calculations, indeed, confirmed the key role of the cerebrospinal fluid in drug release.

REFERENCES: [1] G. Perale et al. (2012) *J Control Release* **in press**, DOI: http://dx.doi.org/10.1016/j.jconrel.2011.12.025. [2] R.B. Bird, W.E. Stewart, E.N. Lightfoot (2002) *Transport phenomena*, Wiley International ed.

In vitro studies of osteoblast activity on biphasic calcium phosphate ceramic surfaces

A. Dubnika[1], D. Loca[1], J.B. Nebe[2], L. Berzina-Cimdina[1]

[1] *RTU Riga Biomaterials Innovation and development Center, Riga, Latvia,* [2] *University of Rostock, Biomedical Research Centre, Rostock, Germany*

INTRODUCTION: Hydroxyapatite (HAp) and β-tricalcium phosphate (β-TCP) ceramics are widely used as bone replacement materials due to their bioactivity and osteoconductive properties. The use of biphasic calcium phosphate (BCP) bioactive ceramics is based on an optimum balance between more stable phase – HAp and more soluble phase – β-TCP. β-TCP supplies surrounding bone and soft tissues with calcium and phosphate ions, HAp enhances biocompatibility and improves mechanical strength.[1,2] Hence it is important to find an optimal ratio between HAp and β-TCP, to ensure the material replacement with the bone tissue during the implant resorbtion. Sintering temperature directly affects the surface area and microporosity of the material. Increasing the sintering temperature decreases both the surface area and microporosity.

METHODS: Biphasic calcium phosphate (HAp/β-TCP) synthesis was carried out by wet precipitation method. The dried precipitate was milled to obtain fine powder. Before sintering, powder was uniaxially pressed into pallets. BCP was sintered at 1000 ^{o}C and 1150 ^{o}C temperature. Obtained samples have HAp/β-TCP ratio 70/30. Porosity, shrinkage, phase composition, surface area and surface morphology of the samples after sintering were evaluated. To determine the adhesion, proliferation and biocompatibility MG63 osteoblast cell line was used. Stability of samples in cell culture medium was determined.

RESULTS: The surface area of samples sintered at 1000 ^{o}C was 8 m^2/g, while surface area of samples sintered at 1150 ^{o}C was ten times lower (0.8 m^2/g). BCP ceramic sintered at 1000°C has a high rate of particle release compared to material sintered at 1150°C. The effect of HAp/β-TCP sintering temperature on osteoblast behaviour was evaluated. Cells are able to adhere and proliferate on both kinds of material, but there are differences in shape and size of cells. Cells seeded on BCP ceramic sintered at 1150°C are more flat and outspread both after 30 min and 24 h than those on material sintered at 1000°C (Fig.1.).

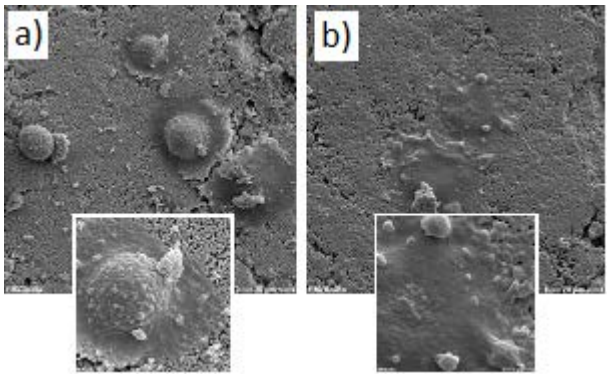

Fig. 1: a)osteoblastic cells MG63 30 min after seeding on BCP sintered at 1000°C; b)osteoblastic cells MG63 30 min after seeding on BCP sintered at 1150°C.

DISCUSSION & CONCLUSIONS: Both kinds of biomaterial are appropriate for cell culture applications. However, the material sintered at 1000°C shows a higher rate of particle release which has a negative effect on cell growth.

REFERENCES: [1] F. Monchau, A. Lefevre, et al (2002) *Biomol. Eng.* **19**:143-152. [2] X. Wang, H. Fan, et al (2006) *Mater. Lett.***60**:455-458.

ACKNOWLEDGEMENTS: This work has been partially supported by the European Social Fund within the project "Multidisciplinary Research in Biomaterials Technology of New Scientist Group", No.2009/0199/1DP/1.1.1.2.0/09/APIA/VIAA/090, and partially supported by the Baltic-German University Liaison Office within the project "Various research methods by comprehensive evaluation of biomaterials characterization".

Determination of the optimal pore size of PLGA scaffolds for healing of critical size bone defects in rat

Y Förster[1*], A Penk[2*], M Hacker[3], M Schulz-Siegmund[3], D Huster[2], S Rammelt[1]

[1] Department of Trauma and Reconstructive Surgery, University Hospital Carl Gustav Carus, Dresden, GER, [2]Institute of Medical Physics and Biophysics, University of Leipzig, GER, [3] Institute of Pharmacy, University of Leipzig, GER

INTRODUCTION: The therapy of critical size bone defects represents a significant clinical problem. The standard treatment for the repair is autologous bone grafting. However, this requires an extra surgical procedure for harvesting with all its potential hazards and complications. Furthermore, the amount of available bone for harvesting is limited. Therefore, research has focused on the development of biodegradable polymer scaffolds that can be implanted into a defect of given size and stimulate the formation of new bone in the defect along with gradual degradation of the scaffold. The aim of the present study was to analyse the new formed bone and extracellular matrix (ECM) in poly(lactic-*co*-glycolic acid) (PLGA) scaffolds with different pore sizes implanted into the rat tibia. Histology, magnetic resonance imaging (MRI), and quantitative magnetic resonance (NMR) spectroscopy were used to determine formation of new bone and ECM.

METHODS: A standardized cylindric defect of 3 mm was created in each tibia head of female Wistar rats using a biopsy punch. The PLGA scaffolds were fitted into the defect but not pressed to conserve the macroporous properties. Animals were sacrificed 2 or 4 weeks postoperatively. The pore sizes of the PLGA scaffolds were 100-300 µm, 300-500 µm, or 500-710 µm.

RESULTS: After 4 weeks, it is shown with histological methods that the scaffolds were invaded completely by newly-formed lamellar bone (Fig. 1A) that was morphological similar to the surrounding cancellous host bone while the control defects were filled only partially by inhomogenous and less mature woven bone. No visible impact of the pore size could be detected with histological staining methods (H/E, Goldner). The scaffold was not detectable.

In contrast, the PLGA scaffolds could still be identified in the MRI scans. The scaffold could clearly be delineated from the surrounding native bone of the tibia (Fig. 1B). Additionally, the *de novo* generated ECM in the PLGA scaffold showed no oriented trabecular structure like that of native bone.

Quantification of NMR spectra showed, that the largest amount of collagen was synthesized in the scaffolds of the middle pore size (300-500 µm) both after 2 and 4 weeks. In addition, the hydroxyapatite content in the scaffold was calculated and referenced to native bone by ^{31}P MAS NMR. Best results were obtained again for the middle pore size.

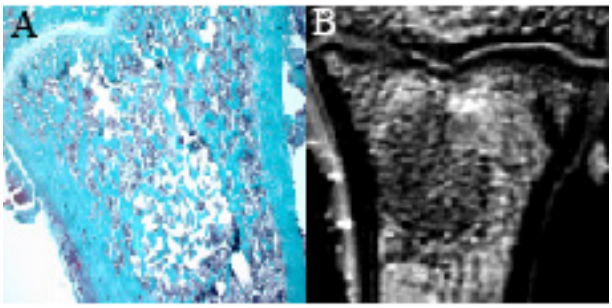

Fig. 1: Representative histological stained (A) and MR images (B) of rat tibiae 4 weeks after defect treatment with PLGA scaffold (pore size 300-500 µm). (A) Goldner stain, magnification x250).

DISCUSSION & CONCLUSIONS: In this study we wanted to evaluate the optimal pore size of PLGA scaffolds by determining new bone and ECM formation. The results, obtained with the various techniques applied, indicated that the PLGA scaffolds are osteoconductive. Further, a pore size of 300-500 µm provides the best results regarding bone and ECM formation and therefore represents the most effective implant. Thus, we will use PLGA scaffolds with this pore size for further studies that will focus on biofunctionalization of those scaffolds with ECM components and growth factors.

ACKNOWLEDGEMENTS: The authors would like to acknowledge the DFG and the collaborators within the Transregio 67 and the CRTD.*Both authors contributed equally to this work.

Photocatalytic and antimicrobial properties of a TiO2 implant coating deposited through cathodic arc evaporation

J Forsgren[1], M Lilja[1,3], M Åstrand[3], M Strømme[1], H Engqvist[2], K Welch[1]

[1] *Division for Nanotechnology and Functional Materials and* [2] *Division of Applied Materials Science, The Ångström Laboratory, Uppsala University, Sweden.* [3] *Sandvik Tooling Sverige AB, Stockholm, Sweden*

INTRODUCTION: Post surgical infections and infections associated with metallic implants are a major concern in the clinical setting. These infections are often difficult to treat and result in great suffering for afflicted patients and substantial costs to the society. This study investigated the structural, morphological and antibacterial properties of a physical vapour deposited TiO_2 coating intended for metallic implants.

METHODS: Disks (Ø =9 mm, thickness 1 mm) of commercially available grade 5 (Ti-6Al-4V) titanium were used as reference samples and substrates for the arc evaporation coating process described elsewhere [1].The resulting TiO_2 coating was characterized by grazing incidence X-ray diffraction (XRD) measurements and scanning electron microscopy (SEM). The photocatalytic activity (PCA) of reference and TiO_2 coated surfaces was tested via a degradation of rhodamine B under UV illumination (λ=365 nm). Free radicals formed at the surface of photocatalytically active samples when illuminated with UV-light causes degradation of rhodamine B in solution. The rhodamine B degradation was monitored spectroscopically as a function of illumination time, and the degradation rate was calculated assuming a pseudo first order reaction.

Antibacterial testing of the reference and TiO_2 coated surfaces was performed using *Staphylococcus epidermidis* as model bacteria. *S. epidermidis* was used as it is commonly associated with implant infections, particularly those implants that penetrate the skin. 8 µl of bacteria suspension containing approximately $8x10^6$ bacteria was spread out over the surface of the disks and the disks were illuminated with a UV light source (λ=365 nm) with an intensity of 20 mW/cm^2 at the disk surface. A series of disks were tested in which the illumination time was varied from 0 to 15 minutes. Viability of the bacteria was assessed using a metabolic assay containing resazurin and making fluorescent measurements after 14 h incubation at 37 C.

RESULTS: XRD measurements of the as-deposited TiO_2 coating showed the coating to be crystalline with anatase as the primary polymorph. Scanning electron microscopy of the coating surface and cross-section showed a columnar grain structure of several hundred nm in thickness.

PCA results of the surface using rhodamine B under UV illumination showed good photocatalytic activity, that was roughly equivalent to similarly produced, but thinner, arc-evaporated TiO_2 coatings that have been previously investigated [1].

Antibacterial tests were performed on anatase TiO_2 coated disks and reference grade 5 titanium disks. While both disks showed a reduction of viable *S. epidermidis* bacteria with high UV doses, the TiO_2 coated disks showed a significantly greater reduction in viable bacteria for illumination times less than 10 minutes.

DISCUSSION & CONCLUSIONS: In this study we have demonstrated that cathodic arc evaporated, anatase thin films on titanium grade 5 substrates not only show UV-induced photocatalytic activity but also exhibit bactericidal effect against *S. epidermidis*. A significant difference in this study compared to previous antibacterial tests with photocatalytic coatings on metallic substrates is that a higher intensity UV light source was utilized, enabling inactivation of bacteria within a more clinically relevant treatment timeframe. The coating deposition method described here is believed to be an important contribution towards development of antimicrobial coatings on metallic implants that also have additional beneficial properties such as bioactivity.

REFERENCES: [1] M. Lilja, K. Welch, M. Åstrand, H. Engqvist, M. Strømme (2012) *J Biomed Mater Res B*, DOI: 10.1002/jbm.b.32674.

ACKNOWLEDGEMENTS: The Swedish funding agencies Vinnova and VR are acknowledged for financial support.

Preparation and characterization of PLGA nanoparticles as anticancer drug delivery carriers

MF Frasco, S Rocha, MC Pereira, MAN Coelho

LEPAE, Chemical Engineering Department, Faculty of Engineering, University of Porto, Rua Dr. Roberto Frias, 4200-465 Porto, Portugal

INTRODUCTION: Enthusiastic studies on the design of delivery systems using biocompatible and biodegradable polymeric nanoparticles (NPs) have grown exponentially. Optimizing the properties of nanocarrier formulations is intended to maintain the activity and the bioavailability of the therapeutic loadings, and to minimize undesirable side effects such as short circulation half-life and unspecific targeting. Among the nanoparticulate carriers, poly(lactic-co-glycolic acid) (PLGA) NPs have high potential in nanomedicine, namely for delivery of drug, gene, proteins and peptides combining targeting, imaging, diagnostics and cancer therapy [1]. The ubiquitin-proteasome pathway is the major system for the degradation of intracellular proteins, and studies have shown that its inhibition reduces tumour proliferation and induces apoptosis [2]. In this study bortezomib (BTZ) was chosen as a proteasome inhibitor.

METHODS: PLGA NPs were formulated by a single-emulsion solvent evaporation technique. PLGA Resomer® RG503H (10 mg) was dissolved in ethyl acetate (0.1 mL). An aqueous solution of 1% (w/v) Pluronic F127 (0.2 mL) was added dropwise and the emulsion obtained by sonication (60 s). This mixture was poured into 2.5 mL of 0.1% (w/v) Pluronic F127 and stirred (800 rpm) at room temperature for 3 h. The suspension was filtered (0.2 µm) and the NPs were collected by centrifugation (14500 rpm, 30 min) and resuspended in ultrapure water. PLGA NPs were loaded with BTZ (1 mg) or with the fluorescent dye coumarin 6 (C6) (0.1 mg) to track cellular uptake. The hydrodynamic diameter was evaluated by dynamic light scattering (DLS) and the size and morphology were analysed by transmission electron microscopy (TEM) (Zeiss microscope operated at 60 kV). The zeta potential was determined by laser doppler velocimetry. DLS and zeta potential analyses were performed in a Zetasizer Nano ZS (Malvern Instruments, Malvern, UK).

RESULTS: The PLGA NPs produced were nearly monodisperse and the negative zeta potentials sustain the stability of the suspensions by electrostatic repulsion between the colloids (Table 1). TEM analysis showed similar sized NPs with uniform spherical morphologies (Figure 1a), and no aggregation was observed. PLGA NPs were loaded densely with C6 as visualized by fluorescence microscopy (Figure 1b). The efficiency of BTZ encapsulation up to 60% was evaluated by UV measurements at 270 nm.

Table 1. Mean size, polydispersity index (PDI) and zeta potential of the studied PLGA NPs (n>3).

	Mean diameter (nm)	PDI	Zeta potential (mV)
Plain PLGA	197 ± 22	0.10 ± 0.03	-24 ± 3
BTZ-PLGA	197 ± 16	0.10 ± 0.06	-28 ± 4
C6-PLGA	185 ± 16	0.14 ± 0.04	-20 ± 2

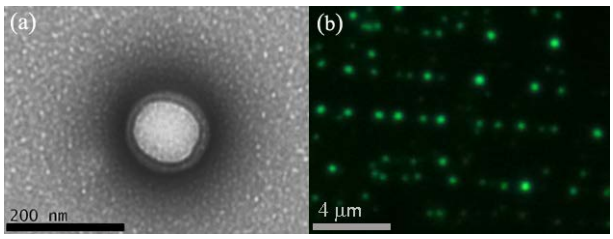

Fig. 1: PLGA NPs: (a) TEM image; (b) PLGA NPs loaded with C6.

DISCUSSION & CONCLUSIONS: In the current study we have shown the efficient loading of PLGA NPs with an anticancer drug and a fluorophore, maintaining the properties of monodispersity and stability of the nanocarrier. Foreseen assays will focus on the inhibition kinetics of the proteasome and on the cellular internalization, sustained drug-release and cytotoxicity of the developed formulations.

REFERENCES: [1] S. Hamdy, A. Haddadi, R.W. Hung, A. Lavasanifar (2011) *Adv Drug Deliv Rev* **63**: 943-55. [2] M. Groll, R. Huber (2004) *Biochim Biophys Acta* **1695**: 33-44.

ACKNOWLEDGEMENTS: This work was supported by *Fundação para a Ciência e a Tecnologia* (FCT) (MF Frasco Post-Doctoral grant SFRH/BPD/40876/2007) and by FCT research project PTDC/QUI-BIQ/115449/2009.

Unexpected mechanism of Zn^{2+} insertion in calcium phosphate bioceramics.

S Gomes[1,2], JM Nedelec[1,2], E Jallot[3], G Renaudin[1,2]

[1] Clermont Université, ENSCCF, ICCF, Clermont-Ferrand, France. [2] CNRS, UMR 6296, ICCF, Aubière, France. [3] Clermont Université, Université Blaise Pascal, CNRS/IN2P3, Laboratoire de Physique Corpusculaire, Clermont-Ferrand, France

INTRODUCTION: Basic understanding of ionic substitutions in hydroxyapatite is a major issue. In effect, natural apatites are strongly substituted and deliberate doping with specific ions can bring new properties to these bioceramics. Zinc doping is now focussing a lot of attention due to the interesting biological properties of this cation.

METHODS: The crystallographic study of eight well crystallized Zn-substituted BCP samples have brought new important information on the structural location of Zn^{2+} cation in both HAp and β-TCP phases. Rietveld refinement of XRPD patterns is a useful tool to reach a fine description of well crystallized substituted materials. Rietveld refinement on powder patterns allows one to generate electronic density maps within the unit cell. This is a direct method to locate the substitution elements when allowed by the electronic contrast. Local information brought by Raman spectroscopy allows confirming structural details.

RESULTS: Zn^{2+} is incorporated in the β-TCP structure by substituting calcium atoms in the low-density column (i.e. in Ca4 and Ca5 sites). Zn^{2+} enters the HAp structure and is located on the 2b Wyckoff site. Zn atoms do not substitute Ca atoms in Ca1 or Ca2 sites, but insert an interstitial site leading to the general formula $Ca_{10}Zn_x(PO_4)_6O_{2x}(OH)_{2-2x}$. Zn atoms are unusually 2+6 coordinated in HAp (with two short Zn-O distances of about 1.7 Å leading to the formation of linear O-Zn-O groups), contrary to recent spectroscopic interpretations that have indicated a tetrahedral configuration for Zn atoms located in calcium sites [1,2]. Such an insertion process induces an excess of cations, compensated by the replacement of hydroxyls by O^{2-} anions (forming the O-Zn-O group). These inserted Zn^{2+} cations are managed by the Ca/P ratio (of 1.67 with a nominal $Ca_{10}Zn_x(PO_4)_6O_{2x}(OH)_{2-2x}$ composition) instead of (Ca+Zn)/P ratio (with nominal $Ca_{10-x}Zn_x(PO_4)_6(OH)_2$ composition when considering usual substitution mechanism). The previously reported inhibiting effect of zinc on HAp crystallisation, or destabilizing feature of zinc for HAp, is not inevitably intrinsic to Zn, but could be due to the nominal constituent ratio as clearly demonstrated here. These results pertain to sample that were annealed at high temperature, so the as-precipitated, less crystalline samples may be quite different.

So in a second step, Rietveld analysis on X-ray powder diffraction patterns recorded from 28 hydroxyapatite samples containing various amount of zinc (0, 1.6, 3.2 and 6.1 wt. Zn %) and heat treated at various temperatures (between 500°C and 1100°C) have allowed to finely characterizing the Zn insertion mechanism into the HAp crystal structure. The formation of Zn-doped HAp was achieved above 900°C only. Zn-doped HAp has the $Ca_{10}Zn_x(PO_4)_6(OH)_{2-2x}O_{2x}$ ($0 < x \leq 0.25$) chemical composition with a constant Ca/P ratio of 1.67 due to the insertion mechanism into the hexagonal channel. Samples heat treated at 500 °C were almost single phase, HAp did not incorporate Zn and about half of the Zn atoms incorporated during the synthesis are not observable by X-ray powder diffraction (contained in an amorphous compound or physisorbed at the HAp surface). The reversible formation of Zn-doped β-TCP phase was observed at 600°C, reached its maximum content at 900°C and almost vanished at 1100°C.

DISCUSSION & CONCLUSIONS: The results presented here strengthen the mechanism of Zn insertion in the interstitial 2b Wyckoff position of the HAp structure, and explain the origin of the contradictory reports in the corresponding literature.

REFERENCES: [1] K. Matsunaga, H. Murata, T. Mizoguchi, A. Nakahira, *Acta Biomater*., 2010, **6**(6):2289-93. [2] Y. Tang, H.F. Chappell, M.T. Dove, R.J. Reeder, Y.J. Lee (2009) *Biomater*, 2009 **30**(15):2864-2872. [3] S. Gomes, J.-M. Nedelec, E. Jallot, G. Renaudin (2012), *Acta Biomater* **8:**1180-89. [4] S. Gomes, G. Renaudin, E. Jallot, J.-M. Nedelec (2011) *Chem Mat* **23**(12) 3072-85.

Silver-nanoparticle induced cytotoxicity in rat brain endothelial cell culture

S Grosse[1], T Syversen[1]

[1] *Department of neuroscience, NTNU, Trondheim, NO*

INTRODUCTION: Silver nanoparticles are among the most widely used nanomaterials in medicine, household products and industry [1]. Due to increasing exposure of these particles to humans, it is necessary to examine potential adverse health effects. It has been shown that nanoparticles are able to migrate to the brain [2]. However, studies on nanoparticle-induced neurotoxicity are limited. Therefore, this *in vitro* study investigated the cytotoxic effects of 10, 50 and 100 nm sized, citrate-coated silver nanoparticles (AgNPs) in rat brain endothelial (RBE4) cells. In addition, metal ion release from the particles was measured to elucidate the toxicity mechanism of AgNPs.

METHODS: Characterisation of the AgNPs was done by the manufacturer (Nanocomposix, San Diego). Original AgNP solutions were diluted in cell culture medium with 10% FBS to the desired particle test concentrations and vortexed thoroughly before each experiment to assure proper dispersion and reduce agglomeration. $AgNO_3$ was used as silver ion-source. RBE4 cells were treated with various concentrations of AgNPs and $AgNO_3$ for a maximum of 24h (exception: colony formation assay). As cytotoxicity endpoints were used membrane integrity and proliferation ability, assessed with Neutral red (n=3) and colony formation assay (n=2), respectively.

AgNPs were separated from Ag^+-ions using ultracentrifugation. The supernatant containing the Ag^+-ions was measured with HR-ICP-MS. The amount of released Ag^+-ions was used in the cytotoxicity assays for comparison with the effects observed with the AgNPs.

Results of cytotoxicity tests are given as mean ± SD. Student's t-test was used to calculate significant difference from control ($p < 0.05$).

RESULTS: Exposure of RBE4 cells to AgNPs lead to impairment of membrane integrity, dependent on particle size (with the smallest particles being most toxic), particles surface area, dose and exposure time (Fig.2). Colony formation was inhibited by 1 µg/ml AgNPs. Only a low amount of Ag^+-ions (54 ng/ml to 3 µg/ml) was found to be released from the particles within 24h. Exposure to these Ag^+-ion-concentrations induced less damage to RBE4 cells – in terms of membrane integrity and proliferation ability.

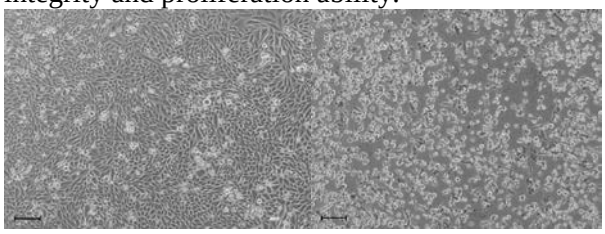

Fig.1: Right: RBE4 cells after 24h exposure to 10 nm AgNPs at 25 µg/ml; left: Control. Pictures are shown with 50 µm magnification bar.

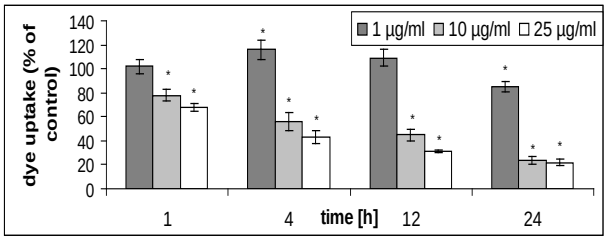

Fig.2: Neutral red uptake in RBE4 cells after exposure to 10 nm AgNPs at 1, 10 and 25 µg/ml for 1, 4, 12 and 24h. Data shown as mean ± SD. Asterisk (*) denotes significant difference from control ($p < 0.05$).

DISCUSSION & CONCLUSIONS: Citrate-coated AgNPs impaired membrane function and proliferation ability of RBE4 cells (10 nm AgNPs were most toxic). Our findings suggest that AgNP toxicity is not solely explainable by the release of toxic silver ions. These results are in agreement with findings from other studies on AgNPs [3,4]. It is likely that other properties attributed to the nanoparticles contributed to the observed effects.

REFERENCES: [1] S. Wijnhoven, W. Peijnenburg, C.A. Herberts, et al (2009) *Nanotoxicology* **3**:109-38. [2] G. Oberdorster, Z. Sharp, V. Atudorei, et al (2004) *Inhal Toxicol* **16**:437-45. [3] C. Beer, R. Foldbjerg, Y. Hayashi, et al (2012) *Toxicol Lett* **208**:286-92. [4] E. Navarro, F. Piccapietra, B. Wagner, et al (2008) *Environ Sci Technol* **42**:8959-64.

ACKNOWLEDGEMENTS: We thank Lars Evje for the HR-ICP-MS measurements.

The chemical and mechanical debridement combined effect is more effective on smooth than rough titanium surface

E Gustumhaugen[2], J Lönn-Stensrud[3], AA Scheie[3], A Ekfeldt[2], SP Lyngstadaas[1], S Taxt-Lamolle[1]
[1]*Department of Biomaterials*, [2]*Department for Prosthodontics*, *Institute for Clinical Dentistry*,
[3]*Department of Biofilm and Signaling*, *Institute for Oral Biology, University of Oslo, Norway*

INTRODUCTION: The success of an implanted titanium (Ti) dental implant is measured by its stability over time. However, implant failure have been reported to be due to bacteria infection and biofilm establishment in the peri-implant area affecting soft and hard tissue [1]. A wide range of decontamination techniques have been suggested, both chemical and mechanical, but few scientific reports exist on the topic. The aim of this *in vitro* study was to quantify the efficiency of combining chemical and mechanical debridement methods on three different Ti surfaces inoculated with Staphylococcus epidermidis (S. epidermidis), contra chemical debridement alone.

METHODS: Three Ti surfaces were characterised and S. epidermidis were inoculated on these surfaces. NaCl (0.9 vol.%), EDTA (12 vol.%), H_2O_2 (3 vol.%) or H_2O_2+TiO_2 nanoparticles (Degussa Aeroxide P25, Hanau-Wolfgang, Germany) served as chemical debridement agents, while TiBrush™ (Straumann, Basel, Switzerland) was used as mechanical debridement tools. The contaminated surfaces were cleaned either by chemical debridement alone, or combined with mechanical debridement. Biomass still attached to surfaces after cleaning was measured by safranin staining, while its viability was assessed by re-incubating the samples after debridement.

RESULTS: Surface average roughness (S_a) of the samples were measured at 2.22 ± 0.19 µm for group A, 0.19 ± 0.02 µm for group B, and 1.99 ± 0.10 µm for group C. *Fig. 1* shows these surfaces before and after incubation. When chemical debridement agents were used alone, H_2O_2-containing products were the most efficient in reducing biomass from the three surfaces as well as viability (*Fig. 2*). When combining chemical and mechanical debridement, further reduction of biomass and viability was observed with higher effects surface with low S_a value (group B).

DISCUSSION & CONCLUSIONS: Combining H_2O_2-containing chemical agents with mechanical debridement (TiBrush™) provided best biomass removal and lowest bacterial re-growth. Smooth Ti surfaces were easier to clean than rough ones.

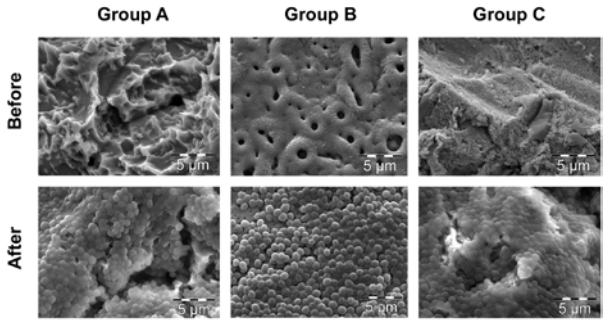

Fig. 1: SEM scans before and after inoculation of the test surfaces (5000x).

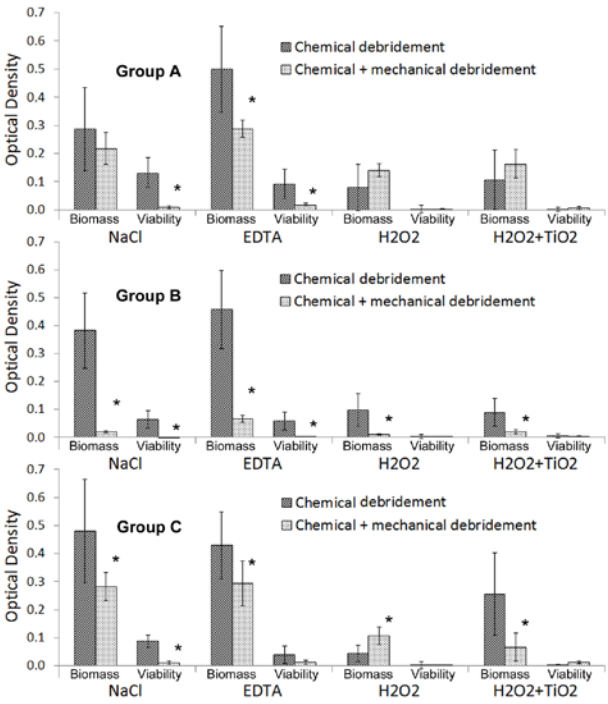

*Fig. 2: Biomass and viability optical densities after chemical and chemical+mechanical debridement. Statistical analysis was run for each pair comparing debridement techniques (N=6, * if p<0.05).*

REFERENCES: [1] A. Mombelli, N.P. Lang (2000) *Periodontol* **4**:81-5.

ACKNOWLEDGEMENTS: To Institut Straumann AG (Basel, Switzerland) for kindly providing material for this study.

Ultra-porous ceramic titanium dioxide scaffold show excellent bone healing when placed in rabbit peri-implant cortical defect model

Håvard J. Haugen[1*], Marta Monjo[2], Marina Rubert[2], Anders Verket[1], S. Petter Lyngstadaas[1], Jan Eirik Ellingsen[3], Hans Jacob Rønold[3], Johan Caspar Wohlfahrt[1]

[1]Department of Biomaterials, [2]Department for Prosthetic Dentistry, Institute for Clinical Dentistry, University of Oslo, Norway, [3]Department of Fundamental Biology and Health Sciences, IUNICS, University of Balearic Islands, Palma de Mallorca, Spain

INTRODUCTION: A variety of bone substitutes from natural to synthetic materials have been developed. One of the major obstacles with synthetic osteogenic bone grafts is their lack of mechanical strength. However, we have showed that it is possible to produce mechanical loadable ceramics based on TiO2 [1]. This is the very first study were the ultra-porous TiO2 bone grafts are used in vivo. The aim was to evaluate the performance of the recently developed ultra-porous TiO2 bone bone grafts in a rabbit peri-implant tibial bone critical size defect model.

MATERIALS & METHODS: The bone grafts were prepared by the polymer sponge method as previously described [1]. The animal model used is a modification of a well-established rabbit tibia model [2]. Seven New Zealand White female rabbits, 6 months old and 3.0-3.5 kg, were used in this study. Real-time PCR was performed to determined inflammation: interleukin-6 (IL-6), interleukin-10 (IL-10) and tumour necrosis factor-α (TNF-α). The specimens were examined using a microCT. Histological sections were prepared according to the cutting-grinding technique described [3] and stained with Van Gieson.

RESULTS: Gene expression of selected inflammatory markers, IL-6, IL-10 and TNF-alpha, showed no significant differences between sham and TiO2 bone graft. 3D bone morphometric parameters and BMD from the cortical section of the tibial bone showed significantly higher bone volume ($p = 0.037$), bone surface ($p < 0.001$) and bone surface to volume ratio ($p < 0.001$) for TiO2 bone graft as compared to sham. Also for the bone marrow section there was significant difference between the bone volume ($p = 0.007$), percentage bone volume ($p = 0.0028$), bone surface to volume ratio ($p = 0.006$) and BMD ($p < 0.001$) for TiO2 bone graft when compared to sham (*Fig 1*).

The histological evaluation of the defects implanted with the TiO_2 bone graft showed predominantly newly formed woven bone in the cortical compartment of the defects. Signs of newly formed blood vessels were also seen indicating an active bone regrowth in the area of interest. There were no signs of pathology, inflammatory reactions or foreign body reactions in any of the examined sections, and no instances of fibrous encapsulation of the bone graft material were observed.

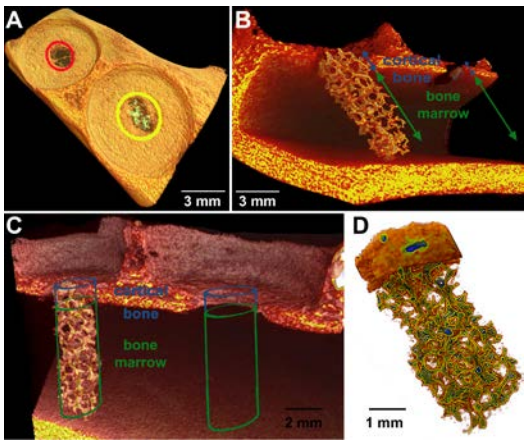

Fig. 1 3D model from microCT of peri-implant defect model (A), where the bone graft was placed (B-D) and integrated to cortical bone

DISCUSSION & CONCLUSION: The results demonstrate that the novel ultra-porous TiO2 bone graft promotes new bone formation in a peri-implant critical size bone defect, and that the open porosity of this scaffold promotes bongrowth also onto the adjacent implant surface.

REFERENCES: [1]Fostad G et al (2009) *J Eur Ceram Soc* **29**:2773-81. [2]Ronold HJ et al (2002) *Biomaterials* **23**:4211-19. [3]Donath K, Breuner G. (1982) *J Oral Pathol* **11**:318-26.

ACKNOWLEDGEMENTS: This work was supported by Eureka-Eurostars Project E!5069 NewBone, Interempresas Internacional Program (CIIP20101024) from the Centre for the Development of Industrial Technology (CDTI) and the Ministry of Science and Innovation from the Spanish Government (Torres Quevedo contract to MR and Ramón y Cajal contract to MM).

In vitro performance of Sr-doped calcium phosphate hollow spheres

G Hulsart Billström[1], E Carlsson[1], S Larsson[1], W Xia[2], H Engqvist[2]

[1] *Department of Orthopedics, Uppsala University, Sweden,*[2] *Department of Engineering Sciences, Uppsala University, Sweden*

INTRODUCTION: Strontium is an interesting element proposed to induce bone, where the true mechanism of action is not fully known [1]. Previous in vitro studies have indicated that Sr might have a positive effect on bone formation by inhibiting bone resorption and through enhanced endosteal and trabecular bone formation [2]. The aim of this study was to create a novel Sr-doped calcium phosphate composite in the form of hollow spheres (SrCaP) and examining its biological effects in vitro in a cell viability study.

METHODS: SrCaP were synthesized and examined in scanning electron microscopy, X-ray diffractometry and scanning transmission electron microscope. SrCaP extractions at concentrations between 0-1000 µg/ml were made by incubating material with complete medium at 37° C for 24 h, then adding it to cells. Cell viability was assessed using MTS assay after 7 days.

RESULTS: The SrCaP particles were spherical, with a hollow core. The particles were approximately 1 µm in diameter and the shell had a thickness of approximately 150 nm. None of the concentrations were cytotoxic in vitro. Significantly higher metabolism was seen with the concentrations of 400 and 600 µg/ml compared to control.

*Table 1. Cell viability of UMR 106 cells after 7 days after exposure to concentrations of SrHA. Significantly higher viability in the 400 and 600 µg/ml groups compared to the control (One way, ANOVA, Dunnett's multiple comparisons test; n=6; ***P<0.0001).*

SrHA concentration in extract	Cell viability (mean ± SD)
0 µg/mL	0,406 ± 0,081
50 µg/mL	0,408 ± 0,072
100 µg/mL	0,410 ± 0,010
200 µg/mL	0,806 ± 0,396
400 µg/mL	1,419 ± 0,368 ***
600 µg/mL	1,189 ± 0,446 ***
800 µg/mL	0,596 ± 0,087
1000 µg/mL	0,707 ± 0,046
*** P<0.0001	

DISCUSSION & CONCLUSIONS: Sr CaP spheres showed a good biocompatibility in vitro with elevated cell viability, which corresponds to earlier studies with strontium substituted bioactive glass by Gentleman et al [3].

REFERENCES: [1.] W.E. Cabrera, I. Schrooten, M.E. De Broe et al (1999) *J Bone Miner Res* **14**(5):661-8.[2.] P.J. Marie, D. Felsenberg, M.L. Brandi (2011) *Osteoporos Int* **22**(6):1659-67. [3.] E. Gentleman, Y.C. Fredholm, G. Jell et al (2010) *Biomater* **31**(14):3949-56.

ACKNOWLEDGEMENTS: The Swedish Research Council and BIOMATCELL, VINN Excellence Center of Biomaterials and Cell Therapy are gratefully acknowledged for financial support.

α-Tricalcium phosphate hydration to calcium deficient hydroxyapatite in calcium phosphate cements

Z Irbe[1], N Borodajenko[1], J Locs, L Berzina-Cimdina[1]

[1] *Institute of General Chemical Engineering, Riga Technical University, Riga, LV*

INTRODUCTION: Calcium phosphate cements (CPC) are inorganic bone cements, that are bioactive and bioresorbable. In this work cements based on α-tricalcium phosphate (α-TCP) are investigated. α-TCP is hydrated during cement setting and aging to form calcium deficient hydroxyapatite (CDHA). CDHA in set bone cements is more similar to mineral phase of bone than stoichiometric hydroxyapatite ceramics. Properties of CDHA (also biological [1]) can vary substantially and are dependent on conditions during crystallization. In previous research it is found that by changing initial pH of the cement liquid (sodium phosphate buffer solutions) cement setting [2] can be controlled as it affects reaction rate [3]. Therefore it was investigated how initial pH of the cement affects the crystallization of CDHA.

METHODS: α-TCP was synthesized by heating a mixture of $CaCO_3$ and $CaHPO_4 \cdot 2H_2O$ (molar ratio – 1:2) to 1300°C for 3h and 1400°C for 1h and quenching to room temperature. α-TCP was milled to obtain particles sized 10 - 0.5 µm. Sodium phosphate buffer solutions (0.5 M phosphate ions, pH range 9.0 – 4.3) were used as liquid phase. Solid/liquid ratio 1.75 g/ 1 ml was used. Cement paste was placed in simulated body fluid after mixing and incubated at 37°C for 0.5 h to 4 days. Cement reaction was stopped by suspending in ethanol and drying at 50°C.

Samples were investigated by Fourier-transform infared spectroscopy (FTIR), X-ray diffraction (XRD) and scanning electron microscopy (SEM).

RESULTS: Morphology of cements differs from the first minutes after mixing, and continued to differ between them even after 4 days. Newly formed crystals in cements are larger if initial liquid phase pH is more acidic (see Fig. 1). Thin plate-like crystals are characteristic of octacalcium phosphate.

XRD results show that conversion of α-TCP to CDHA is slower if more acidic initial pH is used, compared to more basic initial pH of liquid phase. After α-TCP hydration is complete, CDHA peaks are higher and sharper if more basic initial liquid phase pH is used. For cements with acidic initial liquid phase pH (< 7), there is a peak at 4.7° 2θ, identifying presence of octacalcium phosphate, which is most prominent at 5 h. FTIR results show that there are no [OH] groups (characteristic of CDHA) until cement is 1-2 days old.

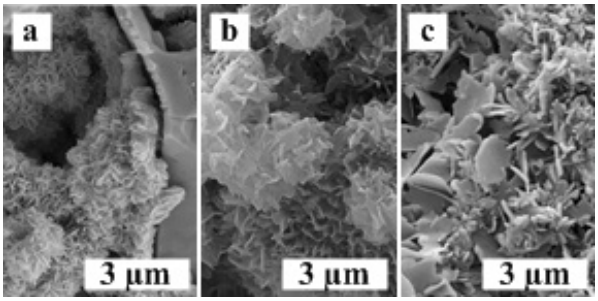

Fig. 1: SEM micrographs of cement mass, aged 5 h (fracture surface). a – initial liquid phase pH 8, b – pH 7, c – pH 6.

DISCUSSION & CONCLUSIONS: Results show that initial pH of the liquid phase for α-TCP based cements significantly influences crystal morphology and setting reaction.

FTIR results show that CDHA formation process continues for several days, even after all α-TCP is hydrated. CDHA phase formed after hydration of α-TCP lacks characteristic [OH] groups during first 2 days.

In vitro tests using osteoblast cell line (MG63) show differences between cements (after reactions in cements are complete). In vivo tests in rabbits show good compatibility and complete healing for all cements tested (initial liquid phase pH 8, 7 und 6).

REFERENCES: [1] P. Sponer, M. Strnadova, K. Urban (2011) *Int Orthop* **35**:1553-60. [2] Z. Irbe, L. Vecbiskena, D. Loca, et al (2011) *Proceedings of ECERS XII*, 340. [3]M. Bohner, T.J. Brunner, W.J. Stark (2008) *J Mater Chem* **18**:5669-75.

ACKNOWLEDGEMENTS: This work has been supported by the European Social Fund within the projects «Support for the implementation of doctoral studies at Riga Technical University» and «Multidisciplinary Research in Biomaterials Technology of New Scientist Group», No.2009/0199/1DP/1.1.1.2.0/ 09/APIA/VIAA/090.

Controlled drug-delivery using mesoporous implants to enhance osseointegration

J Karlsson[1,*], N Hermankaya[2], A Palmquist[2], M Halvarsson[3], P Tengvall[2] and M Andersson[1]

[1] Dept. Chemical and Biological Engineering, Applied Chemistry, Chalmers University of Technology, Gothenburg, Sweden. [2] Dept. Biomaterials, Sahlgrenska Academy at University of Gothenburg, Gothenburg, Sweden, and [3] Dept. Applied Physics, Microscopy and Microanalysis, Chalmers University of Technology, Gothenburg, Sweden

INTRODUCTION: There is an ongoing development in the field of implants to enhance osseointegration [1]. In this study, a drug-delivery system has been developed to further enhance the osseointegration. The system consists of a mesoporous TiO_2 thin film that is deposited on titanium implants, with the purpose of controlling the local delivery of active substances that stimulate bone growth. Drug release studies from mesoporous TiO_2 thin films have been evaluated using quartz crystal microbalance with dissipation monitoring (QCM-D) [2]. Two drugs were evaluated, the osteoporosis drug, Alendronate, and the estrogen receptor, Raloxifene.

METHODS: Mesoporous TiO_2 was synthesized using the evaporation induced self assembly (EISA) method [3]. Spin-coating was used as coating procedure to form mesoporous (test) and nonporous (control) TiO_2 thin films. To characterize the samples, transmission electron microscopy (TEM), scanning electron microscopy (SEM), X-ray photoelectron spectroscopy (XPS), X-ray diffraction (XRD) and nitrogen adsorption were used. Quartz crystal microbalance with dissipation monitoring (QCM-D) was used to monitor the adsorption and the release for both Alendronate and Raloxifene (0.8 mg/ml) from mesoporous and nonporous surfaces coated on QCM crystals.

RESULTS: TEM, SEM and nitrogen adsorption analysis showed that mesoporous TiO_2 films were obtained, having a narrow pore size distribution, and that the pore size was 6 nm. From SEM images, it could be seen that pores were facing out from the surface. QCM-D results presented as the real mass as a function of time is shown in Figure 1. The results show that the presence of mesopores brought a 30 times higher adsorption of Alendronate. Furthermore, the Alendronate was released slowly from the mesoporous films. In the case of Raloxifene, which is less polar then Alendronate, the TiO_2 films were surface modified with dichlorodimethylsilane using silane chemistry. QCM-D monitoring the adsorption of Raloxifene showed that the amount adsorbed was about twice as high on the mesoporous compared to the nonporous films. As for Alendronate a controlled release profile was obtained.

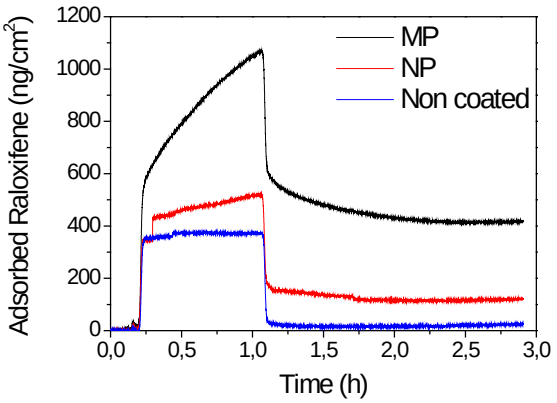

Fig. 1: QCM-D monitoring of adsorption and release of Raloxifene from a mesoporous (MP), a nonporous (NP) and a non coated surface. At 0.2h, the flow of Raloxifene (0.8 mg/ml) is added and continuous up to 1.1h, then rinsing with methanol starts.

DISCUSSION & CONCLUSIONS: Mesoporous TiO_2 thin films were successfully prepared having pores directed out from the surface, and with a pore size of 6 nm. QCM-D was shown to be suitable for monitoring the drug release from the films. A controlled release could be achieved using mesoporous thin films, both for a polar (Alendronate) and a non-polar (Raloxifene) drugs. Mesoporous TiO_2 thin films are interesting candidates to be used as implant coatings for controlled local drug-delivery.

REFERENCES: [1] R. Jimbo, et al (2011) *Acta Biom.*, **7**:4229-4234. [2] M. Rodahl and B. Kasemo (1996) *Sensors and Actuators a-Physical* **54**:448-456. [3] M. Andersson, et al (2005) *Chem. Mater.*, **17**:1409-1415.

ACKNOWLEDGEMENTS: We gratefully thank the Materials Area of Advance at Chalmers University of Technology for providing the financial support.

Improved surface resolution for porous titanium implants manufactured through Electron Beam Melting

J Karlsson[1], A Snis[2,5], A. Palmquist[3,5], H Engqvist [4,5], J Lausmaa [1,5]
[1] SP Technical Research Institute of Sweden, Borås, Sweden. [2] Arcam AB, Mölndal, Sweden, [3]Department of Biomaterials, Sahlgrenska Academny at University of Gothenburg, Göteborg, Sweden, [4] Applied Materials Science, Uppsala University, Uppsala, Sweden, [5] BIOMATCELL Vinn Excellence Center of Biomaterials and Cell Therapy

INTRODUCTION: Electron Beam Melting (EBM) is an additive manufacturing process that can produce parts in biocompatible titanium grades from a powder stock material. In EBM, parts are manufactured layer-by-layer based on a 3D CAD model. It allows the production of advanced geometries that are not possible to manufacture with conventional machining [1]. An attractive feature is the production of porous lattice structures for medical applications [2]. Such porous structures (Fig 1) have been evaluated in a sheep model, where a high degree of osseointegration was shown [3]. However these structures are rough and control of the strut size and appearance are limited with today's EBM technology [4]. This study presents the result from the use of a small sized powder stock material. The aim was to use the smaller powder to enhance surface resolution and produce EBM lattice structures with better surface control and finer morphology for biomedical applications.

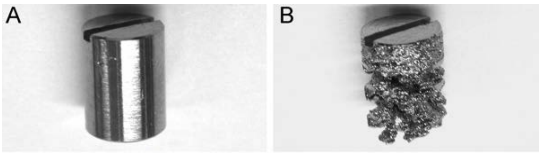

Fig. 1: A) surface manufactured through conventional machining. B) a porous structure manufactured by EBM.

METHODS: Ti6Al4V powder of size 25-45 µm was used to produce solid parallelepipeds and cylinders of varying thickness in an Arcam A1 machine. The same geometries were also produced using a powder of size 45-100 µm, which is the current standard. Parts with a defined porous structure in the form of lattice structures were also produced using both powders. Chemical composition was analysed with Time-of-Flight Secondary Ion Mass Spectroscopy (ToF-SIMS), X-ray Photoelectron Spectroscopy (XPS) and Inductive Coupled Plasma Optical Emission Spectroscopy (ICP-OES). Scanning Electron Microscopy (SEM) was used to characterize the appearance of powders and produced parts. Stereo SEM was used to characterize surface roughness parameters.

RESULTS: The SEM pictures in Fig. 2 show the surfaces of EBM built parts. The left picture (a) show a surface built from 45-100 µm powder. The right image (b) show a surface built with 25-45 µm powder.

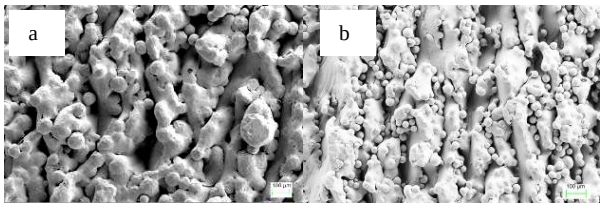

Fig. 2: a) SEM picture of EBM built surface with powder 45-100 µm. b) SEM picture of EBM built surface with powder size 25-45 µm.

In Fig. 3 the elemental composition of the built parts are shown. XPS and ToF-SIMS analyses showed that the surfaces are covered by a surface oxide composed mainly of TiO_2.

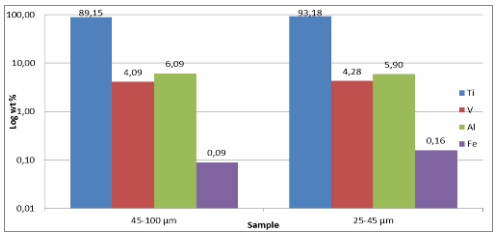

Fig.3: Chemical composition of parts built from 45-100 µm and 25-45 µm.

DISCUSSION & CONCLUSIONS: The surface appearance and surface resolution will differ between the builds of the two different powders. This will in turn affect the resolution of the porous structures built in lattice structures with the EBM. No differences are found in chemical composition between the builds.

REFERENCES: [1] www.arcam.com, [2] O.L.A. Harrysson et al (2008) *Materials Science and Engineering: C* **28**(3): 366-73, [3] A Palmqvist et al (2011) *J Biomater Appl* **In Press**, [4] L.E. Murr et al (2009) *Materials Characterization* **60**(2): 96-105.

Novel approach for the synthesis of fluorescent silica nanoparticles

A Lemelle[1], S Morgan[2]

[1] *Laboratoire d'Ingénierie et Sciences des Matériaux, University of Reims, France.* [2] *Cranfield Health, Cranfield University, UK*

INTRODUCTION: The use of fluorescent silica nanoparticles (FSNPs) is being widely investigated for medical applications [1]. However, FSNPs still face some limitations due to the inability of the traditional synthesis methods (Stöber method and microemulsions) to encapsulate all fluorophores. This gap translates by the near absence of systems containing photosentizers (for photodynamic therapy) and sensor dyes (for diagnostics). Furthermore, it also precludes the design of multifunctional nanoparticles containing several dyes simultaneously for combined diagnostics, imaging, and/or therapy.

To develop a "universal" carrier, we have adopted a method based on the alteration of the silica matrix with organic moieties (hydrophobic or charged groups) to stabilize the fluorophores. We also use the amino acid catalysis route as a mean to produce very small particles [2]. We have investigated the effects of the particle composition and tested the capacity of the hybrid particles to carry fluorophores with various physical and chemical properties.

METHODS: Fluorescent silica nanoparticles were synthesised by hydrolysis and co-condensation of tetraethyl orthosilicate (TEOS) and vinyltriethoxysilane (VTEOS) in an aqueous arginine solution containing a fluorescent dye. Ten fluorophores differing in terms of hydrophilicity, charge, and excitation/emission wavelengths were tested. Phenyltriethoxysilane (PhTEOS) and aminopropyltriethoxysilane (APTES) were also employed instead of/in combination with VEOS.

The nanoparticle size was characterised by both SEM and DLS, whilst their composition was determined by infrared spectroscopy. The optical properties of the particles were assessed by fluorescent spectroscopy.

RESULTS: SEM and DLS results indicate that the hybrid nanoparticle diameter varies with the organosilane/TEOS ratio. In the VTEOS and PhTEOS cases, the particle diameter remained smaller than 100 nm except for full VTEOS and PhTEOS systems that yielded particles several hundreds of nanometres in diameter. Addition of APTES to the VTEOS hybrids did not induce any variation up to 10 molar% of APTES above which a strong aggregation was observed. Infrared spectroscopy confirmed the formation of the silica network and of the presence of vinyl, phenyl, and/or amine groups in the particles.

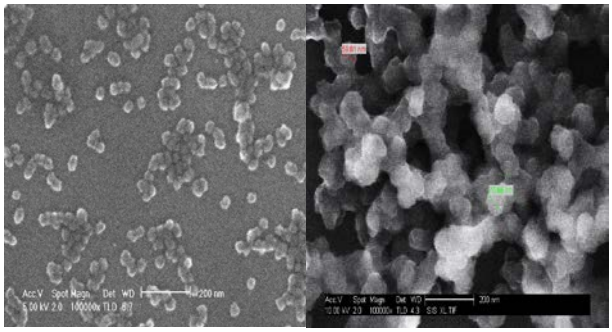

Fig. 1: SEM images of VTEOS (50 % VTEOS, left) and PhTEOS hybrids (10 % PhTEOS, right)

Neither the VTEOS nor the PhTEOS hybrid particles were able to entrap all of the fluorophores tested. More precisely, none of the negatively charged dyes were combined with the nanoparticles. However, addition of small amount of the positively charged APTES to the VTEOS hybrids was a paying strategy and was a solution for the encapsulation of all ten fluorophores.

DISCUSSION & CONCLUSIONS: We have shown that modulating the particle composition according to the fluorophore charge is a solution to get closer to a universal carrier. Furthermore, the amino acid route is naturally able to restrict the particle diameter to a few tens of nanometers. We have still to demonstrate that it is possible to synthesize core-shell structures formed of successive hybrid layers or to coat other nanoparticles such as superparamagnetic particles. Yet, our system opens new opportunities for the design of multifunctional nanosystems by combining into a single structure fluorophores such as, photosnsitizers, photoluminescent and sensor dyes.

REFERENCES: [1] J. Yan, M. Estevez, et al (2007) *Nano Today*, **2**:44-50. [2] K.D. Hartlen, A.P. Athanasopoulos, V. Kitaev, (2008) *Langmuir* **24**:1714-20.

Sol-gel synthesis of bioactive glass powders using weak acids as catalyst

A Lemelle[1], H Benhayoune[1], J Faure[1]

[1] *Laboratoire d'Ingénierie et Sciences des Matériaux, Université of Reims, France*

INTRODUCTION: Bioactive glasses (or bioglasses) are used for bone repair and regeneration. Their bioactivity is strongly influenced by their composition but also by their synthesis route. The most bioactive glass is known as 45S5 Bioglass® (45 wt.% SiO_2, 24.5 wt.% Na_2O, 24.5 wt.% CaO, 6 wt.% P_2O_5) and is traditionally produced by melting-quenching [1]. Elaborating 45S5 bioglass by the sol-gel method is of high interest owing to the increased porosity and specific surface of the materials that in turn enhance their bioactivity. However, the exact 45S5 composition has not been achieved by sol-gel yet. Here, we explore the potential of weak acids - including amino acids - to catalyse the sol-gel reactions. We investigate the effects of various parameters such as acid concentration, heat treatment, or double catalysis on the ceramic composition and further assess the powders' bioactivity.

METHODS: Bioglass gels were synthesised by mixing the silicon and phosphorous precursors to an aqueous solution of either citric acid (CA), aspartic acid (AA), or glutamic acid (GA). In a second time, the sodium and calcium precursors were slowly added and the sols were stirred until gelation. Resulting gels were dried and the powders were grounded for characterization.

The bioglass composition was assessed by energy-dispersive X-ray spectroscopy (EDX) as well as Fourier transform infrared spectroscopy (FTIR) and Raman spectroscopy. X-ray diffraction (XRD) analyses were carried out to determine the crystallinity and phases of the gels. Bioactivity was determined by immersion of the powders in simulated body fluid (SBF) followed by imaging with a scanning electron microscope (SEM) and FTIR, Raman, and XRD analyses.

RESULTS: EDX spectra showed that CA is the most promising catalyst and is nearly able to produce the 45S5 bioglass (Table 1). In comparison, conditions with AA and GA were less optimal and the powders generally lacked of silica and sodium. For the three acids, raising the temperature had little effect on the composition whilst the double catalysis (addition of a second basic catalyst at the end of the procedure) tended to lower the silicon percentage. FTIR and Raman spectra revealed the presence of Si-O-Si peaks from the silica network as well as P-O bonds.

XRD diffractograms displayed some peaks related to the $Na_2Ca_2Si_3O_9$ phase, which is known to play a key role in the ceramic bioactivity, and showed a high crystallinity. In contrast, the commercial 45S5 bioglass displayed a very weak peak of the $Na_2Ca_2Si_3O_9$ phase but was overall amorphous. The crystallinity of the sol-gel powders was further confirmed by FTIR and Raman spectroscopy.

The formation of a hydroxyapatite layer onto a material immersed in SBF is the sign of its bioactivity. Here, our test demonstrated that a calcium phosphate layer had been created after only 4 hours with partial dissolution of the bioglasses. Changes were hardly detectable in the commercial 45S5 under the same conditions and required longer immersion in SBF.

Table 1. Atomic composition of some CA and amino acid-catalysed powders.

At %	O	Na	Si	P	Ca
Theory	55.3	17.1	16.3	1.8	9.5
45S5©	56.2	15.9	16.5	1.7	9.7
CA	54.5	16.7	15.9	1.6	11.3
AA	56.2	15.6	13.9	1.9	12.4
GA	55.6	14.4	13.5	1.8	14.7

DISCUSSION & CONCLUSIONS: CA catalysis appears as a better strategy than the traditional nitric acid to synthesize 45S5 powders, also with some minor elemental variations. Compared to the commercial 45S5 produced by melting-quenching, the sol-gel powders were more crystalline and also more bioactive. This is an important feature translating the ability of the new bioglasses to quickly create bonds with bones. Amino acids proved less successful. However the possibility of keeping these biomolecules into the powders may reveal important for the cellular response. Further work will include assessing the toxicity and the response of bone cells to the sol-gel powders.

REFERENCES: [1] L. Hench, (2006) *J Mater Sci: Mater Med*, **17**:967-78.

Photocatalytic and bioactive TiO_2 thin films deposited by vaccum arc

M Lilja[1,3], K Welch[1], M Åstrand[3], H Engqvist[2], M Strømme[1]

[1]Division for Nanotechnology and Functional Materials, [2]Division of Applied Materials Science, Department of Engineering Sciences, The Ångström Laboratory, Uppsala University, Sweden, [3]Sandvik Tooling Sverige AB, Lerkrogsvägen 19, 12680 Stockholm, Sweden

INTRODUCTION: Improving biomedical implants via deposition of functionalised surface coatings is a growing field of research. With respect to implant surfaces, infections present a major problem, and result mostly from the contamination of the surface by bacteria during surgery. UV irradiation induced photocatalysis on crystalline TiO_2 implant surfaces may present a promising way to decontaminate surfaces while at the same time providing a bioactive surface for enhanced tissue integration.

METHODS: Four coating series on Ti-6Al-4V substrates (Ø=9mm) were made with variations in deposition time, temperature, bias voltage and oxygen flow and denoted as CAD-time, CAD-temp, CAD-bias and CAD-gradient. The coating microstructure was evaluated by grazing-incidence X-ray diffraction (XRD). Bioactivity tests of all coatings were performed in Phosphate Buffer Saline (PBS) for 24 hours and 7 days at 37°C. The precipitated Hydroxyapaptite (HA) coatings were examined using Scanning electron microscope (SEM) and XRD. The photocatalytic activity (PCA) of the as deposited TiO_2 films was determined from the degradation of Rhodamine B monitored as a function of time.

RESULTS: The PCA of the as deposited coatings was shown to increase with increasing oxide coating thickness up to a thickness of about 250 nm.

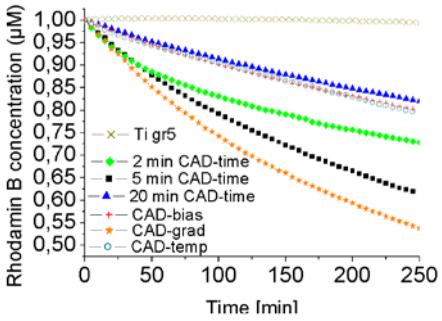

Fig. 1: Photocatalytic activity of the as deposited TiO_2 coatings

Furthermore, the PCA was promoted by the anatase phase, and a tendency of obtaining a higher photocatalytic activity with smaller anatase grain size was also indicated. Bioactivity of all as deposited coatings was confirmed by the growth of uniform layers of HA after 7 days in PBS at 37 °C. After 24 hours enhanced HA formation was seen on coatings with small titanium dioxide grains of the rutile and the anatase phase.

Table 1. Coating structural characteristics

Coating	TiO_2 thickness (nm)	Dominating phase[1]
2 min CAD-time	70	R(110)
5 min CAD-time	150	A(101)
20 min CAD-time	500	A(101)
CAD-temp	450	R(110)
CAD-bias	650	A(101)
CAD-gradient	250 (600)[2]	R(110)

[1]Measured using XRD, where A and R denote the anatase and rutile phases, respectively

[2]total coating thickness is ~600 nm, consisting of a metallic phase of ~350 nm and a gradient oxide phase of ~250 nm

CONCLUSIONS: The results of this study provide an outline for the development of new bioactive implant coatings with photocatalytically induced on-demand antibacterial properties.

ACKNOWLEDGEMENTS: We wish to thank the Swedish Research Council (VR) and the Swedish funding agency Vinnova for financial support of this study.

Apatite coating co-doped with strontium and fluoride using a mineralization method

C Lindahl[1,2], W Xia[1,2], H Engqvist[1,2]

[1] *Applied Materials Science, Department of Engineering Sciences, Uppsala University.*
[2]*BIOMATCELL, VINN Excellence Center of Biomaterials and Cell Therapy, Gothenburg, Sweden.*

INTRODUCTION: Improving the bonding between implant and bone can reduce the risk of implant failure and revision surgery [1]. Strontium is known to have beneficial effects on bone formation by increasing the activity of osteoblast and decreasing the number of osteoclasts [2,3]. Fluoride is known to increase the activity and proliferation of osteoblastic cells [4]. Doping HA coatings on metallic implants with both strontium and fluoride could enable a local delivery of strontium and fluoride ions near the implant site.

METHODS:

Oxidation of Ti plates: Titanium plates (grade 2) were heat treated at 800°C for 1h. Afterwards the plates were immersed in 5M NaOH for 24h and thereafter washed in H_2O and left to dry at 37 °C over night.

Coating method: Modified D-PBS solution was prepared with different concentrations of strontium and fluoride added. Strontium nitrate was used as a strontium source and sodium fluoride was used as a fluoride source. The treated Ti plates were immersed in the modified PBS solution containing strontium and fluoride at 37°C and 60°C for 1 week. Afterwards the plates were gently washed in H_2O and dried at 37°C prior to analysis.

Analysis: The coatings were analyzed using scanning electron microscopy (SEM), Thin film X-ray diffraction analysis (TF-XRD).

RESULTS: Figure 1 show SEM images of strontium and fluoride co-doped apatite coating. The morphology is plate-like and similar to pure HA coatings prepared with the same method. XRD spectra show apatite peaks in the pattern, see Figure 2. The apatite peak around 26° is much sharper than those around 32°.

DISCUSSION & CONCLUSIONS: In this study an apatite coating containing strontium and fluoride was prepared by a mineralization method. This co-doped strontium and fluoride apatite coating can be used to simultaneously deliver strontium and fluoride ions near the implant site *in vivo* combining the positive biological effects of these ions.

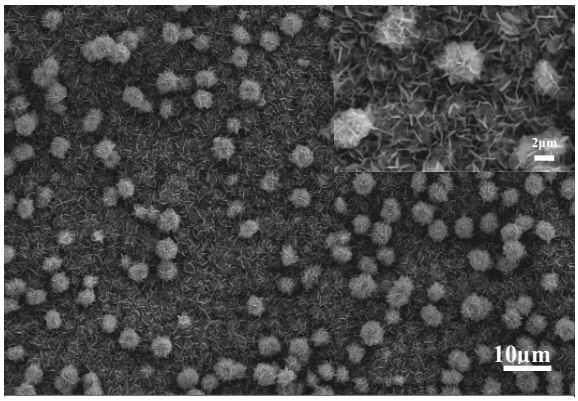

Fig. 1 SEM image of co-doped apatite coating prepared at 37 °C in D-PBS containing 0.06mM Sr and 0.4mM F (006Sr04FPBS-37).

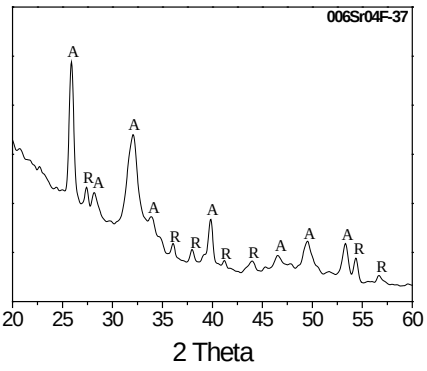

Fig. 2 XRD pattern of strontium and fluoride co-doped apatite coating (A: apatite; R: rutile).

REFERENCES: [1] A.V Zavgorodniy, et al (2011) *J Biomed Mater Res B Appl Biomater* **99B** 58-69. [2]E Canalis, et al (1996) *Bone* **18**: 517-23. [3]PJ Marie, et al (2001) *Calcif Tissue Int* **69**:121–9. [4]J.P Bilezikian, et al (1996) *California: Academic Press Inc.*

ACKNOWLEDGEMENTS: This work was supported by BIOMATCELL VINN Excellence Center of Biomaterials and Cell Therapy

Acrylic bone cement modified with oligo(trimethylene carbonate)

A López[1], A Hoess[1], H Fathali[1], M Ott[1], H Engqvist[1], C Persson[1]

[1] *Materials in Medicine, Division of Applied Materials Science, Department of Engineering Sciences, The Ångström Laboratory, Uppsala University, Sweden*

INTRODUCTION: Some of the clinical and biomechanical data from the past fifteen years, suggests that vertebroplasty increases the risk of additional adjacent vertebral fractures, and that it may be due to the relatively high Young's modulus of poly(methyl methacrylate) (PMMA)–based bone cements [l]. One approach to reduce the modulus could be to copolymerize PMMA with a more flexible polymer. Poly(trimethylene carbonate) (PTMC) is used in biomedical applications [2] and is an excellent candidate for this purpose, due to its low modulus and high strain at break [3]. This study aimed to modify two commercial PMMA bone cements with low molecular weight PTMC, also called oligo(trimethylene carbonate) (oTMC), to test their mechanical properties, and to evaluate the cytotoxicity of their extracts.

METHODS: oTMC 1500 Da was synthesized by bulk ring-opening polymerization of TMC using 1,4-butanediol as co-initiator (100:8 feed ratio) at 160°C in argon. This hydroxyl-terminated prepolymer (0.1 eq) was modified with acrylic endgroups by acrylation with acryloyl chloride (2 eq) in the presence of N,N-diisopropylethylamine (2 eq) and 4-dimethylaminopyridine (0.2 eq). The product was purified by filtration through a column of activated alumina and rotoevaporation of the solvent. The structure of the resulting oTMC-α,ω-acrylate (oTMC-da) was confirmed by H^1 NMR spectroscopy. Selected amounts of oTMC-da were dissolved in the monomeric components of Osteopal®V (Heraeus Medical) and Simplex®P (Stryker), by either adding it or replacing an equal volume of the monomer with it. The cements were cured by mixing the modified monomeric component with the powder as indicated by the fabricant. The mechanical properties were determined from the stress-strain compression data, using an AGS-H universal materials testing machine, according to ASTM F-451. Additionally, the cytotoxicity of cement extracts was investigated on MG-63 cells according to ISO 10993-5.

RESULTS: H^1 NMR spectroscopy confirmed the structure of oTMC-da, which exhibited characteristic peaks at 2.03 (m, -CH_2-), 4.00-4.30 (m, -CH_2-O-), 5.80 (d, *CH, chiral terminal), 6.10 (m, *CH, chiral terminal), 6.40 (d, *CH, chiral terminal). Fig. 1 shows an example of the stress-strain curves for the modified Osteopal®V, in which the Young's modulus varied from 1.60 to 0.05 GPa. The moduli were generally higher for Osteopal®V than for Simplex®P, at the same concentration of oTMC. The extraction media from the modified cements showed slightly higher cytotoxic effects than the extracts from the unmodified ones.

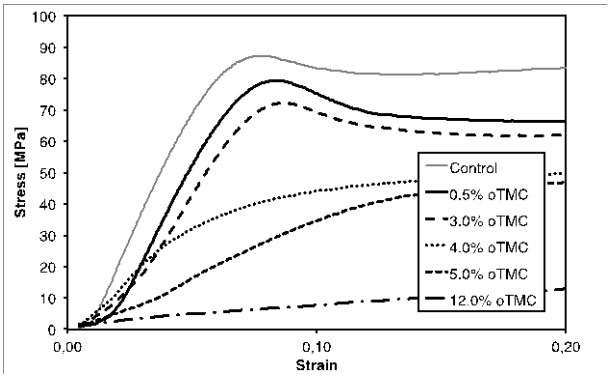

Fig. 1: Stress-strain curves for Osteopal®V including 0.0; 0.5; 3.0; 4.0; 5.0; and 12.0% oTMC added to the monomer.

DISCUSSION & CONCLUSIONS: The results indicated that it is possible to reduce the Young's modulus of PMMA bone cements, and to control their stress-strain curves, by incorporating small amounts of oTMC-α,ω-acrylate 1500 Da. Even though modifying the cements altered the cell viability, the monomer replacement approach reduced the extracts cytotoxicity, probably due to a reduced monomer release. In summary, these materials are potential candidates to develop a new generation of bone cements for treating specific pathologies and different degrees of vertebral osteoporosis.

REFERENCES: [1] A. Boger, P. Heini, M. Windolf, et al. (2007) *Eur Spine J* **16**(12):2118-2125 [2] L.S. Nair, C.T. Laurencin (2007) *Prog Polym Sci* **32**:762-798. [3] A.P. Pêgo, D.W. Grijpma, J. Feijen (2003) *Polymer* **44**:6495-6504.

ACKNOWLEDGEMENTS: Funding from the European Union (VPHOP FP7-ICT2008-223865 and SPINEGO PERG07-GA-2010-268134) as well as VINNOVA (VINNMER 2010-02073) is gratefully acknowledged.

A self-hardening biodegradable cement as a drug delivery vehicle

T Mellgren[1], J Forsgren[2], A Mihranyan[2], H Engqvist[1], C Persson[1]

[1] *Applied Material Science, Department of Engineering Sciences, Uppsala University, Uppsala, Sweden.* [2] *Nanotechnology and Functional Materials, Department of Engineering Sciences, Uppsala University, Uppsala, Sweden*

INTRODUCTION: Injectable, resorbable cements are commonly studied for bone repair, but rarely considered as vehicles for sustained drug release in tissues other than bone. In this study, a self-hardening biodegradable calcium carbonate cement containing the drug hydroxyflutamide was developed. Hydroxyflutamide is used for treatment of pancreas cancer, which is a possible indication for this drug delivery system. Drug release measurements showed a sustained release of the drug for several days.

METHODS: A cement precursor of vaterite phase calcium carbonate was prepared according to a method first descried by Buzágh [1].

First the calcium carbonate powder was prepared as follows. Calcium hydroxide was dispersed in methanol. During stirring, carbon dioxide was bubbled through the dispersion until all of the calcium hydroxide had reacted and formed a gel. When the gel was subsequently dried in air at 70 °C a white powder was obtained. The powder was then stored in a nitrogen atmosphere at 5 ° C. Secondly the cement was prepared by mixing of the calcium carbonate powder with a PBS solution and 10 wt % of the model drug, hydroxyflutamide. The cement was then put into rubber moulds and left to cure at 37 °C and 100 % humidity.

Compression tests were performed on cured cement to evaluate the mechanical strength. The tests were performed on 6 x 12 mm rods after 24 and 48 hours. The chemical compositions of the samples were studied by means of X-ray diffraction analysis. Furthermore, the drug elution properties of the cement were measured with a dissolution tester and UV-absorption analysis. The elution was carried out in deionized water at 37 °C on 3 x 6 mm cylinder shaped samples.

RESULTS: X-ray diffraction analysis of the synthesized calcium carbonate powder indicates that it consisted of vaterite, calcite and amorphous calcium carbonate (ACC). 24H after the same powder was mixed with PBS, cured at 100 % humidity at 37 °C, the vaterite and ACC had transformed into aragonite.

The result from the drug elution measurements is presented in figure 1. 80 % of the drug had been released after four days and 100 % had been released after 11 days.

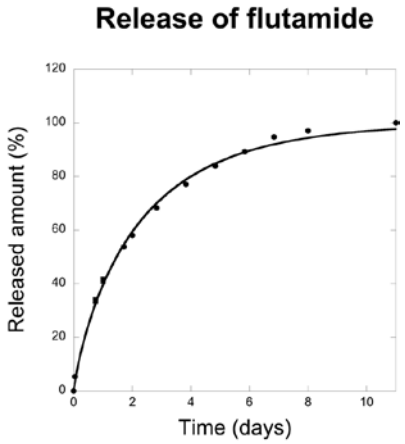

Fig. 1: Release of flutamide in deionized water at 37 °C.

The compression strength of the cement without hydroxyflutamide was 3.1 MPa (std 0.4 MPa) after 24H and 3.3 MPa (std 0.9 MPa) after 48H. With 10 wt % of hydroxyflutamide in the cement the compression strength was measured to be 1.9 MPa (std 0.6 MPa)

DISCUSSION & CONCLUSIONS: The results from this study prove the possibility of using biodegradable calcium carbonate cement as a drug-eluting vehicle. Further studies are needed to determine the setting time of the cement in order to show that the cement can function in an injectable drug delivery system. The drug elution properties are however very promising for such an application.

REFERENCES: [1]A. Buzágh (1926) *Kolloid-Zeitschrift* **38**:222-26.

QCM-D - a useful tool for cell studies?

E Nilebäck,[1, 2] N Tymchenko,[1] J Gold,[1] B Kasemo,[1] S Svedhem[*, 1]
[1] Dept. of Applied Physics, Chalmers University of Technology, 412 96 Göteborg, Sweden. E-mail: sofia.svedhem@chalmers.se. [2] Q-Sense, 426 77 Västra Frölunda, Sweden

INTRODUCTION: Morphological changes in cells are connected with important phenomena such as cell spreading, motility, activity, and potentially even differentiation. For this reason, there is a demand for label-free, real-time techniques as complements to conventional fluorescence microscopy and patch clamp methodology. It is especially attractive to screen properties of cells based on monitoring of global cell properties (e.g. electrical or mechanical). Recently quartz crystal microbalance with dissipation monitoring (QCM-D) has been employed successfully in e.g. cytotoxicity assays [1], or to detect cellular responses in response to growth factors [2]. Here, reversible changes in QCM-D responses were induced in fibroblasts by the cytomorphic agent cytochalsin D.

METHODS: QCM-D is a surface sensitive technique that measures changes in mass and viscoelastic properties of an adsorbed layer close to the sensor surface (from nm to µm). Specifically the measurement consists of monitoring of changes in the shear oscillation frequency (related to changes in the acoustically coupled mass) of a piezoelectric quartz crystal sensor and the energy dissipation/damping of the oscillator (related to viscoelastic properties and dissipative processes). However, the QCM-D results from cells have been proven to be non-trivial to interpret without complementary data from e.g. microscopy.

RESULTS: Fibroblasts were seeded to collagen or fibronectin-coated sensors *in situ*. QCM-D and light microscopy data were recorded in real-time simultaneously on the same substrate as fibroblasts were attached, spread, and subjected to the cytoskeleton perturbing agent cytochalasin D. Cell attachment did not result in significant frequency shifts, but was associated with large dissipation shifts Reversible morphological changes were repeatedly seen both visually in the light microscopy images and in the dissipation factor from the QCM-D measurements. The attached fibroblasts responded reversibly to the cytomorphic agent cytochalasin D by retraction of the cell body, clearly seen in the microscopy images, and also detected as large dissipation shifts.

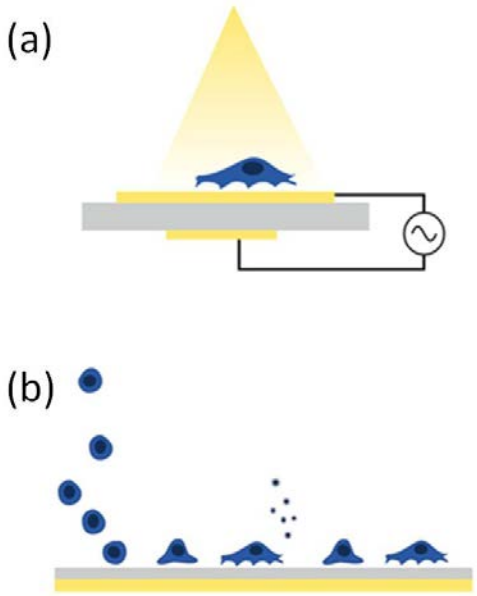

Fig. 1: Schematic illustration of the experimental outline, using (a) a combined setup with a windowed QCM-D module mounted on a microscope. (b) The cells were seeded on the QCM-D sensor in situ where they were allowed to attach and spread. Their reversible responses due to rearrangements in the cytoskeleton were followed in real time.

DISCUSSION & CONCLUSIONS: In this study, cytoskeletal changes in fibroblasts were monitored by QCM-D. Integration of QCM-D and light microscopy gives a unique opportunity to not only see morphological changes visually but also to construct models to quantify this in physical parameters such as viscosity and shear elastic modulus of cells in real-time.

REFERENCES: [1] J. Fatisson, F. Azari, and N. Tufenkji (2011) *Biosens Bioelectr* **26**:3207-12. [2] J.Y. Chen, M.H. Li, L.S. Penn, and J. Xi (2011) *Anal Chem* **83**:3141-6.

ACKNOWLEDGEMENTS: These results were obtained with funding from the EU 7th Framework Programme (FP7/2007-2013) under grant agreement no NMP4-SL-2009-229292 (Find&Bind).

Properties and cell compatibility of mineralized alginate hydrogel beads

M Olderøy[1], M Xie[1], M Westhrin[2], J-P Andreassen[3], Z Zhang[4], B L Strand[2], T Standal[2], P Sikorski[1]

[1]Department of Physics, Norwegian University of Science and Technology, Trondheim, Norway. [2]Department Cancer Research and Moleculer Medicine, Norwegian University of Science and Technology, Trondheim, Norway. [3]Department of Chemical Engineering, Norwegian University of Science and Technology, Trondheim, Norway. [4]School of Chemical Engineering, University of Birmingham, Birmingham, United Kingdom

INTRODUCTION: Hydrogels have long been recognized for their applications in tissue engineering, either as encapsulation matrices for cells and growth factors or for the use in wound management aids. However, only recently they have shown potential applications in tissue engineering of hard tissues, due to development of strategies for mineralization and control of cell-matrix interactions. Here, we describe alginate hydrogel beads mineralized by bioinspired method, where calcium phosphate is precipitated within the gel network. Two methods to create super-saturation are used, one based on enzyme ALP which produces phosphate ions form organic phosphate precursor [1] and counter-diffusion [2] methods where phosphate ions are mixed with alginate solution and calcium phosphate is made at the same time as the gel is formed in a bath containing Ca-ions. Encapsulation of human cell types relevant for bone tissue engineering in those materials is described.

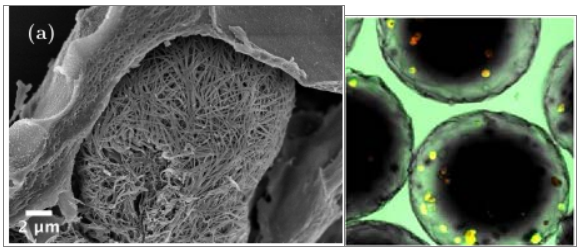

Figure 1: (a) Scanning electron micrograph showing Collagen produced by BMSCs within alginate matrix. (b) BMSCs in alginate beads after 8 days in culture (dark colour is due to extensive mineralisation). Beads are approximately 500µm in diameter.

METHODS: Alginate beads in the size range of 500µm are made by electrostatic dripping method and are mineralised with enzymatic or counter diffusion method. Encapsulated cells were pre-mixed with the alginate solution priory to formation of the beads. Produced cell containing composites were characterized with various microscopy techniques, at different time points during culture.

RESULTS: Human mesenchymal stem cells (MSCs) derived from bone marrow (BMSCs) were shown to be compatible with encapsulation in beads mineralized by enzymatic and counter-diffusion methods. The beads mineralized by counter-diffusion with encapsulated BMSCs were shown to be extensively mineralized after 21 days of culture in a differentiation medium. BMSCs encapsulated in beads mineralized enzymatically [1] showed differentiation towards OST phenotypes when cultured in differentiation medium, and scanning electron microscopy showed that the cells secreted collagen. However, the initial mineralization was necessary for further mineralization of the beads. Viscoelastic properties of single beads in which cells after prolonged cultured have been investigated using micromanipulation based compression and hold method [3]. Significant increase in instantenious (3-fold) and relaxed (4-fold) Young's moduli have been observed.

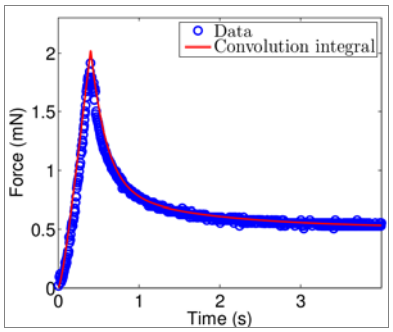

Figure 2: Force curve for compression and hold experiment of a single mineralised alginate bead.

REFERENCES: [1]M. Xie, M.O. Olderoy, Z. Zhang, J.P. Andreassen, B.L. Strand, P. Sikorski (2012) *Biocomposites prepared by alkaline phosphatase mediated mineralization of alginate microbeads*. RCS Advances 2012. [2]M. Xie, M.O. Olderøy, J-P. Andreassen, S.M. Selbach, B.L. Strand, P. Sikorski (2010) *Acta Biomater* **6**:3665–3675. [3]M.O. Olderoy, M. Xie,, J.P. Andreassen, B.L. Strand, Z. Zhang, P. Sikorski (2012) *Viscoelastic properties of mineralized alginate hydrogel beads*. **Submitted**.

An in-situ crosslinking, citric acid based composite for osteonecrosis of the femoral head.

M Palmer[1], R. Tran[1], HK. Kim[2], J. Yang[1*]

[1] *Department of Bioengineering, University of Texas at Arlington, U.S.A.* [2] *Center for Excellence in Hip Disorders, Texas Scottish Rite Hospital for Children, U.S.A.*

INTRODUCTION: Osteonecrosis, resulting from bone resorption imbalance, is difficult to treat. The collapse of weight bearing bone prevents normal regeneration from occurring [1]. We have developed an injectable, elastomeric citrate-based composite that can polymerize in situ, with appropriate material properties to support the collapsed femoral head and facilitate regeneration.

METHODS: The poly-poly ethylene glycol-maleate-citrate (PEGMC) pre-polymer was synthesized as described previously [2], combined with varied amounts of hydroxyapatite (HA) and initiators ammonium persulfate and TEMED. Crosslinked composites were mechanically tested on an MTS insight, under uniaxial unconfined compression according to ASTM D695-10. Composites were soaked in 1x and 5x simulated body fluid (m-SBF) for 1, 7 or 14 days and evaluated for mineralization by scanning electron microscopy (SEM) and energy dispersive X-ray spectrometer (EDS). Degradation studies were carried out in PBS for three months and the resulting surface topography was evaluated with SEM.

Cytocompatibility of PEGMC/HA was assessed with the pre-osteoblast MC3T3 cell line. Cells were incubated with the prepolymer, initiators, degradation or leach products and cytotoxicity was evaluated by MTT, according to ISO 10993-5. Composites were seeded with 20,000 cells/cm^2 and incubated in 50 ug/mL ascorbic acid for 3, 7 or 14 days. Osteoblast adhesion was evaluated by SEM.

RESULTS: The compressive strength and moduli of PEGMCHA composites reached 5 MPa and 15 MPa, respectively. The rate of degradation slowed significantly with increasing amounts of hydroxyapatite ($p<.05$). Composites with higher hydroxyapatite content mineralized extensively in SBF and in all cases hydroxyapatite nanocrystals were observed (figure 1). The prepolymer demonstrated minor toxicity below concentrations of 10 mg/mL and leach product toxicity comparable to control polymer polyethylene diacrylate (PEGDA). Seeded osteoblasts displayed spread morphology, indicative of differentiation.

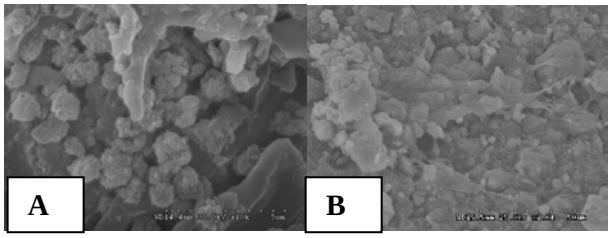

Fig. 1: SEM image of mineralized composites (7 day, 1x SBF) (A), and adherent osteoblasts (7 day) (B).

DISCUSSION & CONCLUSIONS: PEGMC composites with 50% hydroxyapatite can support physiologically appropriate levels of stress (5 MPa) which is within reported values of cancellous bone. The presence of citrates in composites enhanced mineralization and bound to hydroxyapatite to prevent particulate leaching. In 1x SBF hydroxyapatite nanocrystals were observed, suggesting that citrate-based composites mineralize similar to normal bone. Seeded osteoblasts attached, proliferated and differentiated on PEGMC/HA composites, thereby demonstrating excellent cytocompatibility. We have developed the first injectable, citrate-based elastomeric composite for repair of the femoral head. Future work will include cell and drug delivery formulations for bone tissue engineering.

REFERENCES: [1] HK. Kim (2007) *J Musculoskelet Neuronal Interact* **7**(4):350-3. [2] D. Gyawali (2010) *Biomaterials* **31**(34):9092-105.

ACKNOWLEDGEMENTS: The authors acknowledge support from a NSF CAREER award 0954109, a NIH R01 EB012575, and a TSRHC grant.

QUANTITATIVE CHARACTERIZATION OF BIOMATERIALS AND THEIR INTERACTION WITH LIVING CELLS BY AFM

C. Pettersson[1], T. Neumann[1], T. Neicke[1]

[1]*JPK Instruments AG, Applications department, Berlin, Germany*

INTRODUCTION: Topography, roughness and mechanical properties of biomaterials are crucial parameters influencing cell adhesion/motility, morphology and mechanics as well as the development of stem/progenitor cells [1,2,3,4]. Atomic force microscopy (AFM) is a powerful tool not only to study the morphology in terms of high resolution imaging and roughness measurements, but also to map mechanical and adhesive properties. Combining these remarkable abilities with advanced optical microscopy allows for extensive characterization of biomaterials.

METHODS: AFM is based on a flexible cantilever stylus that is scanned over the sample. The probe-sample interaction induced deflection of the cantilever is finally converted into sample topography and interaction force. The sensitivity of the detection system and the accuracy of piezo actuators and capacitive sensors allow for resolving structures of less than 1 nm and forces in the pN scale. Different imaging modes can resolve structures of biomaterials in physiological conditions without the Abbe diffraction limit. In force spectroscopy mode, interaction forces between the (modified) cantilever and any substrate can be measured. Using Single Cell Force Spectroscopy (SCFS), cell-substrate or cell-cell interactions can be measured down to single protein unbinding (fig. 1). The cantilever can also serve as a nano-indentation tool to analyse mechanical properties like the Young's modulus of biomaterials or cells.

RESULTS: Using AFM imaging, the nanostructure of biomaterials like aligned collagen matrices have been resolved as well as cell alignment on such structures [4,5]. SCFS quantified the adhesion force and the contribution of different components, e.g. from the extra cellular matrix of living cells, to implant materials as from cochlear implants [6]. Force-indentation measurements on cells using colloidal probes showed a significant effect of micro-patterned substrates on cellular elasticity [2].

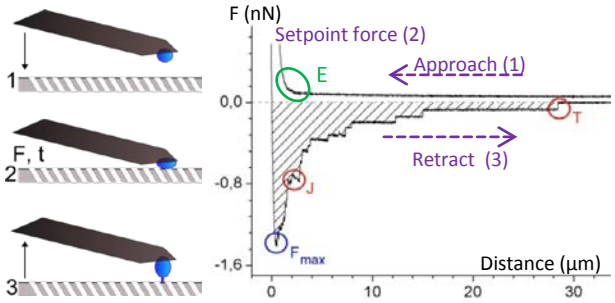

Fig. 1: Sketch of a SCFS experiment. The probe cell is approached to (1) and pressed against the substrate (2) with a defined Setpoint force (F) for a defined time (t). When the cell is separated from the sample (3) interactions like maximum adhesion force (F_{max}) and single unbinding events (force jumps (J) and those that are preceded by membrane tethers (T)) are visible in the force distance curve. The contact part of the Approach curve allows for applying elasticity models (E).

DISCUSSION & CONCLUSIONS:
AFM is a multipurpose technology which is much more than simple imaging. Interaction forces from single molecule unbinding to cell adhesion and analysis of surface and mechanical properties of biomaterials and cells make AFM to a key technology in biomaterial research. Nano-mechanical analysis of cells increasingly gains in importance in different fields in cell biology like cancer research [7] and developmental biology [8]. We present a strategy to comprehensively characterize biomaterials as well as their interaction with cells and influence on cell behavior.

REFERENCES: [1]Elter et al., Eur Biophys J 2011:40(3): 317-327. [2]McPhee et al., Med Biol Comput 2010:48(10):1043-53. [3]Engler et al., Cell 2006:126(4):677-689. [4]Kirmse et al., J Cell Sci 20100:124(11):1857-66. [5]Cisneros et al., Small 2007:3(6):956-63. [6]Aliuos et al., Biomed Tech 2010:55:66-68. [7]Cross et al., Nat Nanotech 2007:2(12):780-783. [8]Krieg et al. Nat Cell Biol 2008:10(4):429-36.

Characterization of BMP-2 delivery from hydrogels via radiolabeling

S Piskounova[1], L Gedda[1], G Hulsart-Billström[1], J Hilborn[1], T Bowden[1]

[1] *Uppsala University, Uppsala, Sweden*

INTRODUCTION: The use of bone morphogenetic protein 2 (BMP-2) in clinical applications has been shown to be excessively complicated due to this growth factors short biological half-life, localized action and rapid clearance. A hyaluronan-based hydrogel system has been previously evaluated as a delivery vehicle for bone morphogenetic protein 2 (BMP-2) for bone induction purposes. The release of the growth factor from the hydrogel system was quantified by Enzyme-Linked Immunosorbent Assay (ELISA). However, only a fraction of the total loaded BMP-2 was detected to be released after 4 weeks in vitro. [1] Since then we have hypothesized that since ELISA requires sampling and dilution of BMP-2 it may not the most reliable methods for BMP-2 quantification. Therefore in this work we employed radiolabeling of BMP-2 with ^{125}I in an attempt to perform a more accurate characterization of the growth factor release from the hydrogel both in vitro and in vivo.

METHODS: BMP-2 (InductOs, Pfizer) was radiolabeled using a modified chloramine-T method. To prevent loss during handling, adsorption to sample tubes was studied at different times and temperatures. Hydrogels containing mixture of labelled and non-labelled BMP-2 were prepared by addition of the mixture to one of the hydrogel components. The vitro the release profile of ^{125}I-labelled BMP-2 was compared to the alkaline phosphatase (ALP) expression in response to BMP-2. The hydrogels were also evaluated in vivo in a subcutaneous ectopic model in male Sprague–Dawley rats in order to correlate the retention of the growth factor to bone formation.

RESULTS: The data shows that Protein LoBind tubes exhibit the lowest protein affinity. The release study showed a biphasic release profile of biologically active BMP-2 in vitro *(Fig. 1)*. In vivo the release was similar, though somewhat faster. Mineralization was observed in vivo at day 8, with increasing bone mineral volume and bone mineral content until day 14.

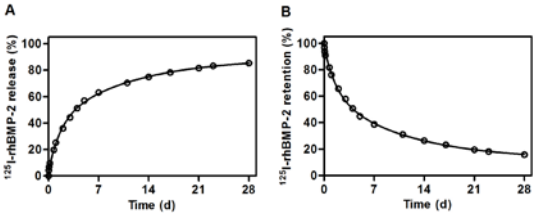

Fig. 1: The in vitro (A) release and (B) retention profiles of BMP-2 from hydrogels.

DISCUSSION & CONCLUSIONS: The results confirm that the initial BMP-2 characterization by means of ELISA was not entirely correct, as large amount of the growth factor were not detected by this technique. Most importantly the study illustrates the importance of cautions handling and reliable quantification techniques for successful design of a carrier for BMP-2.

REFERENCES: [1] K. Bergman (2009) *J Biomed Mat Res* **91A**(4):1111-18.

ACKNOWLEDGEMENTS: This work has benefited from research funding from the European Community's Seventh Framework Program in the project AngioScaff (NMP-LA-2008-214402).

The effects of nanotopography on promoting osteogenic differentiation

S Pujari[1], L Tang[2], M Karlsson Ott[1]

[1] *Department of Engineering, Uppsala University, Uppsala, SE.* [2] *Department of Bioengineering, School of Engineering, University of Texas at Arlington, Arlington, TX, USA.*

INTRODUCTION: There are many osteogenic biomaterials to choose from when designing an orthopaedic prosthesis. Nanoporous alumina demonstrates a greater surface area to volume ratio and more closely mimics the topography of the native extracellular matrix than many other biomaterials. In this study, nanoporous alumina was evaluated as an osteoinductive and drug eluting nanomaterial. A murine mesenchymal stem cell (MSC) line (W20-17) was cultured on multiple pore sized alumina (20-, 100-, and 200nm in diameter) to characterize the effect of nanotopography on osteogenic behavior.

METHODS: Nanoporous alumina membranes were soaked overnight in a BMP-2 solution (120ng/ml). Tissue culture polystyrene (TCPS) was used as the control. MSCs were seeded on nanoporous alumina surfaces, with or without the addition of BMP-2, at a density of 5,000cells/cm^2. Cell proliferation and osteogenic differentiation were then evaluated by AlamarBlue and alkaline phosphatase (ALP) activity respectively, at 2, 7, and 14 days. Cell morphology was studied by Scanning Electron Microscopy (FESEM, Leo 1550, Zeiss).

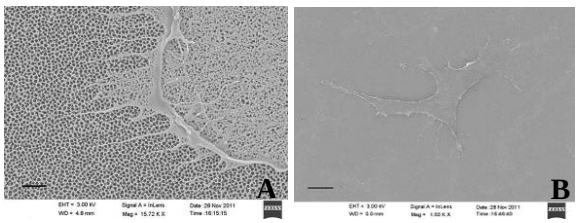

Fig.1 SEM images of W20-17 on A)100nm nanoporous alumina, and B) 200nm nanoporous alumina.

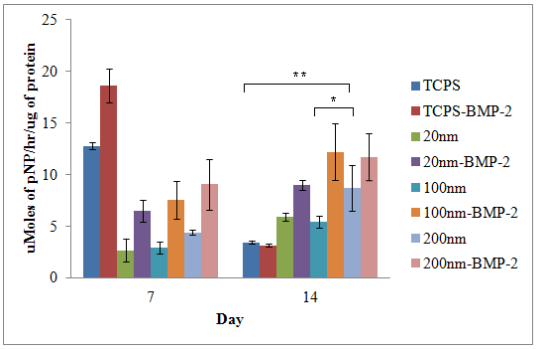

Fig. 2 ALP protein expression levels.

RESULTS: Our results suggest that changing the pore sizes on nanoporous alumina surfaces result in difference in MSC behavior. Cell spreading, an indicator of adhesion, is enhanced on larger pore size membranes (Fig.1,100 and 200nm). Although cell proliferation was not affected by pore size, MSC differentiation was different between pore sizes without BMP-2. After 14 days of culture ALP expression was significantly greater on 200nm as compared to 100nm pore size and the control ($p < 0.05$) (Fig.2). As for the BMP-2 loaded alumina, a similar trend was observed.

DISCUSSION & CONCLUSIONS: Alkaline phosphatase, the most common indicator of differentiated osteoblasts, levels increased gradually from 7 to 14 days on samples incubated with and without BMP-2 indicating that a range of nano-sized pores can guide MSCs towards osteogenic differentiation. MSCs grown on 200nm pores had higher ALP levels as compared to the other surfaces suggesting that larger pore sizes are conducive to promoting an osteogenic phenotype [1]. Cells grown on larger pore size substrates elicited an elongated morphology with filipodia extending into the pores, further supporting the conclusion that pore size affected differentiation.Finally, ALP expression was consistently higher on BMP-2 loaded nanoporous alumina surfaces as compared to unloaded surfaces, indicating that not only is nanoporous alumina osteoinductive, but also has the potential to be used as a drug eluting bone coating.

REFERENCES: [1] S. Oh et al (2008) *PNAS* **106**: 2130-35.

ACKNOWLEDGEMENTS: The authors acknowledge support from STINT.

Reconstruction of large bone defects using 3 dimensional, resorbable, textile implants. A pilot study on rabbit calvaria defects.

C Rentsch[1], B Bischoff[1], B Rentsch[2], S Heinemann[3], R Bernhard[3], H Zwipp[1]
[1]*University Hospital Carl Gustav Carus, Clinic and Polyclinic for Trauma and Reconstructive Surgery, Dresden, Germany,* [2]*Catgut GmbH, Markneukirchen, Germany,* [3]*Max Bergmann Center of Biomaterials, Dresden, Germany*

INTRODUCTION: The majority of cranial bone defects are the outcome of heavy skull traumata which often require a decompressive craniectomy. The skull bone has to be reconstructed after the treatment of the brain hematoma. Autografts, allografts, mineral bone substitutes, metal meshes or other commonly used materials for large bone reconstruction have their advantages and disadvantages in biocompatibility, stability, storage, immune reaction, infection risk, pain, availability and aesthetic. The need for alternative osteogenic bone substitutes has led to the development of many strategies to recreate functional and structural tissue *in vitro* or *in vivo*. The aim of this study was to characterize embroidered and surface modified poly (caprolactone-*co*-lactide) (PCL, trade name of Catgut GmbH)) scaffolds (Fig. 1), implanted in a rabbit calvaria defect, in consideration of new bone formation, vascularization, mechanical stability and resorption of the implant material.

METHODS: The defect was made using a 13 mm (in diameter) dental trephine without injuring the dura mater. Four groups (n = 8) were compared after 6 months of implantation: empty defect, autologous bone, PCL scaffolds uncoated and PCL scaffolds collagen I plus chondroitin sulfate coated (coll I/cs). Microcomputer tomography (µCT), histology and biomechanical analyses were used to evaluate new bone formation, vascularization, mechanical stability and implant status.

RESULTS: The autologous bone group showed vascularized bone in the defect area, whereas the single autologous bone fragments were still detectable. The empty defect group showed the lowest new bone formation (26.6 %) compared to the autologous (68.6 %), uncoated PCL (43.3 %) and the coll I/cs coated PCL group (47.1 %) (Fig. 2). The coll I/cs surface coating of the PCL scaffold resulted in a significant more uniform defect bridging compared to the uncoated scaffold.

The biomechanical testing revealed that the coll I/cs coated scaffolds reached with 0.22 MPa the mechanical stability of autologous bone (0.21 MPa). Histological analyses showed new bone formation directly enclosing PCL fibers lacking detectable connective tissue spacing. Degrading scaffold material was visible without inflammation signs.

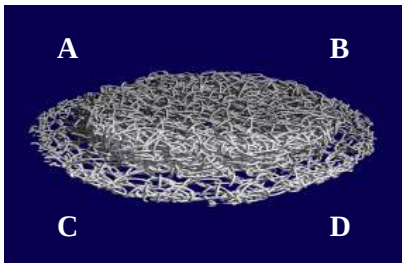

Fig. 1: 3 dimensional reconstruction of PCL scaffold using µCT, porosity 80 % and pore size 0.2-1 mm

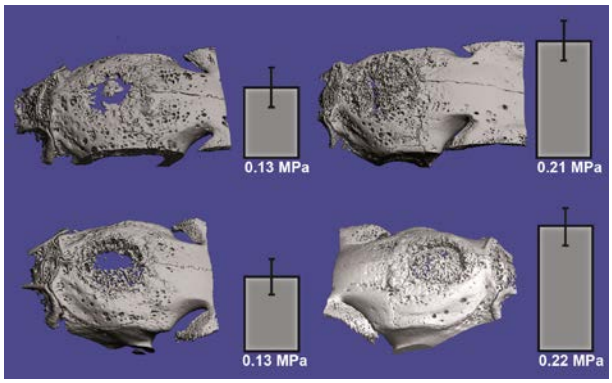

Fig. 2: representative µCT reconstruction of explanted rabbit calvaria after 6 months of bone healing plus biomechanical testing results, A: empty defect, B: autologous bone, C: uncoated PCL, D: coll I/cs coated PCL

DISCUSSION & CONCLUSIONS: This study describes a promising alternative approach using bioresorbable, embroidered, tissue engineered scaffolds for reconstruction of large bone defects.

ACKNOWLEDGEMENTS: The authors would like to acknowledge the Sächsische AufbauBank for financing and the Möckel Embroidery and Engineering Company (Auerbach, Germany) for producing the PCL scaffolds.

Development of alginate hydrogels loaded with synthetic proline-rich peptides for bone repair

M. Rubert[1], J. M. Ramis[1], J. Vondrasek[2,3], J. Calvo[4], A. Gayà[4], S. P. Lyngstadaas[5], M. Monjo[1]

[1]Research Institute on Health Sciences (IUNICS). University of Balearic Islands, Palma de Mallorca, ES. [2] Institute of Biotechnology and [3] Institute of Organic Chemistry and Biochemistry, Prague, CZ. [4]Fundació Banc de Sang i Teixits de les Illes Balears, Palma de Mallorca, ES. [5]Department of Biomaterials, Institute for Clinical Dentistry, University of Oslo, NO.

INTRODUCTION: Proline-rich proteins control the microstructure of vertebrate bones and teeth by serving as a scaffold to control the assembly of biological apatites [1]. In order to find new treatments for bone repair, we first aimed to design the structure of artificial peptides based on the common characteristics of the proline-rich region in hard tissue extracellular matrix proteins and to evaluate if such peptides could be used for induction of bone formation and biomineralization. The activity of the designed peptides was tested on osteoblast-like cells (MC3T3-E1) and in human umbilical cord mesenchymal stem cells (hUCMSCs) compared to the effect of the commercially available amelogenin formulation (Emdogain®, EMD). We further aimed to find a suitable formulation in order to facilitate their use for bone tissue engineering. Alginate is one of the main polymers chosen to form hydrogels for tissue engineering due to favourable properties as biomaterials such as non-toxicity, biodegradability, and ease of processing into desired shape under normal physiological conditions. Thereby, alginate was evaluated as a carrier of synthetic proline-rich peptides to stimulate osteoblast cell differentiation and mineralization.

METHODS: A peptide that contains a polyproline consensus sequence of 25AA length, further comprising a systematic variation of non-proline residues was designed [2,3]. Six different variants of the designed peptide (P1 to P6) were used in further experiments. Emdogain® was kindly supplied by Institut Straumann GMbH (Basel, Switzerland). Final concentrations of 50 µg/ml of peptides and of EMD were used to assay their effect on cytotoxicity by measure of LDH activity, cell differentiation by determination of relative mRNA expression levels for bone formation and mineralization related genes, ALP activity determination and analysis of calcium deposition.

RESULTS: MC3T3-E1 and hUCMSCs cells treated with the synthetic peptides showed decreased cytotoxicity compared to control. MC3T3-E1 cells treated with EMD showed lower expression of osteoblast markers genes than cells treated with P2, except for collagen type I. ALP activity was markedly increased in MC3T3-E1 cells incubated with P2 compared to other treatments. Further, P2 increased calcium deposition rate compared to EMD or control either in MC3T3-E1. Different synthetic peptides induced osteocalcin mRNA levels in both, hUCMSCs cells treated with the different synthetic peptides in combination with osteogenic supplements and in MC3T3-E1 cells treated with the formulated synthetic peptides compared to untreated and to EMD alginate-gel.

DISCUSSION & CONCLUSIONS: Osteocalcin, the most specific and the latest of expressed osteoblast markers, has been found to be significantly induced by treatment with the synthetic peptides regardless of the means of administration or the cell type used and in a recent in vivo study where titanium implants were coated with the peptides [4]. This finding suggests that the cells treated with the synthetic peptides are at a more mature stage of the differentiation process.

REFERENCES: [1] T. Jin, Y. Ito, X. Luan, et al (2009) *PLoS Biol* **7(12)**:e1000262. [2] M. Rubert, J.M. Ramis, J. Vondrasek, et al (2011) *J Biomater Tissue Eng* **1:**198-209. [3] J.M. Ramis, M. Rubert, J. Vondrasek, et al (2012) *Tissue Eng A* **In press**. [4] C. Petzold, M. Monjo, M. Rubert, et al (2012) *Oral Craniofac Tissue Eng* **In press.**

ACKNOWLEDGEMENTS: This work was supported by the Norwegian Research Council; Conselleria de Comerç Industria i Energia de les Illes Balears; MICINN (Torres Quevedo contract to MR and JMR, and Ramón y Cajal contract to MM) and Eureka-Eurostars Project Application E!5069 NewBone, and Interempresas Internacional Program from the CDTI.

Strontium-releasing CaP bone cements for osteoporotic bone defects

M Schumacher[1], A Lode[1], M Gelinsky[1]

[1] *Centre for Translational Bone, Joint and Soft Tissue Research, Medical Faculty and University Hospital, Technische Universität Dresden, Dresden, DE.*

INTRODUCTION: The therapeutic benefit of strontium ions is used in the clinical treatment of osteoporotic bone disease by systemic administration of Sr-containing drugs [1]. Sr is known to inhibit bone resorption as well as to positively affect bone formation. Therefore, the concept of local release of Sr^{2+}-ions from bone cements for the treatment of osteoporotic bone defects has been proposed [2]. In this study, a CaP bone cement (setting to hydroxyapatite) has been modified with divalent strontium and characterised by means of compressive strength and Sr-release. Furthermore, the influence of the cement modification on human mesenchymal stem cells (hMSC) was studied *in vitro*.

METHODS: Strontium modified CaP bone cements were prepared by the addition of $SrCO_3$ to an α-tricalcium phosphate based, hydroxyapatite-forming cement (CPC) as described by Driessens et al. [3] or by the substitution of Ca^{2+} by Sr^{2+}-ions in the cement powder. Compressive strength of the set cements was measured (Instron). Sr^{2+}-ion release was determined during ageing in buffered salt solution by atomic absorption spectroscopy. Primary human mesenchymal stem cells were cultured in α-MEM containing 9% FCS, 1% L-glutamine and 1% PS. To induce osteogenic differentiation 5 mM β-glycerophosphate, 50 µM ascorbate-2-phosphate and 10 nM dexamethasone were added. Cell proliferation and osteogenic differentiation were measured by intracellular lactate-dehydrogenase (LDH) activity and alkaline phosphatase (ALP) activity quantification, respectively.

RESULTS: Compressive strength was found to increase with Sr-substitution (up to 57 MPa compared to 29 MPa for pure CPC) but to decrease with higher $SrCO_3$ addition (14 MPa). For all cement formulations ion release increased with higher strontium content (figure 1, left). Cell proliferation was significantly faster on Sr-containing cements, the highest proliferation was found on CPC with 8.4% Sr substitution. Osteogenic differentiation (as determined by specific ALP activity) was also increased on Sr-cements (figure 1, right).

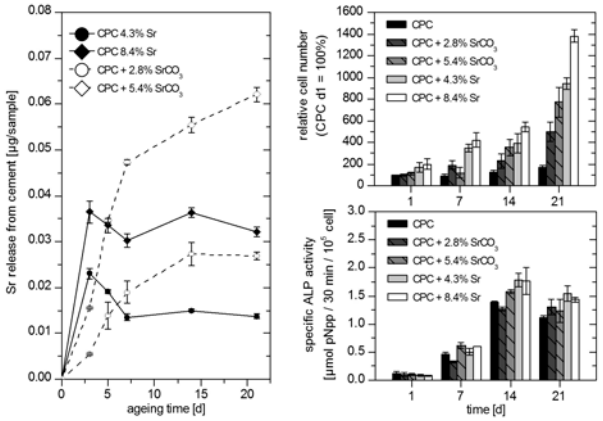

Fig. 1: Left: Sr-ion release from modified CaP cements as determined by AAS. Right: hMSC proliferation and differentiation on Sr-modified cements.

DISCUSSION & CONCLUSIONS: Sr-substitution of CaP cement can significantly improve its mechanical strength and result in sustained release of Sr-ions from the material. Cell proliferation as well as osteogenic differentiation were shown to be promoted by the presence of Sr in the cement. Therefore, a positive effect on the bone regeneration can be expected. Taking into account the known effect of Sr-ions in the treatment of osteoporosis, such modified bone cements could be beneficial on the healing of osteoporotic bone defects.

REFERENCES: [1]P.J. Marie (2005) *Osteoporos Int* **16**(1):7-10. [2]Y.W. Li, J.C. Leong et al. (2000) *J. Biomed. Mater. Res.* **52:**164-70. [3]F.C.M. Driessens, M.G. Boltong et al. (1994) *J Mater Sci Mater Med* **5**:164-70.

ACKNOWLEDGEMENTS: The authors thank InnoTERE GmbH (Dresden, Germany) for the kind supply of cements powders. This work was funded by the DFG and part of SFB/TR79.

Structural characterization of mesoporous titania containing silver nanoparticle inclusions for antibacterial implant applications

T Thersleff, K Grandfield, W Xia, K Welch, H Engqvist

Division for Applied Materials Science, Department of Engineering Sciences, Uppsala University, Uppsala, SE

INTRODUCTION: Titanium dioxide is a well-known biomaterial, ideal for use in implant coatings due to its biocompatibility and surface topography. It can also be fabricated as a porous structure, with a pore size ranging between 5 – 50 nm in diameter, also known as mesoporous titania. This enables the coating to act as a reservoir for nanoparticles and drugs, while not significantly compromising its mechanical properties. Recently, it was demonstrated that mesoporous titania can be used as a novel surface drug-delivery system when loaded with Cephalothin [1]. In this study, the ability of this mesoporous matrix to hold silver nanoparticles is investigated. Such a nanocomposite structure would be capable of acting as an antimicrobial surface combining the effects of ultraviolet radiation with those of silver ions. The success of such nanocomposites depends, to a large extent, on the spatial distribution of silver nanoparticles within the mesoporous titania matrix. This study is designed to make a detailed assessment of the nanoparticle distribution and structure-property relationship of silver nanoparticle-doped mesoporous titania coatings.

METHODS: Mesoporous titania films approximately 200 nm in thickness were deposited on bulk titanium using an Evaporation Induced Self-Assembly (EISA) method. Silver nanoparticles were introduced into the mesoporous coatings by soaking in a silver nitrate solution, followed by treatment with UV light (254 nm) to decompose the nitrate into silver nanoparticles or silver oxides. All coatings were initially characterized using x-ray diffraction in the Bragg-Brentano and grazing incidence geometries. The surface topology of the films was assessed in a Carl Zeiss 1550 scanning electron microscope operated at 3 kV in secondary electron mode. One doped and one undoped specimen were then prepared for structural and chemical analysis in a transmission electron microscope using the focused ion beam in-situ lift-out method. The structure of the films was locally assessed using electron diffraction and high resolution imaging with both parallel and convergent beams and related to the x-ray data. The chemical distribution was investigated by generating real-space elemental maps using energy dispersive x-ray and electron energy loss spectroscopy.

RESULTS: Figure 1 below shows an SEM image of the undoped mesoporous titania surface, revealing an average pore diameter of 5.44 ± 1.30 nm and an average "roundness" of 1.31 ± 0.21, where "roundness" is determined by the P2A measurement:

$$P2A = Perimeter^2/4\pi Area$$

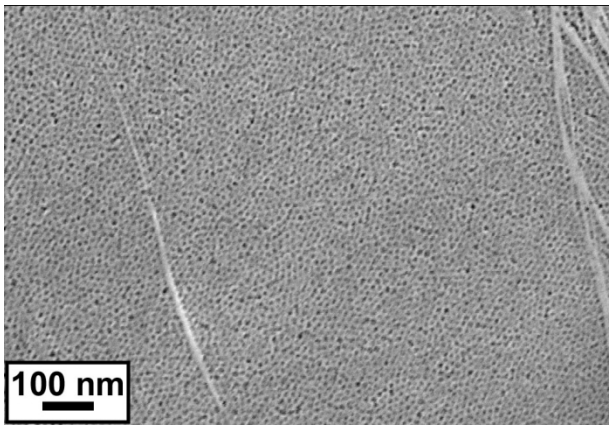

Fig. 1: Secondary electron micrograph of the surface of undoped mesoporous titania captured in a scanning electron microscope. The nanoporous structure can be clearly delineated.

DISCUSSION & CONCLUSIONS: Silver nanoparticles can be incorporated into the bulk of mesoporous titania. The spatial distribution of these particles plays a significant role in understanding their usefulness as implant coatings. This study assesses the feasibility of producing an antimicrobial mesoporous titania implant coating with silver nanoparticles.

REFERENCES: [1] W. Xia, K. Grandfield, A. Hoess, A. Ballo, Y. Cai, H. Engqvist (2012) *J Biomed Mater Res* **100B**:82–93.

ACKNOWLEDGEMENTS: The authors are grateful for the support from VINNOVA.

Compressive strength of highly porous ceramic TiO_2-ZrO_2 foams

H Tiainen[1], G Eder[1,2], HJ Haugen[1]

[1]*Department of Biomaterials, Institute of Clinical Dentistry, University of Oslo, Norway.* [2]*Institute of Medical and Polymer Engineering, Chair of Mechanical Engineering, Technische Universität München, Germany*

INTRODUCTION: Highly biocompatible crystalline TiO_2 has been identified as a promising scaffolding material for the restoration of large bone defects [1], whereas the more bioinert ZrO_2 is know for its excellent mechanical properties. The aim of the present study was to investigate the effect of ZrO_2 addition on the compressive strength of highly porous ceramic TiO_2 bone scaffolds.

METHODS: Highly porous TiO_2 foams were produced using polymer sponge replication with 0-40 wt.% of TiO_2 raw material substituted with ZrO_2. Microstructure, chemical composition, and pore architectural features were characterised using SEM, XRD, and micro-CT. These characteristics were then related to the compressive strength of the prepared ceramic foams.

RESULTS: Typical appearances of the microstructure of the prepared ceramic foams are shown in Fig.1. ZrO_2 additions < 20 wt.% resulted in single-phase ceramic foams consisting of Zr-dissolved rutile TiO_2, whereas foams with higher ZrO_2 content exhibited two-phase microstructure of $ZrTiO_4$ and Zr-dissolved rutile. Intergranular porosity and transgranular cracks became more frequent as the ZrO_2 concentration increased.

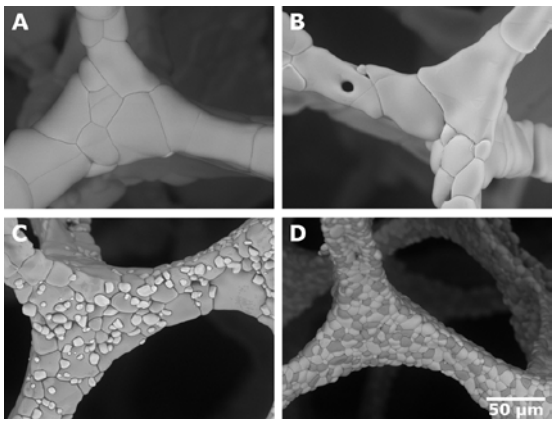

Fig. 1: Microstructure of ceramic foams containing 0 (A), 10 (B), 20 (C), and 40 wt.% (D).

Overall, the added ZrO_2 did not significantly affect the desired pore architectural features of the TiO_2 foams. However, ZrO_2 addition was generally found to have an adverse effect on the mechanical properties of the scaffold structure as only the lowest ZrO_2 concentration resulted in increased strength (Fig.2).

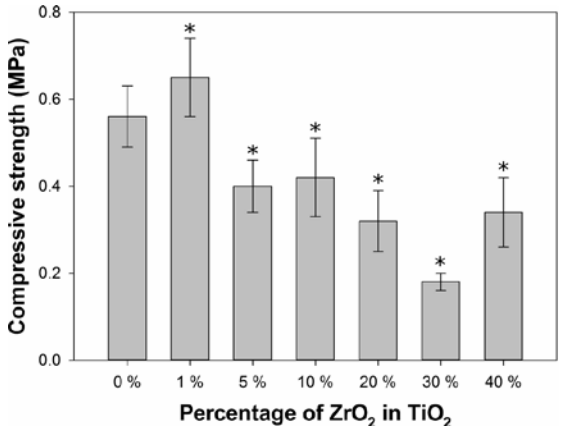

*Fig. 2: Compressive strength of the prepared ceramic foams.*statistical significance against 0% ZrO_2 ($p<0.05$).*

DISCUSSION & CONCLUSIONS: Dissolution of ZrO_2 in the TiO_2 lattice and the formation of the intermediate $ZrTiO_4$ phase prevent the use of ZrO_2 particles to toughen the TiO_2 scaffold material by crack deflection or by transformation toughening mechanism. The appearance of $ZrTiO_4$ in samples containing ≥ 20 wt.% ZrO_2 considerably reduced the average grain size of TiO_2 but also led to poor densification in the absence of sintering aids, which had a detrimental effect on the mechanical properties of the scaffold structure. Furthermore, the achieved improvement in the compressive strength of the scaffolds containing 1 wt.% ZrO_2 was rather limited with only 16 % increase in the average compressive strength in comparison to scaffolds containing no ZrO_2. Therefore, it may be concluded that ZrO_2 addition does not markedly increase in the mechanical properties of highly porous TiO_2 bone scaffolds.

REFERENCES: [1] H. Haugen, Will, J. et al (2004) *J Eur Ceram Soc* **29**:661-8.

ACKNOWLEDGEMENTS: This study was supported by Eureka-Eurostars Project Application E!5069 NewBone.

Microscratching of silicon nitride and silicon carbonitride coatings

S Tkachenko[1,2], M Pettersson[1], S Schmidt[3], T Berlind[3], S Jacobson[1], L Hultman[3], C Persson[1], H Engqvist[1]

[1] *Applied Materials Science, Department of Engineering Sciences, Uppsala University, Sweden*
[2] *Institute for Problems of Materials Science, National Academy of Sciences, Kiev, Ukraine*
[3] *Department of Physics, Chemistry and Biology (IFM), Linköping University, Sweden*

INTRODUCTION: Previous studies have shown that silicon nitride coatings are promising candidates for bearing surfaces of total joint replacements [1]. These coatings are intended to reduce the inflammatory response to wear debris and prolong the lifetime of joint replacements. Screening tests on silicon nitride coatings have demonstrated higher wear resistance than the conventional cobalt chromium alloy (CoCr) commonly used today. An understanding of the cohesion and adhesion of these coatings is therefore of great importance. This study investigates these properties for silicon nitride (SiN) and silicon carbonitride (SiCN) coatings using microscratching.

METHODS: SiN- and SiCN-coatings, deposited on silicon wafers and CoCr plates by High Power Impulse Magnetron Sputtering (HiPIMS), were studied. Deposition parameters such as target power, temperature, time and sample rotation were varied to obtain different chemical compositions and microstructures.

Scratch tests were performed using a commercial CSM nano scratcher with a sphero-conical stylus (apex 90°; tip radius 2 µm). The scratching was performed in three steps: pre-scan (load 3 mN), progressive loading up to 500 mN over 600 µm (loading rate 150 mN/min) and post-scanning (load 3 mN). Critical loads L_{C1} and L_{C2}, responsible for cohesive and adhesive failure of the coatings respectively, were determined using load vs. depth-profiles in combination with optical and scanning electron microscopy.

RESULTS: The resulting coatings present three different types of microstructure: dense SiN-coatings (thickness between 2 and 6 µm) and SiCN-coatings showing either laminar or columnar microstructure (thickness of 0.5 to 1 µm). The SiN-coatings deposited on silicon wafers failed at critical loads in the range of 260-440 mN. This was found to be 3-5 times higher than for SiCN-coatings. Failure of SiN-coatings occurred by extensive flaking-off without formation of cohesive failure cracks (Fig. 1a). Critical loads for the SiCN-coatings of similar thickness were higher for the coatings with laminar microstructure and low carbon content than for the coatings with columnar microstructure and high carbon content (Fig. 1b, c). SiCN-coatings with columnar microstructure, deposited on silicon wafers, demonstrated better adhesion than the same coatings on CoCr substrates.

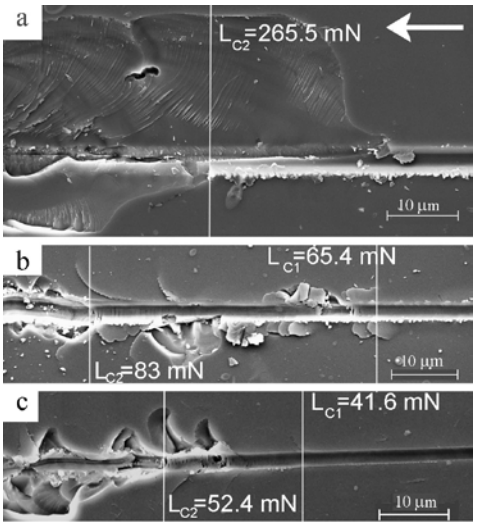

Fig. 1 Scratches on coatings deposited on silicon wafers for a) SiN-coating with dense microstructure, b) SiCN-coatings with laminar microstructure and c) SiCN-coating with columnar microstructure. The arrow indicates the direction of scratching.

CONCLUSIONS: The SiN-coatings demonstrated higher adhesion to silicon substrates than the coatings containing carbon. However, the adhesion of coatings on CoCr substrate needs to be improved. Thick (2-6 µm) SiN-coatings exhibiting a dense structure are of great interest for further studies due to their high adhesive loads, indicating better load-carrying abilities.

REFERENCES: [1] M. Pettersson, J. Olofsson, N. Teuscher, S. Jacobson, C. Persson, A. Heilmann, et al. (2011) Ball-on-disc testing of SiN_x-coatings for hip joint implants, The International Conference on BioTribology (ICoBT), 18-21 September 2011 London.

ACKNOWLEDGEMENTS: The authors are grateful for funding from the Swedish Foundation for Strategic Research, SSF, and the Swedish Institute, SI.

Antibacterial properties of contemporary dental luting agents

E Unosson[1], Y Cai[2], X Jiang[1], J Lööf[3], K Welch[2], H Engqvist[1]

[1]*Applied Materials Science, The Ångström Laboratory, Uppsala University, Sweden,*
[2]*Nanotechnology and Functional Materials, The Ångström Laboratory, Uppsala University, Sweden,*
[3]*Doxa AB, Uppsala, Sweden*

INTRODUCTION: In prosthetic dentistry, acid-base reacting or self-etching cements are used to fixate crowns and bridgeworks onto supporting teeth. In addition to biocompatibility, mechanical integrity and good handling properties, effective dental cements should also inhibit caries or plaque formation. Restoration failures are most often caused by secondary caries [1], developing in small gaps or margins where bacteria can proliferate unhindered. Antibacterial properties of the cement thus becomes of critical importance to preserve the integrity of the restoration for as long as possible. The current study was aimed at evaluating the antibacterial properties of four commercially available dental cements (RelyX™ Unicem, Ketac™ Cem, Ceramir® C&B and Harvard zinc phosphate cement) and two reference materials (glass-ionomer cement and calcium aluminate cement), compared to a negative control material (PMMA).

METHODS: After being prepared in accordance with manufacturer instructions and allowed to set in 1.5 mm deep and 5 mm diameter moulds, the cement samples were aged in 37°C and 100 % relative humidity for 10 min, 1 day or 7 days before testing for antibacterial properties. *S. mutans* suspension, adjusted to 10^9 CFU/mL, was used to determine growth inhibition activity of the investigated cements, as well as the effects of varying pH and the bactericidal effect of fluoride. A method allowing direct contact between the bacteria and the surface under investigation was employed [2], and a metabolic assay was used to quantify remaining viable bacteria. Optical density (OD) measurements were used to determine bacterial proliferation in solutions with pH ranging from 1.5 to 9, as well as in solutions containing up to 2000 ppm fluoride.

RESULTS: The strongest antibacterial properties were found for calcium aluminate, followed by Ceramir and RelyX. Ketac, Harvard and the reference glass-ionomer showed bacteria content either higher than, or not significantly different from the PMMA control in all instances. pH levels below 6.3 and above 9.0 were found to have negative effects on bacterial proliferation, and a continuous reduction in the bacterial growth rate was observed with increasing fluoride concentration

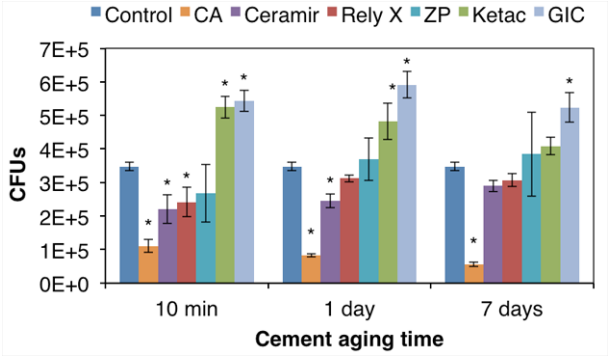

*Fig. 1: CFUs present in solution after direct contact tests. Significant differences ($p < 0.05$) from control indicated by *. Note: First bar in each group shows the same control PMMA data since these samples were not aged.*

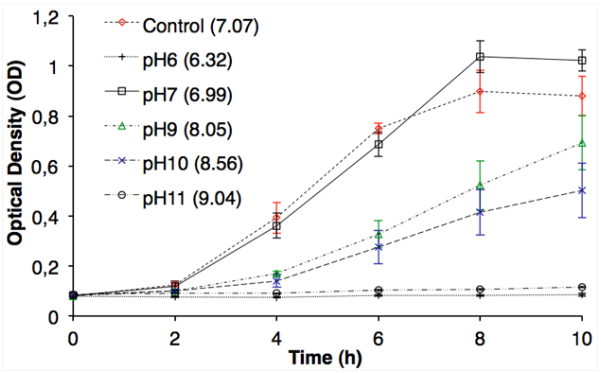

Fig. 2: Growth curves of S. mutans in BHI at different pH buffer/BHI solutions. Value in brackets indicates the resulting pH of buffer/BHI solution.

DISCUSSION & CONCLUSIONS: Low pH and high fluoride concentration reduces bacterial growth rates. However, no correlation between either acidic materials (Ketac, GIC, ZP) or fluoride release (RelyX, Ceramir, GIC) and antibacterial properties could be seen in this study; rather, basic materials (CA, Ceramir) showed stronger antibacterial properties.

REFERENCES: [1] G. Libby et al (1997) *J Prost Dent* **78**:127-31. [2] E. Weiss et al (1996) *Endod Dent Traumatol* **12**, 179–84.

Patterned electrospun microfibers integrated in a microfluidic system to study cells in complex microenvironments

Patric Wallin[1], Carl Zandén[2], Björn Carlberg[2], Johan Liu[2], Julie Gold[1]

[1] *Biological Physics, Applied Physics, Chalmers University of Technology, Gothenburg, SWE*
[2] *Bionano Systems, MC2, Chalmers University of Technology, Gothenburg, SWE*

INTRODUCTION: Cell microenvironments play a very important role in basic cell research, drug discovery and tissue engineering among others. The ability to define, create and control such microenvironments is rapidly increasing due to the application of microfluidic technologies in cell research. Electrospinning of polymeric fibers is a method that has been applied for many years in tissue engineering and biosensing applications. Electrospun fibers are used as cell culture substrates as they mimic native extracellular matrix properties. We have recently developed and evaluated a device that combines microfluidic networks with electrospun fibers.

METHODS: We have previously shown the ability to spatially pattern random as well as directionally-oriented electrospun fiber pads on a single glass substrate by direct photolithographic processing [1]. In the current study, a PDMS microfluidic channel was irreversibly bonded to a glass slide containing such patterned e-spun fiber pads. A flow-based gradient generator was used which relies on repetitive splitting and recombining fluid streams with different concentrations. This principle allows the formation of linear and parabolic gradients with varying gradient steepness/profiles. The microfluidic device was characterized by computational fluid dynamic (CFD) simulations (COMSOL) to investigate if placing three-dimensional pads of micron-diameter fibers in a microfluidic channel would disrupt or disturb the laminar flow and concentration gradient profiles in the liquid. Further, soluble gradient properties were measured with fluorescein/PBS by fluorescence microscopy and compared between channels with and without incorporated electrospun fibers. Additionally, 3T3 fibroblast attachment within the channels was evaluated by fluorescently staining cells with DAPI and phalloidin.

RESULTS: It was shown that patterned fiber pads with defined fiber alignment can be produced and that the PDMS channels could be positioned over the pads and subsequently bonded to the underlying substrate. CFD simulations as well as experimentally determined linear concentration gradients showed that the fiber pads do not significantly disturb the laminar flow in the microfluidic channel. There is a small eddy forming at the edge of the fiber pad which is only locally extending into the free media flow on the length scale of one cell. It was shown that cells can be cultured in the system under mild flow conditions (less than 2 dynes/cm2) for at least 24 hours, and that cells can be visualized in situ by bright field and fluorescent microscopy techniques.

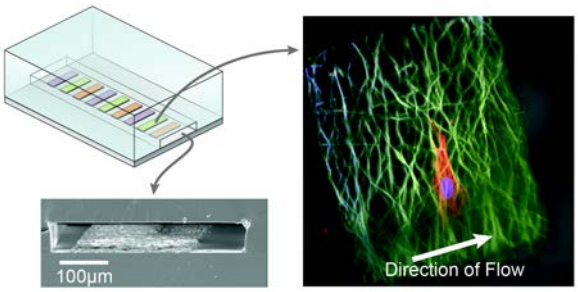

Fig. 1: Sketch of the microfluidic channel containing multiple electrospun fiber pads with different alignment and orientation to the direction of flow. Fibroblast cell attached to a fiber pad, 24hr.

DISCUSSION & CONCLUSIONS: The results of the system characterization presented in this work clearly demonstrate the suitability of integrating spatially and geometrically electrospun patterns with a microfluidic generated defined liquid microenvironment. The production method and resulting microfluidic system open the possibility for many investigations into the behavior of cells in well-defined microenvironments.

REFERENCES: [1] B. Carlberg, T. Wang, and J. Liu, *Langmuir* **26**, 2235-9 (2010)

ACKNOWLEDGEMENTS: The research leading to these results has received funding from the EU 7th Framework Programme (FP7/2007-2013) under grant agreement NMP3-SL-2009-229294 NanoCARD, from Vinnova under contract no: 2009-00227, and was carried out within the Sustainable Production Initiative and the Production Area of Advance at Chalmers.

Calcium phosphate sphere/PMMA composite: preparation, ion and drug release

W Xia[1,2], M Z Mujo[1], H Engqvist[1,2], C Persson[1]

[1] *Applied Materials Science, Department of Engineering Sciences, Uppsala University, Uppsala, SE.* [2] *BIOMATCELL, VINN Excellence Center of Biomaterials and Cell Therapy, Gothenburg, SE*

INTRODUCTION: Treatment of prosthesis-related infection is difficult, and generally focuses on removal of the foreign body material combined with surgical removal of infected tissue around the prostheses area. Thereafter antibiotics are administrated. To reduce the incidence of infections and avoid systemic treatment, bone cements have been developed for local drug release (PMMA containing antibiotics). However, the release of antibiotics from PMMA generally consists of a burst release with little maintained elution. Furthermore, PMMA do not show bioactivity. Therefore, a combination of slow release of antibiotics with bioactivity would be a significant improvement of PMMA as bone cement. Via the addition of drug loaded bioactive calcium phosphate hollow spheres to PMMA a high drug loading capacity and good bioactivity can be achieved.

METHODS: Strontium doped hollow calcium phosphate spheres (HCPS) were prepared using a previously described method [1]. The PMMA used was Osteopal V (Heraeus Medical). Four groups were studied: (1) PMMA / HCPS (10wt%), (2) PMMA / Vancomycin (2.5wt%), (3) PMMA / Vancomycin loaded HCPS (10wt%) and (4) PMMA/HCPS (10wt%) / Vancomycin (2.5wt%). All samples were prepared in 6 mm × 12 mm molds. 20 ml PBS of pH value 4, 7.4 and 8 was added to the PMMA groups and the release was carried out at 37°C on an orbital shaker. The ion concentration in the solutions was analyzed by ICP-AES. The release of vancomycin was studied by UV-VIS. The ion and drug release behavior was evaluated using Korsmeyer-Peppas model.

RESULTS: Vancomycin release from all four groups showed a similar trend, a burst release within 8 hours followed by a slow release. The pH value of the release medium did not significantly influence the release rate. Strontium release from all four groups also showed a similar behaviour. However, the initial quick release lasted for 120 hours followed by the slow release. Furthermore, for Sr the pH value had a significant influence on the release, see Fig. 1. Sr release in PBS (pH=4) showed the quickest rate. Incorporation of HCPS into PMMA increased the drug release rate (group 2 vs. group 4). Both the drug and ion release mainly followed a Fickian diffusion profile based on the calculation from the Korsmeyer-Peppas model.

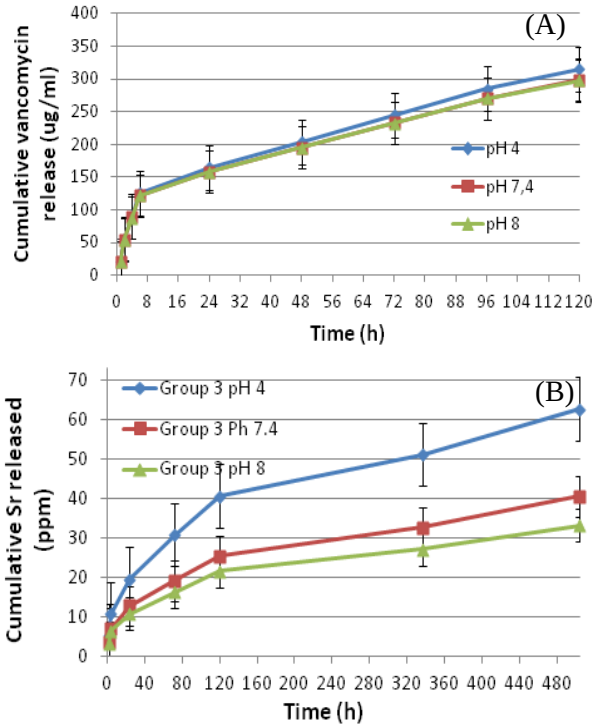

Fig. 1 Vancomycin (A) and strontium (B) release profiles for PMMA composite group 3 in PBS (pH 4, 7.4 and 8).

DISCUSSION & CONCLUSIONS: Incorporation of drug loaded hollow calcium phosphate spheres into PMMA influenced the release of the drug and ions. The pH value of the release medium affected the Sr release, but not the vancomycin release. Incorporation of HCPS into PMMA increased the drug release rate. Both drug and ion releases were mainly controlled by Fickian diffusion.

REFERENCES: [1]. W. Xia, K. Grandfield, A Schwenke, H. Engqivst (2011) *Nanotechnology* **22**: 305610

ACKNOWLEDGEMENTS: The authors are grateful for funding from VR (Swedish research council), EU and VINNOVA (SPINEGO FP7-PEOPLE-2010-268134 and VINNMER 2010-02073 projects, respectively).

Structural and chemical features of modified Ti and TiZr surfaces and their biocompatibility for human gingival fibroblasts

R Xing[1], M Gomez-Florit[2], M Monjo[2], HJ Haugen[1], SP Lyngstadaas[1], SF Taxt-Lamolle[1]

[1]*Department of Biomaterials, Institute for Clinical Dentistry, University of Oslo, Norway.*
[2]*Department of Fundamental Biology and Health Sciences, IUNICS, University of Balearic Islands, Palma de Mallorca, Spain*

INTRODUCTION: Bone loss around dental implants has been suggested to be due to bacteria infection from the mouth. Therefore, sealing the implant's neck to prevent oral pathogen from penetrating this region can be of great importance. Many efforts have been made to optimize surface structures for soft tissue growth.

Titanium (Ti) is one of the mostly used implant materials. It can be alloyed with zirconium (Zr) to improve mechanical properties, which allows for thinner implants, e.g. for placement in thinner alveolar bones.

This research aimed at modifying and characterising Ti and TiZr surfaces, and to test their biocompatibility in human gingival fibroblast cells.

METHODS: Both Ti and TiZr coin-shaped specimens were surface-modified and separated into three groups: (1) polished, (2) machined, and (3) polished pickled hydride [1-2]. Surface topography and roughness were analyzed by interferometry and profilometry. Surface morphology was investigated by SEM (Scanning Electron Microscopy). SIMS (Secondary Ion Mass Spectroscopy) was used for characterizing surface elemental compositions. LDH (Lactate Dehydrogenase) activity of human gingival fibroblasts (HGF-1) cultured on the samples was assayed to evaluate surface cytotoxicity.

RESULTS: Six different surfaces were created (Fig. 1): polished Ti (poTi) and TiZr (poTiZr), machined Ti (MTi) and TiZr (MTiZr), polished pickled hydrided Ti (ppHTi) and TiZr (ppHTiZr). Among them, roughness (Sa) is increasing in the following order: poTi, poTiZr, MTiZr, MTi, ppHTiZr and ppHTi.

Hydrogen amount on ppHTi and ppHTiZr were found higher than all the other groups, while MTi and MTiZr coins showed the lowest hydrogen intensity. Furthermore, both poTi and ppHTi showed higher hydrogen intensity than their corresponding TiZr surfaces: poTiZr and ppHTiZr.

For the *in vitro* test using HGF, all the samples presented low cytotoxicity compared to plastic cell culture plate in different degrees. More *in vitro* studies are being investigated to further test how surface topography and chemistry affect cell proliferation and differentiation.

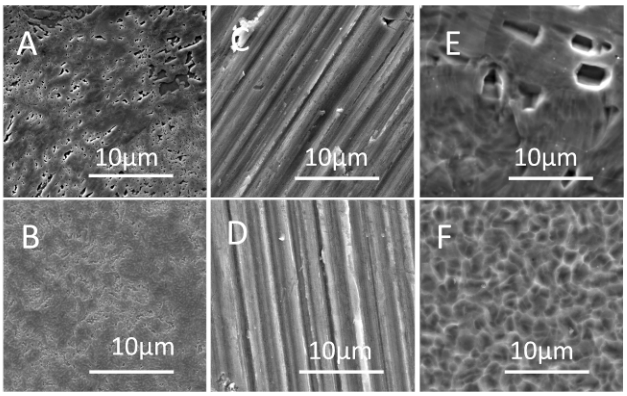

Fig. 1: *SEM pictures of Ti and TiZr surface topographies: A. polished Ti; B. polished TiZr; C. machined Ti; D. machined TiZr; E. polished pickled hydrided Ti; F. polished pickled hydrided TiZr.*

DISCUSSION & CONCLUSIONS: Three different types of surfaces (polished, machined, and polished pickled hydrided) were prepared on Ti and TiZr coins. TiZr surfaces were more wear and corrosion resistant than Ti since the surface modifications did not affect as much TiZr as Ti (roughness). All surfaces possessed their specific topographies and hydride content. Process of pickling and hydridation was proven to be able to increase the hydrogen amount on the surface. Moreover, all of the manufactured surfaces could be applied as abutment, since they showed low cytotoxicity levels compared to plastic cell culture plates.

REFERENCES: [1] S. Lamolle, M. Monjo, et al (2009) *J Biomed Mater Res A* **88**(3): 581-88. [2] K. Videm, S. Lamolle, et al. (2008). *Applied Surface Science* **255**(5): 3011-15.

Biomimetic calcium-phosphate coatings on artificial spider silk fibres

L Yang[1], M Hedhammar[2], T Blom[3], K Leifer[3], J Johansson[2], P Habibovic[1], CA van Blitterswijk[1]

[1]Department of Tissue Regeneration, University of Twente, Enschede, The Netherlands. [2]Department of Anatomy, Physiology and Biochemistry, Swedish University of Agricultural Sciences, Uppsala, Sweden. [3] Department of Engineering Sciences, Uppsala University, Uppsala, Sweden

INTRODUCTION: A successful synthetic bone graft substitute needs to satisfy the requirements of biocompatibility, as well as bioactivity in terms of osteoconductivity and osteoinductivity. Furthermore, sufficient mechanical properties are needed to obtain initial stability at the defect location and to avoid stress shielding. Calcium phosphate (CaP) coatings, applied on surfaces of metallic and polymeric biomaterials, can improve their performance in bone repair and regeneration. Spider silk is biocompatible, strong and elastic, and hence an attractive biomaterial for applications in connective tissue repairs. Recently, artificial spider silk, with mechanical and structural characteristics similar to those of native spider silk, has been produced from recombinant minispidroins [1].

METHODS: In the present study [2], supersaturated simulated body fluid (SBFx5A and B) was used to deposit calcium phosphate coatings on recombinant spider silk fibres. The mineralization process was followed in time using scanning electron microscopy (ESEM) equipped with an energy dispersive x-ray (EDX) detector and Raman spectroscope. Focused ion beam technology was used to produce a cross section of a coated fibre, which was further analysed by EDX. Preliminary *in vitro* experiments using the coated fibres for culture of bone marrow-derived human mesenchymal stem cells (hMSCs) were also performed.

RESULTS: After only 10 min of immersion in the SBFx5A solution, polygon-like particles with a size of 0.5–1 μm started depositing on the surface of the fibres. Elemental mapping using EDX showed that these particles were sodium chloride crystals. After 1 h of immersion, formation of new globules was also observed. Elemental mapping showed that these globular deposits consisted of CaP with approximate calcium to phosphorus ratio of 1.5. After 24 h, silk fibres were completely covered with a CaP layer consisting of globules, 0.2–0.5 μm in size. EDX analysis indicated only the presence of calcium and phosphorus, suggesting that the coating was relatively thick. When these pre-calcified fibres then were immersed in a SBFx5B solution, with lower concentration of magnesium and carbonate ions, crystal growth was promoted. This could be confirmed with a shift in peak position in the Raman spectra and by ESEM analysis.

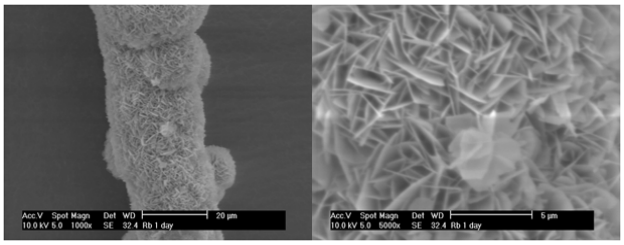

Fig. 1: ESEM micrographs of spider silk fibres after immersion in the SBFx5A solution for 24 h followed by immersion in the SBFx5B solution for 10 min. Scale bar is 20 μm (left) and 5 μm (right).

DISCUSSION & CONCLUSIONS: The results of this study showed that recombinant spider silk fibres could successfully be coated with a homogeneous and thick crystalline CaP layer using a two-step biomimetic procedure. The mineralization process started with the formation of sodium chloride crystals, prior to deposition of CaPs, which contrasts the findings of mineralization of other substrates, such as metallic surfaces. It was qualitatively shown that the coated silk fibres supported the attachment and growth of bone marrow-derived hMSCs.

REFERENCES: [1] M. Stark, S. Grip, A. Rising, et al (2007) *Biomacromolecules* **8**:1695-1701. [2] L. Yang, M. Hedhammar, T. Blom, et al (2010) *Biomed Mater* **5**:045002.

ACKNOWLEDGEMENTS: This study was financially supported by the EC 'Spiderman' project (G5RD-CT-2002-00738).

In vitro bioactivity studies of bone substitutes based on titanium or magnesium doped hydroxyapatite and calcium sulfate

A Zima[1], D Siek[1], J Czechowska[1], W Mróz[2], A Ślósarczyk[1]

[1] *AGH – University of Science and Technology, Faculty of Materials Science and Ceramics, Cracow, Poland.* [2] *Institution of Optoelectronics, Military Academy of Technology, Warsaw, Poland*

INTRODUCTION: Calcium phosphates (CaPs) are widely used in hard tissue replacement [1]. The interesting alternative for high-temperature calcium phosphate ceramics are mouldable, self-setting calcium phosphate cements (CPCs) [2]. The surface properties of biomaterials affect their long-term stability and biological properties. Bioactivity *in vivo* of an implant material can be predicted by assessing apatite formation on its surface *in vitro* in simulated body fluid (SBF) [3]. After implantation, on the surface of these materials an apatite layer is formed, what provides a biological active bone/implant interface [4]. The aim of this study was *in vitro* evaluation of bioactive potential of the composite type bone substitutes on the basis of titanium doped hydroxyapatite, magnesium doped carbonate hydroxyapatite and calcium sulfate hemihydrate.

METHODS: Using the wet chemical method two different calcium phosphate powders: titanium doped hydroxyapatite (Ti-HA) and magnesium doped carbonate hydroxyapatite (Mg-CHA) were synthesized. Obtained powders were heat treated at 1250°C and 800°C, respectively. The modified hydroxyapatite powders were mixed with calcium sulfate hemihydrate (CSH, Acros Organics) at the 2:3 weight ratio. For the pastes preparation the 1.0 wt.% Na_2HPO_4 solution and various chitosan solutions in acetic acid were applied as liquid phases. Changes in the surface morphology of hardened bodies, incubated in simulated body fluid (SBF) for 7 and 28 days, were observed. The bioactivity of calcium phosphate substitutes was assessed using atomic force microscopy (AFM), scanning electron microscopy (SEM), fourier-transformed infrared spectroscopy (FTIR) and X-ray diffraction (XRD).

RESULTS: XRD measurements revealed that Mg-CHA-CSH cement after setting and hardening was composed of calcium sulphate dehydrate (CSD) and hydroxyapatite. While Ti-HA-CSH consisted of hydroxyapatite, tricalcium phosphate and bassanite. The differences in phase compositions of obtained materials influenced their surface morphology (Fig.1). The AFM and SEM studies showed the formation of 'cauliflower' like apatitic crystals layer as soon as after 7 days of incubation in SBF. FTIR measurements confirmed increase in the intensity of bands assigned to hydroxyapatite with elongation of the soaking time.

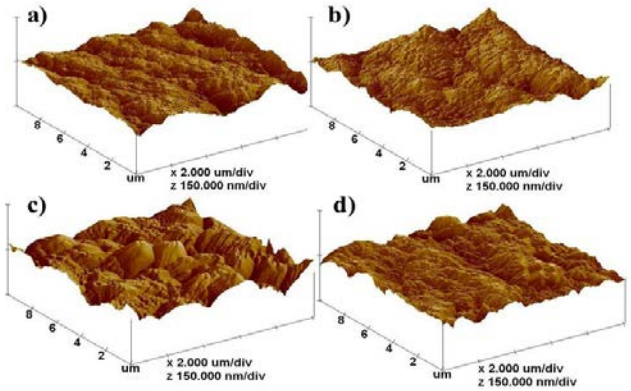

Fig. 1: The surface morphology of the cement type composite Ti-HA-CSH: a) non-incubated, b) incubated in SBF for 7 days, and Mg-CHA-CSH: c) non-incubated, d) incubated in SBF for 7 days.

DISCUSSION & CONCLUSIONS: The new bone substitutes based on titanium doped hydroxyapatite or magnesium doped carbonate hydroxyapatite and calcium sulfate were developed. The formation of apatite layer on the surface of the samples incubated in SBF indicates on high bioactive potential of both obtained materials.

REFERENCES: [1]A. Bigi, B. Bracci, S. Panzavolta (2004) *Biomaterials* **25(14)**:2893-99. [2]M. Bohner (2001) *European Spine Society* **10**:114-21. [3]L. Kong, Y. Gao, G. Lu, Y. Gong, N. Zhao, X. Zhang (2006) *European Polymer Journal* **42(12)**:3171-79. [4]N.A.F. Almeida, M.H.V. Fernandes (2006) *Materials Science Forum* **514-516**:1039-43.

ACKNOWLEDGEMENTS: This work has been supported by the European Union - project No: UDA-POIG-01.03.01-00-005/09.